Fabrication of Macadamia Nutshell Powder-Al/Fe Metal Oxide Modified Diatomaceous Earth Composite Beads for Fluoride and Pathogen Removal from Groundwater.

A Masters Dissertation Submitted to the Department of Ecology and Resource Management, School of Environmental Sciences, University of Venda.

By

Nekhavhambe Humbelani Helga

Student Number: 11631512

Supervisor: Prof Gitari M.W

Co-Supervisor: Dr Mudzielwana R

April 2021

DECLARATION

I, Nekhavhambe Humbelani Helga (Student No: 11631512), hereby declare that this dissertation titled “Fabrication of Macadamia Nutshell Powder-Al/Fe Metal Oxide Modified Diatomaceous Earth Composite Beads for Fluoride and Pathogen Removal from Groundwater” is my own work in design and execution and it has never been submitted for any degree or examination in any other University. All sources of information herein have been dully and appropriately acknowledged by means of comprehensive list of references.

--- ---------- ----03 /09/ 2021----------

H.H Nekhavhambe Date

ACKNOWLEDGEMENT

I would like to express my sincere gratitude to the following, without hesitation because if it was not their assistance my study would not have been possible.

My Heavenly Father, who enable me and give me strength in everything I do, his protection to see me live.

Prof. Gitari M.W.- Your supervision and mentorship were crucial to the compaction of this dissertation and your financial support for my fees will not be forgotten.

Dr Mudzielwana R.-Your supervision, mentorship and your hard work in lab for analysing my sample. Thank you for sacrificing your time and providing such excellent support.

My parents, sister and brothers- for providing me with privilege of studying and their financial support.

Research group (ENVIREN) for always making things easier, willing to assist with all aspect of the study. From helping with proof reading and lab equipment. Thank you for your support.

DEDICATION

This work is dedicated to my parents Mr Nekhavhambe K.K and Mrs Nekhavhambe N.I. To my parents I say thank you for the support and also encouraging me to do the best.

ABSTRACT

Contamination of drinking water due to fluoride and pathogens is a severe health hazard problem. Excess of fluoride (>1.5 mg/L) in drinking water leads to dental and skeletal fluorosis whereas the presence of pathogens in water can lead to adverse health effects, including gastrointestinal illness, reproductive problems, and neurological disorders. This study aims to fabricate macadamia nutshell powder-Al/Fe metal oxide modified DE composite beads for removal of fluoride, pathogen from groundwater. The physicochemical compositions of the material were characterized using Scanning Electron Microscope, Fourier Transform Infrared Spectroscopy, Brunauer Emmett Teller and X-Ray Fluorescence and X-Ray Diffraction. The fluoride removal was evaluated using batch and column experiment and the pathogen removal was done using Well disc diffusion assay method.

First chapter of results focused on physiochemical characterization of macadamia nutshell powder and further evaluates its efficiency in fluoride and pathogens removal from water. Physicochemical characterization revealed that MNS mainly consist of O, C, H and N as the main elements. This was further confirmed by FTIR which showed OH, C-H, C=O, C-C, C-OH together with the band of C-O. The XRD revealed that MNS is crystalline. The batch experiments showed a maximum fluoride sorption capacity of 1.26 mg/g which was achieved at initial fluoride concentration of 5 mg/L, adsorbent dosage of 0.5 g/100 mL, pH 6 and shaking time of 120 min agitation time. The adsorption isotherm data fitted well to Langmuir than to Freundlich isotherm indicating adsorption occurred on monolayer surface. The value ΔG^0 was found to be negative indicating that adsorption of fluoride onto MNS was spontaneous and favourable. The regeneration studies of MNS demonstrated that the adsorbent can be regenerated for up to 7 cycles using 0.01 M HCl and this clearly indicates the reuse potential of the adsorbent. MNS show no zone of inhibition (bacterial activity) towards the *Escherichia Coli* and *Staphylococcus Aureus* and *Klebsiella Pneumoniae.*

Second chapter focused on fabrication of macadamia nutshell powder-Al/Fe metal oxide Modified diatomaceous earth composite beads for fluoride and pathogen removal and to further evaluate their properties and efficiency of fluoride and pathogens removal. The optimum ratio for fabricating the beads was found to be 1:3 (1 MNS: 3 Modified DE) which yield the high fluoride removal. The MNS-Al/Fe metal oxide modified DE beads consist of Al_2O_3 and FeO_3 as major chemical components. Batch experiments showed a maximum fluoride removal capacity of 2.61 mg/g with initial fluoride concentration of 5 mg/L and adsorbent dosage of 0.9 g/ 100 mL at a pH of 4 and equilibration time of 120 mins. The adsorption kinetics data fitted

better to pseudo second order than pseudo first order of reaction kinetics indicating that the rate limiting factor is chemisorption. The adsorption isotherm data fitted better to Langmuir isotherm model indicating that adsorption occurred on monolayer surface. The thermodynamics parameters such as ΔG^{o} and ΔH^{o} revealed that adsorption of fluoride by the composite adsorbent is endothermic and spontaneous and ΔS^{o} indicated that fluoride ions were randomly distributed on the surface of the adsorbent. The presence of Mg^{2+}, Ca^{2+}, SO_4^{2-}, NO_3^{-}, Cl^{-}, and CO_3^{2-} reduced the percentage fluoride uptake by the prepared beads. The adsorbent was regenerated up to 5 cycle using deionised water and this clearly indicates the reuse potential of the adsorbent. The column experiments showed that increasing bed height from 30 mm to 40 mm increases the volume of water treated at breakthrough point from 1.3 To 1.8 L. Moreover, the breakthrough capacity for 40 mm bed height was found to be 0.49 mg/g. Antimicrobial potency study showed that the prepared composite beads have a potency against *Klebsiella Pneumoniae* with 10 mm diameter of inhibition zone.

Based on the findings, it can be concluded that MNS and MNS-Al/Fe metal oxide modified DE beads can be used for fluoride removal from ground water with about 48% (MNS) and 70% (MNS and MNS-Al/Fe metal oxide modified DE beads). MNS and MNS-Al/Fe metal oxide modified DE beads also show microbial potency towards *Klebsiella Pneumoniae*. Moreover, MNS show no microbial potency and the fluoride removal is below 1.5 mg/L as recommended by WHO. Therefore, it is recommended that further study should investigate modification of MNS using inorganic and organic chemical species in order to enhance its performance towards fluoride and pathogen removal. Although MNS-Al/Fe metal oxide modified DE beads showed potency towards *Klebsiella Pneumoniae*, further research must be done use Ag and Au nanoparticles to enhance its effectiveness to bacteria.

EXPECTED ACADEMIC OUTPUT

Peer reviewed articles under preparation:

Nekhavhambe H.H, Gitari W.M & Mudzielwana R. Physicochemical characterization of macadamia nutshells for fluoride and pathogen removal from groundwater. To be submitted to an international peer reviewed journal in 2021.

Nekhavhambe H.H, Gitari W.M & Mudzielwana R. Fabrication of macadamia nutshell powder-Al/Fe metal oxide Modified diatomaceous earth composite beads for fluoride and pathogen removal. To be submitted to an international peer reviewed journal in 2021.

TABLE OF CONTENTS

List of figures

List of tables

Acronym

MNS : Macadamia Nutshell

F^- : Fluoride

DE : Diatomaceous Earth

FTIR : Fourier Transform Infrared Spectroscopy

pH : Potential Hydrogen

WHO : World Health Organisation

WRC : Water Research Council

XRF : X-Ray fluorescence

XRD : X-Ray diffraction

BET : Brunauer Emmett Teller

SEM : Scanning Electron Microscopy

MNS-Al/Fe metal oxide modified beads : Macadamia Nutshell-Al/Fe Modified Diatomaceous Earth Composite Beads

Chapter 1: Introduction

1.1 Background

Water scarcity is gradually becoming a potential threat to human health, food security and national ecosystems with more than 50% of the world projected to experience water shortage by 2025 (Pradhan and Biswal, 2018: Tzanakakis *et al*., 2020). These shortages of water are due to climatic change and pollution from industries. According to the World Health Organization (WHO) reports, about 844 million people lack basic quality drinking-water service, with about 3.4 million people, mostly young children died annually from water-related diseases, most especially in the developing countries (WHO/UNICEF, 2017; Ayinde *et al*., 2018). For these reasons' majority of people in rural areas of Sub-Saharan Africa and other developing countries depends on groundwater as source of drinking water and water for domestic usage (Gitari *et al*., 2015). Depending on the geographical location, groundwater is characterized by a high concentration of ions such as fluoride which is detrimental to human health (Yu *et al*., 2013; Ayinde *et al*., 2018; Odiyo and Makungo, 2012). Excessive levels of fluoride can cause many problems ranging from mild dental fluorosis to crippling skeletal fluorosis as the level and period of exposure increases (WHO, 2017). The World Health Organisation has recommended a guideline value of 1.5 mg/L of fluoride in drinking water in order to reduce the risk of fluorosis (WHO, 2017).

Apart from fluoride, groundwater is vulnerable to other contaminants such as pathogens (Soupir *et al*., 2018; Ayinde *et al*., 2018). The lack of proper sanitation measures, as well as improperly placed wells lead to contamination of groundwater with pathogens carried in faeces and urine. The presence of pathogens in water can lead to adverse health effects, including gastrointestinal illness, reproductive problems, and neurological disorders (Newell, 2010). Regarding this sickness caused by contaminated water there is a need for the development of water treatment techniques that will help reduce the number of people who lacks access to clean water.

Different defluoridation techniques have been developed to remove fluoride in drinking water. Such techniques include precipitation, reverse osmosis, electrodialysis, ion exchange, nanofiltration, and adsorption (Dhillon *et al.*, 2015; Yu *et al*., 2013). Among these various techniques, adsorption is the most suitable and commonly used because of its effectiveness, energy saving, simplicity and cost effective (Bhatnagar *et al*., 2011). Several adsorbents including nanohydroxyapatite, clay and diatomaceous earth have been tested for fluoride

removal from groundwater (Ayinde *et al*., 2018; Mudzielwana *et al*., 2018; Gitari *et al*., 2015; Izuagie *et al*., 2016). However, these materials are more effective at narrow pH range and have poor regeneration potential. Moreover, these adsorbents do not target microbial contaminants. The ways of disinfection, chlorination of drinking water, boiling of water, ceramic filters and ultraviolet (UV) (Ayinde *et al*., 2018: Moran *et al* 2008).

Our previous study has evaluated the efficiency of Al/Fe oxides modified DE in fluoride removal using batch and column experiments (Gitari *et al*., 2017; Nekhavhambe, (2018). The material showed a maximum fluoride adsorption capacity of 5.53 mg/g. (Izuagie *et al*., 2016). The column experiment conducted by Nekhavhambe (2018) showed that the material has a better fluoride removal capacity. However, its application at household level using fixed bed column is limited by its low permeability which results in small volume of water treated after a long period of time. The amount of treated water at breakthrough point was 3.33 L within 62 hours. In the bid to enhance the permeability, combining DE with bio-waste could yield better permeability. The bio-waste used was Macadamia Nutshell powder (MNS) which is known to have high surface area (Pakade *et al*., 2017) which could enhance the permeability and the porosity of the composite material.

South Africa is the third largest producer of Macadamia nutshells which also increase the accumulation of MNS (Mogala, 2014). Macadamia nut shells are composed of Carbon (57.5%), Hydrogen (5.95%), Nitrogen (0.33%), Oxygen (36.2%) and sulphur (0.33%). Macadamia nutshell powder have also been applied in waste-water treatment for removal of chromium (Pakade *et al*., 2017) and they have shown greater performance. The main objective of this study is to create beads and evaluate their efficiency in fluoride and its antimicrobial potency. The beads will be fabricated by making composite with macadamia nutshell powder and Al/Fe Modified DE using sodium alginate as a binder.

1.2 Problem statement

Contamination of groundwater from fluoride and pathogens is of greater concern mainly in rural communities where groundwater is the main source of water for human consumption due to their health impacts on human beings (Ayinde *et al*., 2018). Prolonged exposure to fluoride concentrations beyond the World Health Organization (WHO) recommended limit of 1.5 mg/L leads to dental and skeletal fluorosis (WHO, 2017; Izuagie *et al*., 2016). While consumption of water contaminated by pathogens lead to several diseases including cholera and diarrhoea.

In South Africa, higher fluoride concentration has been reported in Limpopo, North West, Northern Cape, Western Cape, Free State and KwaZulu-Natal provinces (Ncube and Schutte 2005). A study conducted in Siloam Village Limpopo Province, South Africa by Odiyo and Makungo (2012) show that about 50% of children aged between 11 and 14 in Siloam primary school had mottled teeth. These is a result of high concentration of fluoride in Siloam borehole which is greater than 1.5 mg/L. Pathogen related diseases have been observed in Southern Africa, Zimbabwe and Mozambique (WHO, 2019). A study by Johri *et al*. (2014) observed that 41.5% of urban and 60% of rural households were using contaminated water in Africa. Despite water being contaminated people still rely on contaminated groundwater because of lack of pipe born water or centralized municipal water supply. An effort must be done in order to treat water to the level that is recommended by WHO to avoid health effects.

Several adsorbents including activated alumina, diatomaceous earth and bentonite clay have been developed for fluoride removal (Gitari *et al*., 2017; Izuagie *et al*., 2016; Mudzielwana *al et*., 2017). Activated alumina has a great capacity for fluoride adsorption, which is dependent upon the crystalline form, the activation process and the solution pH and alkalinity (Tripathy *et al*., 2006). Moreover, most of the developed adsorbents are not multifunctional meaning that they are able to remove specific contaminant. There is a need to develop a multipurpose adsorbent that can be able to remove both chemical contaminants and pathogens from groundwater at the same time.

Previous studies indicated that Al/Fe oxide modified DE has greater potential for fluoride removal. However, its application is limited by poor permeability and porosity (Izuagie *et al*., 2016). In the present study, the physical properties of Al/Fe oxide modified DE will be improved by fabricating macadamia nutshell powder Al/Fe oxide Modified DE sodium alginate beads composite with the aim of enhancing the permeability as well as antimicrobial potency of the adsorbent. The developed adsorbent will then be tested for fluoride and pathogen removal.

1.3 Objectives

1.3.1 The main objective

The main objective of the study is to fabricate macadamia nutshell powder-Al/Fe modified DE sodium alginate composite beads for removal of fluoride, pathogen from groundwater.

1.3.2 Specific objectives

- To determine the physicochemical composition of macadamia nutshell powder.
- To evaluate the effectiveness of macadamia nutshell powder in fluoride and pathogens removal from groundwater.
- To evaluate the optimum conditions for fabricating macadamia nutshell powder-Al/Fe oxides coated DE sodium alginate beads for fluoride and pathogen removal from groundwater.
- To evaluate the fluoride and pathogens removal efficiency of macadamia nutshell powder Al/Fe oxides coated DE sodium alginate beads composite.
- To determine the regeneration and reusability potential of the synthesized adsorbents using various chemical solution.

1.4 Research question

- What are the mineralogical, chemical, and elemental characterization of macadamia nut powder?
- How effective the macadamia nutshell powder be in fluoride and pathogens removal from groundwater?
- What are the optimum conditions for fabricating macadamia nutshell powder-Al-Fe oxides coated DE sodium alginate beads for fluoride and pathogen removal from groundwater?
- How efficient will the macadamia nutshell powder Al/Fe oxides coated DE sodium alginate beads composite be in removal of fluoride and pathogens using both batch and column flow mode?
- How effective will the regeneration and reusability of the developed adsorbent be using various chemical solutions?

1.5 Hypothesis

Macadamia nutshell powder-Al/Fe oxide modified diatomaceous earth sodium alginate beads will be effective in removal of fluoride and pathogens from groundwater.

1.6 Assumption

It is assumed that removal of fluoride and pathogen using synthesized adsorbent of milled macadamia nutshell-Al/Fe modified diatomaceous earth sodium alginate beads is effective for the removal of chemical contaminants and it can be applied in household treatment devices.

1.7 Motivation

Most people residing in rural areas depend on groundwater which has higher fluoride concentration and contain pathogens as source of water, due to lack of alternative source of drinking water. The high concentration of fluoride can lead to fluorosis and pathogen can cause diseases including cholera and diarrhoea. As such there is a need to develop a low-cost material that can be used to remove the excess fluoride concentration and pathogens from groundwater at household level. Although several materials have been developed for fluoride and pathogen removal some of them suffer from disadvantages such as operating of low pH value and not being chemically stable (Adeleye *et al*., 2016). The production of macadamia nutshell powder-Al/Fe oxide modified diatomaceous earth composite beads adsorbent will contribute to the problem solving of drinking contaminated water, it will improve the health of the people.

The current study contributes to the Sustainable Development Goals (SDG) 6. Goal 6 aims to tackle challenges related to drinking water, sanitation, and hygiene for populations, as well as to water-related ecosystems. This SDG goals will focus much on goal 6.1 which seek to secure safe and affordable drinking water for all. Without quality, sustainable water resources and sanitation, progress in many other areas across the SDGs, including health, education, and poverty reduction, will also be held back (Moran *et al*., 2008).

1.8 Thesis structure

Chapter 1: Introduction

Chapter 2: Literature review

Chapter 3: Physicochemical characterization of macadamia nutshells for fluoride and pathogen removal from groundwater

Chapter 4: Fabrication of macadamia nutshell powder-Al/Fe metal oxide Modified diatomaceous earth composite beads for fluoride and pathogen removal.

Chapter 5: Conclusions and recommendations

1.9 Reference

Adeleye, A.S., Conway, J.R., Garner, K., Huang, Y., Su, Y. and Keller, A.A., 2016. Engineered nanomaterials for water treatment and remediation: costs, benefits, and applicability. *Chemical Engineering Journal*, *286*, pp.640-662.

Ayinde, W.B., Gitari, W.M., Munkombwe, M. and Amidou, S., 2018. Green synthesis of Ag/MgO nanoparticle modified nanohydroxyapatite and its potential for defluoridation and pathogen removal in groundwater. *Physics and Chemistry of the Earth, Parts A/B/C*, *107*, pp. 25-37.

Bhatnagar, A., Kumar, E. and Sillanpää, M., 2011. Fluoride removal from water by adsorption; a review. *Chemical engineering journal*, *171(3)*, pp.811-840.

Dhillon, A. and Kumar, D., 2015. Development of a nanoporous adsorbent for the removal of health-hazardous fluoride ions from aqueous systems. *Journal of Materials Chemistry A*, *3(8)*, pp.4215-4228.

Gitari, W.M., Izuagie, A.A. and Gumbo, J.R., 2017. Synthesis, characterization and batch assessment of groundwater fluoride removal capacity of trimetal Mg/Ce/Mn oxide-modified diatomaceous earth. *Arabian Journal of Chemistry*, *13*(1), pp.1-16.

Gitari, W.M., Ngulube, T., Masindi, V. and Gumbo, J.R., 2015. Defluoridation of groundwater using Fe^{3+} modified bentonite clay: optimization of adsorption conditions. *Desalination and Water Treatment*, *53(6)*, pp.1578-1590.

Izuagie, A.A., Gitari, W.M. and Gumbo, J.R., 2016. Defluoridation of groundwater using diatomaceous earth: optimization of adsorption conditions, kinetics and leached metals risk assessment. *Desalination and Water Treatment*, *57(36)*, pp.16745-16757.

Johari, A., Alkali, H., Hashim, H., Ahmed, S.I. and Mat, R., 2014. Municipal solid waste management and potential revenue from recycling in Malaysia. *Modern Applied Science*, *8(4)*, p.37.

Mogala M 2014. A profile of the South African Macadamia nuts market value chain 2014. Department of Agriculture, Forestry and Fisheries South Africa, Pretoria

Moran, D.D., Wackernagel, M., Kitzes, J.A., Goldfinger, S.H. and Boutaud, A., 2008. Measuring sustainable development nation by nation. *Ecological economics*, *64(3)*, pp.470-474.

Mudzielwana, R., Gitari, M.W., Akinyemi, S.A. and Msagati, T.A., 2018. Performance of Mn $^{2+}$-modified bentonite clay for the removal of fluoride from aqueous solution. *South African Journal of Chemistry*, *71*, pp.15-23.

Ncube, E.J. and Schutte, C.F., 2005. The occurrence of fluoride in South African groundwater: A water quality and health problem. *Water SA*, *31(1).* pp. 35-40.

Newell, A.D., 2010. Mating type distribution of soybean pathogen *Cercospora sojina in Arkansas*. University of Arkansas.

Odiyo, J.O. and Makungo, R., 2012. Fluoride concentrations in groundwater and impact on human health in Siloam Village, Limpopo Province, South Africa. *Water SA*, *38(5)*, pp.731-736.

Pakade, V.E., Ntuli, T.D. and Ofomaja, A.E., 2017. Biosorption of hexavalent chromium from aqueous solutions by Macadamia nutshell powder. *Applied Water Science*, *7(6)*, pp.3015-3030.

Pradhan, R.M. and Biswal, T.K., 2018. Fluoride in groundwater: a case study in Precambrian terranes of Ambaji region, North Gujarat, India. *Proceedings of the International Association of Hydrological Sciences*, *379*, pp.351-356.

Soupir, M.L., Hoover, N.L., Moorman, T.B., Law, J.Y. and Bearson, B.L., 2018. Impact of temperature and hydraulic retention time on pathogen and nutrient removal in woodchip bioreactors. *Ecological Engineering*, *112*, pp.153-157.

Tripathy, S.S., Bersillon, J.L. and Gopal, K., 2006. Removal of fluoride from drinking water by adsorption onto alum-impregnated activated alumina. *Separation and purification technology*, *50*(3), pp.310-317.

Tzanakakis, V.A., Paranychianakis, N.V. and Angelakis, A.N., 2020. Water Supply and Water Scarcity.

World Health Organization, 2017. “Guideline for drinking water, world health organization”. *Geneva*.

Wu, D., Zhao, J., Zhang, L., Wu, Q. and Yang, Y., 2010. Lanthanum adsorption using iron oxide loaded calcium alginate beads. *Hydrometallurgy*, *101*(1-2), pp.76-83.

Yu, X., Tong, S., Ge, M. and Zuo, J., 2013. Removal of fluoride from drinking water by cellulose@ hydroxyapatite nanocomposites. *Carbohydrate polymers*, *92*(1), pp.269-275.

Chapter 2: Literature Review

2.1 Introduction

This chapter present the review of literature related to fluoride and pathogens in groundwater, their occurrence and factors influencing their concentration in water, their health effects, and their health standards and the methods used to remedy them. Lastly, it will review literature surrounding their removal from groundwater.

2.2 Fluoride

Fluoride (F^-) is a chemical which occurs naturally on the earth crust. It is derived from the element fluorine which is the most electronegative of all chemical's elements (Tong *et al.,* 2020). Fluoride exists in the environment through the combination of other elements as fluoride compound and is also found naturally in water, foods, soil, and several minerals such as fluorite and fluorapatite (Kabir *et al.,* 2020; Banerjee *et al,* 2015). Fluoride-bearing minerals such as fluorite, apatite, cryolite, sellaite, amphiboles, topaz, and mica are found in numerous rocks and sediments (Mukherjee and Singh, 2020). The Weathering of this fluoride-bearing minerals are considered to be the first major natural source of inorganic fluorides in the groundwater, whereas the second major natural source is the volcanic eruption, and the third major natural source are marine aerosols (Makoba, 2020 and Kadam *et al.,* 2020). Anthropogenic activities such as excess application of phosphate fertilizers in the agriculture field, coal combustion, aluminum smelting, cement manufacture is also contributing fluoride in the environment (Weldeslassie *et al*., 2018)

Contamination of water by fluoride is directly affected by the adsorption and leaching process (Patel *et al*., 2019). The fluoride adsorption capacity decreases from humid areas to arid areas and from acidic soils to alkaline soils. In arid and semiarid alkaline soil regions, leaching process is higher. Therefore, fluoride could enrich the fluoride concentration in the shallow groundwater, which results in the endemic fluorosis (Narsimha and Rajitha, 2018). Fluoride leaching rate also depends on weathering process and the presence of organic acids in soil. It was found that fluoride leaching rate is higher from highly weathered biotite, compared to fresh biotite (Patel *et al*., 2019). Formation of organic complexes and ionic exchange between biotite and organic acids might lead to the release of fluoride into the pore water which infiltrates through the soil and shallow groundwater could achieve high concentrations fluoride (Singh *et al.*, 2018). Soil sorption capacity generally varies with physicochemical parameters such as pH

and salinity of the soil and types of sorbent present in the soil (Yuan *et al.*, 2019 and Chen *et al.*, 2020).

In general, fluoride is soluble in soil and it is less available for plant uptake. Therefore, most of fluorine compounds are absorbed in the clay and oxyhydroxide in the alkaline environment, and only few dissolves in the soil (Hong *et al*., 2016). Parvaiz (2021) suggested that high salinity of soil solution due to effect of evapotranspiration can increase the risk of fluoride leaching in the groundwater.

The mobility of fluoride in soil depends on concentration gradient of fluoride and increase in soil water content. Formation of the fluoro-aluminium complex due to presence of aluminium in soil enhances the fluoride mobility (Apshankarand, 2018). Luo *et al*. (2018) observed that the fluoride contamination due to aluminium production increases the mobility of humus substances. Phosphatic fertilizers widely used in agriculture often contain fluoride as an impurity, which is released and leached down to the soils by irrigation or rainwater (Mukherjee and Singh, 2020). Excessive use of fluoride-containing groundwater for irrigation may increase amount of fluoride in soils due to leaching of such fluoride-contaminated water from the irrigation field surface (Batabyal and Gupta, 2017).

2.3 Factor influencing the concentration of fluoride in water

Fluoride in groundwater depends upon physical and geological factors such as evaporation rate, residence time, aquifer media, rock water interaction, recharge capacity, and anthropogenic activities

2.3.1 Chemical composition of groundwater

In most case high concentration of fluoride in groundwater are associated with a sodium bicarbonate water type and low calcium and magnesium concentration, they usually have high pH that is above 7 (Adimalla, 2019). The presence of excessive sodium bicarbonates ($NaHCO_3$) increases the dissolution rate of fluoride from fluorite (CaF_2) mineral due to water mineral interaction in groundwater as is shown in Eq. (2.1). High concentration of bicarbonate ions (HCO_3^-) and Na^+ at a higher pH value could be the important reasons for the release of fluoride into groundwater and responsible for fluoride mobilization from fluorite mineral (Eq. 2.1 and 2.2) (Haji *et al*., 2018; and Kumar *et al*., 2017).

$$CaF_2^- + NaHCO_3 = CaCO_3 + 2Na^+ + H_2O + CO_2 \qquad (2.1)$$

$$CaF_2 + 2HCO_3^- = CaCO_3 + 2F^- + H_2O + CO_2 \qquad (2.2)$$

2.3.2 Geology

During weathering of rocks caused by circulations water rocks that results in formation of soil, fluorine can leach out and dissolved in groundwater and thermal gases (Mulago *et al*., 2017). The content of fluoride in groundwater varies greatly depending on the geological settings and type of rocks. The most common fluorine bearing minerals are fluorite, apatite, and micas. Therefore, fluoride problems tend to occur in places where these minerals are most abundant in the host rocks (Mukherjee and Singh, 2018).

2.3.3 Climate

Arid regions are prone to high fluoride concentration in groundwater, due to the flow of groundwater (groundwater flow is slow in arid regions and the reaction times with rocks is therefore long). The content of fluoride in water may increase during evaporation if solution remains equilibrium with calcite and alkalinity is greater than the hardness (Mukherjee and Singh, 2018; Marghade *et al.*, 2020).

2.3.4 Residence time

The concentration of fluoride in groundwater depends on reaction time with the aquifer minerals. Groundwater's that have high concentration of fluoride have long residence time in the aquifer. Such groundwater is associated with deep aquifer and slow groundwater movement (Marghade *et al.*, 2020; Pradhan and Biswal, 2018).

2.4 South African provinces contaminated by fluoride

Figure 2.1 present the distribution of fluoride in South Africa. From the map it is clear that high fluoride ion concentration is prevalent mostly in Limpopo, Northern Cape, North West and Kwa-Zulu-Natal provinces where large populations still live-in rural areas with limited treated water supplies (WRC, 2013). A percentage morbidity of dental fluorosis as high as 97% was recorded in the North-West Province by Ncube and Schutte (2005).

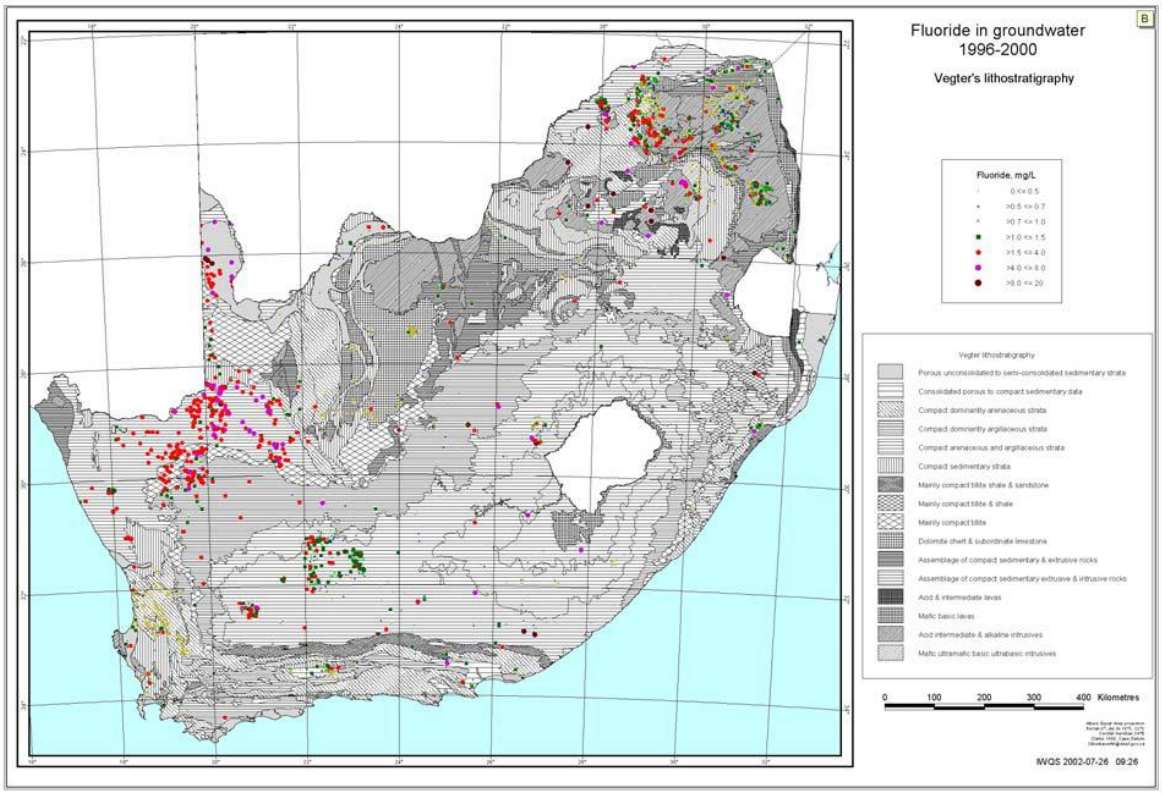

Figure 2.1: Fluoride in groundwater from 1996-2000 by Ncube and Schutte (2005).

2.5 Health impacts caused by drinking water contaminated with fluoride

Fluoride has beneficial effects on teeth at low concentrations in drinking water (0.4 – 1.0 mg/L), especially for young children in that it promotes calcification of dental enamel and protects teeth against tooth decay (WHO, 2018). Excessive levels of F^- on the other hand can cause many problems ranging from mild dental fluorosis to crippling skeletal fluorosis as the level and period of exposure to F^- increases (Kabir *et al*., 2020). The World Health Organisation (WHO, 2018) has recommended a guideline value of 1.5 mg/L as the concentration above which dental fluorosis is likely. Fluorosis is a public health problem in certain areas of South Africa which requires a great attention at various levels (WHO 2018). Table 2.1 shows the effects of prolonged of drinking water that contain fluoride.

Table 2.1: Effects of prolonged of drinking water in human health, related to fluoride (WHO, 2018)

Fluoride concentration (mg/L)	Health outcomes
<0.5	Dental carries
0.5-1.5	Optimum dental health
1.5-4.0	Fluorosis
4.0-10	Dental and skeletal fluorosis
>10	Crippling fluorosis

2.5.1 Dental fluorosis

Dental fluorosis refers to a change in the appearance of tooth enamel that are caused by long term ingestion of fluoride during the formation of teeth (Whelton *et al.*, 2019). Dental fluorosis is effective in children less than 8 years of age during their teeth development stages (WHO, 2017). The changes become apparent once the teeth erupt. Changes noted in the teeth in dental fluorosis include the, the appearance of whitish spots or chalk-like lines, brownish stains on teeth, in severe cases, pitting of teeth. The extent of the damage depends on the amount of fluoride consumed and the duration period. It should be taken into consideration, that fluoride deficiency also affects teeth, making them more prone to tooth decay (WHO, 2017).

2.5.2 Skeletal fluorosis

Symptoms of skeletal fluorosis appear later than dental fluorosis. Structural changes take place in the bones, which make them weak. Ligaments may also calcify and harden, and bony spurs may appear in skeletal fluorosis (Walser *et al.*, 2020). Symptoms of skeletal fluorosis include Pain in small joints, Pain and stiffness in the back, deformity of the hips, knees and other joints. Knock knees may be present and deformity of the spine (Bhowmik *et al.*, 2020; Walser *et al.*, 2020). Spinal deformity can cause compression on the spinal cord and the exiting nerves, resulting in pain, muscle weakness, tingling and numbness and other symptoms along the distribution of the nerves (WHO, 2017).

Other symptoms like digestive tract symptoms like pain in abdomen, diarrhoea, constipation, neurological symptoms like tingling and numbness, increased tendency to urinate and increased thirst, and muscle pain, stiffness and weakness may also be present. These symptoms

may appear before the onset of skeletal fluorosis and therefore may be useful in early diagnosis (Nelson *et al*., 2019).

2.6 Fluoride Removal

Different defluoridation techniques have been developed to remove fluoride in drinking water. Such techniques include precipitation, reverse osmosis, electrodialysis, ion exchange, nanofiltration, and adsorption (Dhillon *et al*., 2015).

2.6.1 Precipitation method

Alum and lime are the most utilised coagulants for defluoridation by the precipitation method (Waghmare and Arfin, 2015). The Nalgonda technique is the best example of a coagulation/precipitation method. It involves the addition of aluminium salts, lime, and bleaching powder to fluoride contaminated water followed by rapid mixing, flocculation, sedimentation, filtration, and disinfection (Dubey *et al*., 2018). After the addition of lime and alum, the disinfection process takes place in the following steps, Insoluble aluminium hydroxide flocs form, sediment sinks to the bottom, and bleaching powder and fluoride co-precipitate (Dubey *et al*., 2018). Although this method is effective for defluoridation, it may not be able to lower the fluoride concentration to a desirable limit (1.5 mg/L) (Barathi *et al*., 2019). The precipitation technique is rarely used because of its high chemical costs, formation of sludge with a high content of toxic aluminium fluoride complex, unpleasant water taste, and high residual aluminium concentration.

2.6.2 Adsorption method

Adsorption method is the second effective method where activated alumina (Al_2O_3) or activated charcoal is used as a strong absorbent. This technique is suitable for both community water supply and household use (Patel *et al*., 2020). The filter material needs to be backwashed when the adsorbent becomes saturated with fluoride ions. Weak acid or alkali solution can be used as a cleaning and regenerating agent (Kurunanithi *et al*, 2019). The effluent from backwashing is enriching with fluoride and disposal should be done carefully to avoid any further fluoride contamination. Adsorption removes a soluble substance from the water. Active carbon is the main tool and it comes in two varieties which is powdered and granulated form of active Carbon (Patel *et al*., 2020).

2.6.2.1 Adsorption using clay

Clays are potentially good adsorbent of fluoride ions since they contain crystalline minerals such as kaolinite, smectite and amorphous minerals such as allophane and other metal oxides

and hydroxides which could adsorb anion (Wang and Wang 2019). The structure of the clay plays a critical role in determining the key charges on the surface of the clay and the type of exchange that will occur with ions in the solution (Biswas *et al*., 2016). The more the positive the clay surface is, the better the sorption will be for negative charged ions.

Many studies have reported on the fluoride adsorption of capacities of clay soils and their potential use as adsorbent. The results showed that, fluoride adsorption capacity vary depending on the soil and clay minerals in particular aluminium hydroxide. It was also found that fluoride adsorption by clay soils is followed by the release of OH^- ions (Mukherjee, and Singh, 2020; Biswas *et al*., 2016). Mudzielwana *et al*., 2017 use Bentonite clay for fluoride removal and the percentage F- removal above 91% was achieved at all evaluated pH levels (2–12), 5 mg/L F- initial concentration, optimum dosage of 1.5 mg/L, and contact time of 30 min at shaking speed of 250 rpm.

2.6.2.2 Powdered Carbon

Some beaten form of carbon particles is employed for making powdered activated carbon. They are beaten to powdered form to allow an easy passage through a fine mesh sieve. Their extremely reduced size induces a large internal surface with small diffusion distance. It is majorly used as gravity filters and mix basins (Mukherjee, and Singh, 2020). Choong *et al*., 2020 use palm shell waste based powdered activated carbon for fluoride removal and found out that the maximum fluoride adsorption capacity 116 mg/g.

2.6.2.3 Granulated Carbon

The large size of granulated activated carbon induces them to form smaller external surface because of their larger size in comparison with powdered active carbon (Asimakopoulos *et al*,.2020). Rashid and Bezbaruah, 2020 use citric acid modified granular activated carbon and the maximum adsorption capacity of fluoride removal found to be 1.65 mg/g.

2.6.3 Membrane process

Membrane filtration is a way of separating components that are suspended or dissolve in liquid (can be efficient and economical). The physical barrier that allows certain compound to pass through, depending on the physical and chemical properties is called membrane. Membrane have porous layers that support it along with thin dense layer that form the actual membrane. Membrane separation processes used for water treatment and purification include reverse osmosis (RO), nanofiltration (NF), ultrafiltration (UF), microfiltration (MF) and electro dialysis (ED) (Sarfraz, 2021). All the types of membrane filtration are based on membrane pore sizes.

Membrane performance is based on many factors, including membrane selectivity and flux, good mechanical, chemical and thermal stability of the membrane material, minimal fouling during operation and good compatibility with the feed solution. For a membrane process to be effective, the membrane must combine high permeability with high selectivity. For liquid separations, the membrane should preferably have both hydrophilic and hydrophobic characteristics (Sarfraz, 2021).

2.6.4 Ion exchange process

Ion exchange is a process in which water flows through a bed of ion exchange material to remove the undesirable ions. Ion exchange are of two types which are the cation exchangers, which exchange positively charged ions (cations), and anion exchangers, which exchange negatively charged ions (anions). The ion exchange process has great potential (up to 95%) for removing fluoride from aqueous solutions. The resins are expensive and make the treatment economically unviable. However, resins can be regenerated easily. Unfortunately, the regeneration process produces large amounts of fluoride-loaded waste and disposal needs for such waste are a disadvantage of this process (Jadhav *et al*., 2015).

Table 2.2. The advantages and disadvantages of technology used for defluoridation (Renuka and Pushpanjali, 2013; Jadhav *et al.*, 2015; Sarfraz, 2021; Mukherjee, and Singh, 2020; Waghmare and Arfin, 2015 and Patel *et al*., 2020).

Method of fluoride removal	**Advantages**	**Disadvantages**
Adsorption method	• Low energy and maintenance costs, • The simplicity and the reliability	• The effectiveness of the adsorption is determined by substance to be removed. • Substances with a high molecular weight and • low water solubility is better adsorbed. • low adsorption capacity, • poor integrity and needs pre-treatment. • Adsorption is possible only at specific pH range. • Needing pre- and post- pH adjustment of water
Membrane process	• Flexible; can be used in the separation, purification of a huge variety of materials across a wide range industry. • The processes can function effectively at low temperatures. • Energy requirements are low. Processes are relatively simple to scale up. • Membranes can be manufactured in a uniform and highly precise manner	• Expensive cleaning and • regeneration schemes may be necessary. • The flow rates can damage shear sensitive materials. • Equipment cost can be high.
Ion exchange process	• It is a very effective and efficient method of water softening. • No perforation of substances into the soft water. • Most of the heavy metals can be reused. • The wastewater that is produced by ion exchange machines is also used for water treatment.	• The level of acidity in the water can be increased. • The machines used to soften the water are known as Iron exchangers. • Their greatest impediment is the fact that they must be cleaned • because of their high level of saturation. • The iron exchangers also require high operational cost

2.7 Pathogens

Pathogens refers to micro-organisms such as bacteria, fungi, and viruses, found commonly in sewage, hospital waste, run-off water from farms, and in water used for swimming, which may cause bacteria such as *E. coli*, staphylococcus aureus, etc. Most pathogens are parasites (live off the host) and the diseases they cause are an indirect result of their obtaining food from, or shelter in, the host. Waterborne disease is caused by the consumption of contaminated water and it can affect many people in a short time (Park *et al*., 2020).

The centre for disease control and prevention (CDCP) reported that about 2.5 billion of people in developing countries lack access to improved water that is safe and hygienic water. Waterborne diseases were reported globally that it causes more than 2.2 million death per year and many illnesses such as diarrhoea, fever, systemic disorders and gastrointestinal (Park *et al*., 2020). Researchers are trying to produce eco-friendly materials towards the development of novel improved antibacterial nanomaterials against multidrug resistant human pathogens like *Escherichia coli*. *Escherichia coli* is one of the deadly contaminants in drinking water (Ayinde *et al*., 2018). Contamination by pathogens in drinking water from groundwater can be explained by combined several factors including the lack of efficient water treatment system, sewage contamination, power infrastructure of water pipelines and microbial biofilms (Lappan *et al*., 2020).

2.8 Pathogens health effect

Sources of drinking water are subject to contamination and require appropriate treatment to remove disease-causing contaminants. The presence of contaminants in water can lead to adverse health effects, including gastrointestinal illness, reproductive problems, and neurological disorders (Varghese *et al*., 2020). Infants, young children, pregnant women, the elderly, and people whose immune systems are compromised because of AIDS, chemotherapy, or transplant medications, may be especially susceptible to illness from some contaminants (Caballero *et al*., 2020). For example, most types of E. coli are harmless and even help keep your digestive tract healthy. But some strains can cause diarrhoea if you eat contaminated food or drink fouled water (Lai *et al*., 2016; Ting *et al*., 2015). Staphylococcus Aureus is one of the most dangerous bacteria (World Health Organization, 2018). Staphylococcus Aureus has the potential to cause a wide range of diseases that are mild and threatening based on the individual. The bacteria even can cause serious medical conditions such as pneumonia and sepsis (Jaradat *et al.*, 2020).

Antibiotics are the most used form of treatment used to treat patients affected with pathogens (Ventola, 2015). The efficiency of this type of medication is high. Most infections can be treated with antibiotics. In some extreme cases where the bacteria have already entered the bloodstream and has started to infect the internal organs, advanced treatment methods such as intravenous antibiotic injections are given (Maciejewska *et al*., 2018).

2.9 Removal of pathogens

Disinfection reduces pathogenic microorganisms in the water to levels designated safe by public health standards. This prevents the transmission of disease. An effective disinfection system kills or neutralizes all pathogens in the water. It is automatic, simply maintained, safe, and inexpensive (Shinde and Apte, 2021). An ideal system treats all the water and provides residual disinfection. Chemicals should be easily stored and not make the water unpalatable. State and federal governments require public water supplies to be biologically safe. Ways of disinfection, chlorination of drinking water, boiling of water, ceramic filters and ultraviolet (UV) (Ayinde *et al*., 2018; Shinde and Apte, 2021).

2.9.1 Methods that are being used for pathogen removal at household level

The method used for disinfecting pathogen for household water use include chlorination, ceramic filters and boiling of water at 100 ^{o}C.

2.9.1.1 Chlorine as a disinfectant

Chlorine is one of the most widely used disinfectants. It is very applicable and very effective for the deactivation of pathogenic microorganisms. Chlorine can be easily applied, measures and controlled (Mazhar *et al*., 2020). It is persistent and relatively cheap. Chlorine has been used for applications, such as the deactivation of pathogens in drinking water, applied in swimming pools and also applied in wastewater, for the disinfection of household areas and for textile bleaching, for more than two hundred years (Jena *et al*., 2020).

Chlorine kills pathogens such as bacteria and viruses by breaking the chemical bonds in their molecules (Mazhar *et al*., 2020). Disinfectants that are used for this purpose consist of chlorine compounds which can exchange atoms with other compounds, such as enzymes in bacteria and other cells. When enzymes meet chlorine, one or more of the hydrogen atoms in the molecule are replaced by chlorine. This causes the entire molecule to change shape or fall apart. When enzymes do not function properly, a cell or bacterium will die (Tsvetanova, 2020).

2.9.1.2 Boiling of water for disinfection of pathogens

Boiling is a very simple method of water disinfection. Heating water to a high temperature, 100°C, kills most of the pathogenic organisms, particularly viruses and bacteria causing waterborne diseases (Espinosa *et al*., 2020). In order for the boiling to be most effective, the water must boil for at least 20 minutes. Since boiling requires a source of heat, rudimentary or non-conventional methods of heat generation may be needed in areas where electricity or fossil fuels are not available (Espinosa *et al*., 2020).

2.9.1.3 Ceramic filter

Ceramic water filters are an inexpensive and effective type of water filter, that rely on the small pore size of ceramic material to filter dirt, debris, and bacteria out of water (Goswami and Pugazhenthi, 2020). This makes them ideal for use in developing countries, and portable ceramic filters are commonly used in backpacking (Goswami and Pugazhenthi, 2020). Chaukura *et al*., 2020 develop low-cost ceramic filter for the removal of methyl orange, hexavalent chromium, and *Escherichia coli* from water. The results suggest that AgNPs played an important role in the removal of *E. coli*. The AgNPs had excellent antibacterial properties against the *E. coli*, showing 100% removal from spiked feed water samples.

2.10 Diatomaceous earth

According to Verleyen *et al*. (2021) Diatomaceous earth is defined as fossilized remains of tiny, aquatic organisms called diatoms. Their skeletons are made of a natural substance called silica. Over a long period of time, diatoms accumulated in the sediment of rivers, streams, lakes, and oceans. Today, silica deposits are mined from these areas (Verleyen *et al*., 2021). Izuagie *et al.* (2016) reported that modified diatomaceous earth has a has high fluoride removal potential.

2.11 Physical and chemical properties of diatomaceous earth

Diatomaceous earth is white, commonly buff to grey in place, and rarely black. Features of the diatomaceous earth is the high content of biogenic amorphous silica, with form of diatom frustules (Verleyen *et al*., 2021). The frustules essentially are chemically inert in most liquids and gases. Moreover, the skeletal of diatomaceous earth, microscopically viewed, have quite complex structure with numerous fine microscopic pores, cavities, and channels and therefore, well proprietor a large specific surface area and high adsorption capacity. Combinations of physical and chemical properties of high-grade diatomaceous earth make it suitable for many specialized applications, especially for filtration (Semiao *et al*., 2020). Semiao *et al*., (2020) classified the chemical composition into three categories: Major, secondary and minor

constituents. Silica (SiO_2) constitutes the major component of diatomaceous earth sediments; however, the secondary constituents are mainly alumina (Al_2O_3) and iron (FeO_3). The minor constituents are (CaO), (MgO), Na_2O) and (SO_3).

2.11.1 Application of diatomaceous earth in water treatment

Izuagie *et al.* (2016) reported that raw diatomaceous earth has a low fluoride removal potential. The use of raw diatomaceous earth for removal of fluoride from drinking water and its limited because it exhibits its fluoride removal characteristics at a very low pH. This limitation lead to surface modification of diatomaceous earth, in such a way that application of the modified diatomaceous earth in drinking water does not require pH adjustment. Diatomaceous earth has pores volumes that can be coated with metal hydroxides/oxides having high affinity for fluoride through precipitation from their salts (Yaun *et al*., 2020). It was also reported by Gitari *et al*., 2017 that trimetal Mg/Ce/Mn oxide-modified diatomaceous earth yelled at about 90% fluoride removal in groundwater. A study by Wambu *et al*., 2011 shows that diatomaceous mineral from Kariandusi mining site in Kenya could greatly be enhanced for F adsorption by simple pre-treatment in dilute HCl. Because of high affinity of the acid pre-treated mineral for F ions, the pH and the presence of other competing ions could not affect the F adsorption onto its surface.

2.12 Macadamia nutshell powder

Macadamia nutshell are bio waste, and they are abundant. They have not been used in defluoridation and pathogen removal. Their main uses are activated carbon, used to make carbon filters, fertilisers (Pakade *et al*., 2017). Most of the study conducted using macadamia nutshell was base of activated carbon (Cobb *et al*., 2012). The shell of macadamia nut is hard and brittle. Macadamia nut shells are composed of Carbon (57.5%), Hydrogen (5.95%), Nitrogen (0.33%), Oxygen (36, 2%) and sulphur (0.33%) (Pakade *et al*., 2017). The main components of the shell are lignin (47%), cellulose (25%), hemicellulose (11%) and ash (0-2%). The shell has bulk density of 680 kg/m^3, and 10% moisture content (Wechsler *et al*., 2011). Very limited study has been carried out on the use of macadamia shell in composite. The utilisation of macadamia shells will promote waste management at little cost, reduce pollution by this waste and increase the economic base of the famers when such waste is sold thereby encouraging more production. MNS have been applied in water treatment for removal of chromium in wastewater and show better removal (Pakade at al., 2017).

2.13 Fluoride and pathogen removal from groundwater

Exposure to fluoride concentration greater than 1.5 mg/L causes dental fluorosis and skeletal fluorosis as the level and period of exposure increases (Fawell *et al*., 2006, WHO, 2017). Generally, most of the study have been conducted for fluoride and pathogen removal but they have their own limitation such, the operation at specific pH. Most of the study were done using batch experiment which is not applicable for household use most especially in rural areas. Gitari *et al*. (2013) evaluated the removal of fluoride from borehole water using raw and Fe^{3+} modified bentonite clay and observed that both raw and modified bentonite clays could remove fluoride from borehole water, however, at different degrees of efficiency. Fe^{3+} modified bentonite clay was found to be more effective than the raw bentonite clay. The degree of fluoride removal was highly dependent on the pH of the solution. Mudzielwana *et al*., 2017 use Bentonite clay for fluoride removal and the percentage F- removal above 91% was achieved at all evaluated pH levels (2–12), 5 mg/L F- initial concentration, optimum dosage of 1.5 mg/L, and contact time of 30 min at shaking speed of 250 rpm.

The presence of pathogens in water can lead to adverse health effects, including diarrhoea, cholera, gastrointestinal illness, reproductive problems, and neurological disorders (Newell *et al*., 2010). Groundwater contamination by pathogenic microorganisms has not received as much attention as surface water pollution because it is generally assumed that groundwater has a good microbiologic quality and is free of pathogenic microorganisms (Orner *et al*., 2021). The lack of documentation of waterborne viral disease outbreaks may be ascribed to limitations in methodology for the detection of viruses in water and relative insensitivity of epidemiologic techniques to detect low level transmission of viral diseases through water (Orner *et al*., 2021). The method used to disinfect pathogens from ground include chlorination of drinking water, boiling of water, ceramic filters and ultraviolet (UV) (Dhillon *et al*., 2015; Ayinde *et al*., 2018). Although this method has been used for pathogen removal some such as UV is not affordable at rural area.

The present study aims to fabricate macadamia nutshell powder-Al/Fe modified DE sodium alginate composite beads for removal of fluoride, pathogen from groundwater. A composite beads adsorbent will be prepared by mixing MNS and Al/Fe oxide modified DE with the use of sodium alginate for formation of beads. Furthermore, the composite beads will be tested for fluoride and pathogen removal from groundwater.

2.14 Conclusion

Base on the discussion, Fluoride is an important mineral and is abundant on earth. Concentration of Fluoride at <1.5 mg/L is beneficial but at > 1.5 mg/L causes dental and skeletal fluorosis. Therefore, there is no cure for this disease, but prevention via defluoridation is necessary. In other hand, the presence of pathogens in water can lead to adverse health effects, including gastrointestinal illness, reproductive problems, and neurological disorders. Different technique has been developed to remove fluoride in water and also different disinfection technique have been developed to make it accessible to rural communities affected.

2.15 Reference

Adimalla, N., 2019. Groundwater quality for drinking and irrigation purposes and potential health risks assessment: a case study from semi-arid region of South India. *Exposure and health*, *11*(2), pp.109-123.

Apshankar, K.R. and Goel, S., 2018. Review and analysis of defluoridation of drinking water by electrocoagulation. *Journal of Water Supply: Research and Technology—AQUA*, *67(4)*, pp.297-316.

Asimakopoulos, G., Baikousi, M., Salmas, C., Bourlinos, A.B., Zboril, R. and Karakassides, M.A., 2020. Advanced Cr (VI) sorption properties of activated carbon produced via pyrolysis of the "*Posidonia oceanica*" seagrass. *Journal of Hazardous Materials*, p.124274.

Ayinde, W.B., Gitari, W.M., Munkombwe, M. and Amidou, S., 2018. Green synthesis of Ag/MgO nanoparticle modified nanohydroxyapatite and its potential for defluoridation and pathogen removal in groundwater. *Physics and Chemistry of the Earth, Parts A/B/C*, *107*, pp.25-37.

Banerjee, S., Adak, K., Adak, M.M., Ghosh, S and Chatterjee, A., 2015. Effect of Some Antinutritional Factors on the Bioavailability of Minerals along with the Study of Chemical Constituents & Antioxidant Property in *Typhonium trilobatum* & *Spinacia oleracea*. *Chemical Science Review and Letters*, *4 (14)*, pp.429-439.

Barathi, M., Kumar, A.S.K. and Rajesh, N., 2019. Impact of fluoride in potable water. An outlook on the existing Defluoridation strategies and the road ahead. *Coordination Chemistry Reviews*, *387*, pp.121-128.

Batabyal, A.K. and Gupta, S., 2017. Fluoride-contaminated groundwater of Birbhum district, West Bengal, India: interpretation of drinking and irrigation suitability and major geochemical processes using principal component analysis. *Environmental monitoring and assessment*, *189(8)*, pp.1-24.

Bhowmik, A.D., Shaw, P., Mondal, P., Chakraborty, A., Sudarshan, M. and Chattopadhyay, A., 2020. Calcium and Vitamin D Supplementation Effectively Alleviates Dental and Skeletal Fluorosis and Retain Elemental Homeostasis in Mice. *Biological Trace Element Research*, pp.1-10.

Biswas, G., Dutta, M., Dutta, S. and Adhikari, K., 2016. A comparative study of removal of fluoride from contaminated water using shale collected from different coal mines in India. *Environmental Science and Pollution Research*, *23*(10), pp.9418-9431.

Caballero, J.R.I., Ata, J.P., Leddy, K.A., Glenn, T.C., Kieran, T.J., Klopfenstein, N.B., Kim, M.S. and Stewart, J.E., 2020. Genome comparison and transcriptome analysis of the invasive brown root rot pathogen, Phellinus noxius, from different geographic regions reveals potential enzymes associated with degradation of different wood substrates. *Fungal Biology*, *124*(2), pp.144-154.

Chaukura, N., Katengeza, G., Gwenzi, W., Mbiriri, C.I., Nkambule, T.T., Moyo, M. and Kuvarega, A.T., 2020. Development and evaluation of a low-cost ceramic filter for the removal of methyl orange, hexavalent chromium, and Escherichia coli from water. *Materials Chemistry and Physics*, *249*, p.122965.

Choong, C.E., Wong, K.T., Jang, S.B., Nah, I.W., Choi, J., Ibrahim, S., Yoon, Y. and Jang, M., 2020. Fluoride removal by palm shell waste based powdered activated carbon vs. functionalized carbon with magnesium silicate: Implications for their application in water treatment. *Chemosphere*, *239*, pp.124765.

Dhillon, J., Liang, Y., Kamat, A.M., Siefker-Radtke, A., Dinney, C.P., Czerniak, B. and Guo, C.C., 2015. Urachal carcinoma: a pathologic and clinical study of 46 cases. *Human pathology*, *46*(12), pp.1808-1814.

Dubey, S., Agrawal, M. and Gupta, A.B., 2018. Advances in coagulation technique for treatment of fluoride-contaminated water: a critical review. *Reviews in Chemical Engineering*, *35*(1), pp.109-137.

Espinosa, M.F., Sancho, A.N., Mendoza, L.M., Mota, C.R. and Verbyla, M.E., 2020. Systematic review and meta-analysis of time-temperature pathogen inactivation. *International Journal of Hygiene and Environmental Health*, *230*, p.113595.

Fawell, J.K., 2006. Fluoride in drinking-water. World Health Organization.

Gitari, W.M., Izuagie, A.A. and Gumbo, J.R., 2017. Synthesis, characterization and batch assessment of groundwater fluoride removal capacity of trimetal Mg/Ce/Mn oxide-modified diatomaceous earth. *Arabian Journal of Chemistry*, *13*(1), pp.1-16.

Goswami, K.P. and Pugazhenthi, G., 2020. Credibility of polymeric and ceramic membrane filtration in the removal of bacteria and virus from water: A review. *Journal of Environmental management*, *268*, p.110583.

Haji, M., Wang, D., Li, L., Qin, D. and Guo, Y., 2018. Geochemical evolution of fluoride and implication for F− enrichment in groundwater: Example from the Bilate River Basin of Southern Main Ethiopian Rift. *Water*, *10*(12), p.1799.

Hong, S.M., Choi, S.W., Kim, S.H. and Lee, K.B., 2016. Porous carbon based on polyvinylidene fluoride: Enhancement of CO_2 adsorption by physical activation. *Carbon*, *99*, pp.354-360.

Izuagie, A.A., Gitari, W.M. and Gumbo, J.R., 2016. Defluoridation of groundwater using diatomaceous earth: optimization of adsorption conditions, kinetics and leached metals risk assessment. *Desalination and Water Treatment*, *57(36)*, pp.16745-16757.

Jadhav, A.S., Amrani, M.A., Singh, S.K., Al-Fatesh, A.S., Bansiwal, A., Srikanth, V.V. and Labhasetwar, N.K., 2020. γ-FeOOH and γ-FeOOH decorated multi-layer graphene: Potential materials for selenium (VI) removal from water. *Journal of Water Process Engineering*, *37*, p.101396.

Jaradat, Z.W., Ababneh, Q.O., Sha'aban, S.T., Alkofahi, A.A., Assaleh, D. and Al Shara, A., 2020. Methicillin Resistant Staphylococcus aureus and public fomites: a review. *Pathogens and Global Health*, pp.1-25.

Jena, S.K., Sahu, J., Padhy, G., Mohanty, S. and Dash, A., 2020. Chlorination roasting-coupled water leaching process for potash recovery from waste mica scrap using dry marble sludge powder and sodium chloride. *International Journal of Minerals, Metallurgy and Materials*, *27*(9), pp.1203-1215.

Kabir, H., Gupta, A.K. and Tripathy, S., 2020. Fluoride and human health: Systematic appraisal of sources, exposures, metabolism, and toxicity. *Critical Reviews in Environmental Science and Technology*, *50*(11), pp.1116-1193.

Kadam, A., Wagh, V., Umrikar, B. and Sankhua, R., 2020. An implication of boron and fluoride contamination and its exposure risk in groundwater resources in semi-arid region, Western India. *Environment, Development and Sustainability*, *22*(7), pp.7033-7056.

Karunanithi, M., Agarwal, R. and Qanungo, K., 2019. A review of fluoride removal from groundwater. *Periodica Polytechnica Chemical Engineering*, *63*(3), pp.425-437.

Lai, T.C., Chiang, C.Y., Wu, C.F., Yang, S.L., Liu, D.P., Chan, C.C. and Lin, H.H., 2016. Ambient air pollution and risk of tuberculosis: a cohort study. *Occupational and Environmental Medicine*, *73*(1), pp.56-61.

Lappan, R., Jamieson, S.E. and Peacock, C.S., 2020. Reviewing the pathogenic potential of the otitis-associated bacteria *Alloiococcus otitidis* and *Turicella otitidis*. Frontiers in Cellular and Infection Microbiology.

Maciejewska, B., Olszak, T. and Drulis-Kawa, Z., 2018. Applications of bacteriophages versus phage enzymes to combat and cure bacterial infections: an ambitious and also a realistic application. *Applied Microbiology and Biotechnology*, *102*(6), pp.2563-2581.

Makoba, E.E., 2020. Geological and hydro-geochemical assessment of fluorine around mount Meru, northern Tanzania.

Malago, J., Makoba, E. and Muzuka, A.N., 2017. Fluoride levels in surface and groundwater in Africa: a review. *American Journal of Water Science and Engineering*, *3*(1), pp.1-17.

Marghade, D., Malpe, D.B., Subba Rao, N. and Sunitha, B., 2020. Geochemical assessment of fluoride enriched groundwater and health implications from a part of Yavtmal District, India. *Human and Ecological Risk Assessment: An International Journal*, *26*(3), pp.673-694.

Mazhar, M.A., Khan, N.A., Ahmed, S., Khan, A.H., Hussain, A., Changani, F., Yousefi, M., Ahmadi, S. and Vambol, V., 2020. Chlorination disinfection by-products in Municipal drinking water. A review. *Journal of Cleaner Production*, p.123159.

Mudzielwana, R., Gitari, W.M., Akinyemi, S.A. and Msagati, T.A., 2017. Synthesis, characterization, and potential application of Mn 2^{+} intercalated bentonite in fluoride removal: adsorption modelling and mechanism evaluation. *Applied Water Science*, *7*(8), pp.4549-4561.

Mukherjee, I. and Singh, U.K., 2018. Groundwater fluoride contamination, probable release, and containment mechanisms: a review on Indian context. *Environmental Geochemistry and Health*, *40*(6), pp.2259-2301.

Mukherjee, I. and Singh, U.K., 2020. Fluoride abundance and their release mechanisms in groundwater along with associated human health risks in a geologically heterogeneous semi-arid region of east India. *Microchemical Journal*, *152*, p.104304.

Narsimha, A. and Rajitha, S., 2018. Spatial distribution and seasonal variation in fluoride enrichment in groundwater and its associated human health risk assessment in Telangana State, South India. *Human and Ecological Risk Assessment: An International Journal*, *24*(8), pp.2119-2132.

Ncube, E.J. and Schutte, C.F., 2005. The occurrence of fluoride in South African groundwater: A water quality and health problem. *Water SA*, *31*(1). pp. 35-40.

Nelson, E.A., Halling, C.L. and Buikstra, J.E., 2019. Evidence of Skeletal Fluorosis at the Ray Site, Illinois, USA: a pathological assessment and discussion of environmental factors. *International Journal of Paleopathology*, *26*, pp.48-60.

Orner, K.D., Symonds, E.M., Madrigal-Solís, H., Orozco-Montoya, R.A., Fonseca-Sánchez, A., Verbyla, M.E. and Cairns, M.R., 2021. Holistically Managing Pathogens and Nutrients in Urbanizing Tropical Towns: Can Sanitation Technologies Create Safer Conditions for Beach Recreation? *ACS ES&T Water*, *27(2)*. Pp.371-388.

Pakade, V.E., Ntuli, T.D. and Ofomaja, A.E., 2017. Biosorption of hexavalent chromium from aqueous solutions by Macadamia nutshell powder. *Applied Water Science*, *7*(6), pp.3015-3030.

Park, J., Shin, E., Park, A.K., Kim, S., Jeong, H.J., Kim, J.S., Jin, Y.H., Park, N.J., Chun, J.H., Hwang, K. and Lee, K.J., 2020. Co-infection With Chromosomally Located blaCTX-M-14 and Plasmid-Encoding blaCTX-M-15 in Pathogenic Escherichia coli in the Republic of Korea. *Frontiers in Microbiology*, *11*, pp.2716.

Parvaiz, A., Khattak, J.A., Hussain, I., Masood, N., Javed, T. and Farooqi, A., 2021. Salinity enrichment, sources and its contribution to elevated groundwater arsenic and fluoride levels in Rachna Doab, Punjab Pakistan: Stable isotope (δ2H and δ18O) approach as an evidence. *Environmental Pollution*, *268*, p.115710.

Patel, A.K., Das, N., Goswami, R. and Kumar, M., 2019. Arsenic mobility and potential co-leaching of fluoride from the sediments of three tributaries of the Upper Brahmaputra floodplain, Lakhimpur, Assam, India. *Journal of Geochemical Exploration*, *203*, pp.45-58.

Patel, S.K., Kumar, P., Srinivasan, G. and Singh, D., 2020. Removal of arsenic from water via solar energy harvesting technique with integrated system of activated alumina absorbent bed and double slope solar still. *Rasa. J. Chemi*, *13*(3), pp.1293-1307.

Pradhan, R.M. and Biswal, T.K., 2018. Fluoride in groundwater: a case study in Precambrian terranes of Ambaji region, North Gujarat, India. *Proceedings of the International Association of Hydrological Sciences*, *379*, pp.351-356.

Rashid, U.S. and Bezbaruah, A.N., 2020. Citric acid modified granular activated carbon for enhanced defluoridation. *Chemosphere*, *252*, p.126639.

Semiao, M.A., Haminiuk, C.W.I. and Maciel, G.M., 2020. Residual diatomaceous earth as a potential and cost effective biosorbent of the azo textile dye Reactive Blue 160. *Journal of Environmental Chemical Engineering*, *8(1)*, p.103617.

Shinde, S.R. and Apte, S., 2021. A Systematic review on advancements in drinking water disinfection technologies: A sustainable development perspective. *Journal of Environmental Treatment Techniques*, *9*(2), pp.349-360.

Singh, G., Kumari, B., Sinam, G., Kumar, N. and Mallick, S., 2018. Fluoride distribution and contamination in the water, soil and plants continuum and its remedial technologies, an Indian perspective–a review. *Environmental Pollution*, *239*, pp.95-108.

Ting, A.S.Y. and Jioe, E., 2016. In vitro assessment of antifungal activities of antagonistic fungi towards pathogenic *Ganoderma boninense* under metal stress. *Biological Control*, *96*, pp.57-63.

Tong, Y., Mao, H., Chen, P., Sun, Q., Yan, F. and Xi, F., 2020. Confinement of fluorine anions in nickel-based catalysts for greatly enhancing oxygen evolution activity. *Chemical Communications*, *56*(30), pp.4196-4199.

Tsvetanova, Z., 2020. Quantification of the bacterial community of drinking water-associated biofilms under different flow velocities and changing chlorination regimes. *Applied Water Science*, *10*(1), p.3.

Varghese, P.M., Tsolaki, A.G., Yasmin, H., Shastri, A., Ferluga, J., Vatish, M., Madan, T. and Kishore, U., 2020. Host-pathogen interaction in COVID-19: Pathogenesis, potential therapeutics and vaccination strategies. *Immunobiology*, p.152008.

Ventola, C. L. (2015). The antibiotic resistance crisis: Part 1: Causes and threats. *Pharmacy and Therapeutics*, *40*, pp277– 283.

Verleyen, E., Van de Vijver, B., Tytgat, B., Pinseel, E., Hodgson, D.A., Kopalová, K., Chown, S.L., Van Ranst, E., Imura, S., Kudoh, S. and Van Nieuwenhuyze, W., 2021. Diatoms define a novel freshwater biogeography of the Antarctic. *Ecography*.

Waghmare, S.S. and Arfin, T., 2015. Fluoride removal by clays, geomaterials, minerals, low cost materials and zeolites by adsorption: a review. *International Journal of Science, Engineering and Technology Research*, *4*(11), pp.3663-3676.

Walser, J.W., Gowland, R.L., Desnica, N. and Kristjánsdóttir, S., 2020. Hidden dangers? Investigating the impact of volcanic eruptions and skeletal fluorosis in medieval Iceland. *Archaeological and Anthropological Sciences*, *12*(3), pp.1-23.

Wambu, E.W., Onindo, C.O., Ambusso, W.J. and Muthakia, G.K., 2011. Fluoride adsorption onto acid-treated diatomaceous mineral from Kenya. *Materials Sciences and Applications*, *2*(11), p.1654.

Wang, W. and Wang, A., 2019. Nanoscale clay minerals for functional ecomaterials: fabrication, applications, and future trends. *Handbook of Ecomaterials; Springer: Cham, Germany*, pp.1-82.

Wechsler, A., Ramirez, M., Crosky, A., Zaharia, M., Jones, H., Ballerini, A., Nunez, M. and Sahajwalla, V., 2011. Physcial properties of furniture panels from macadamia shells. In *Proceedings of the 18th International Conferences on Composite Materials*.

Weldeslassie T., Naz H., Singh B. and Oves M., 2018. Chemical contaminants for soil, air and aquatic ecosystem. In Modern Age Environmental Problems and their Remediation. pp. 1-22.

Whelton, H.P., Spencer, A.J., Do, L.G. and Rugg-Gunn, A.J., 2019. Fluoride revolution and dental caries: evolution of policies for global use. *Journal of Dental Research*, *98*(8), pp.837-846.

World Health Organization, 2018. Guideline for drinking water, world health organization. *Geneva*.

World Health Organization, 2017. Guideline for drinking water, world health organization. *Geneva*.

Yuan, C., Li, M., Wang, M., Zhang, X., Yin, Z., Song, K. and Zhang, Z., 2020. Sensitive development of latent fingerprints using Rhodamine B-diatomaceous earth composites and principle of efficient image enhancement behind their fluorescence characteristics. *Chemical Engineering Journal*, *383*, p.123076.

Yuan, P., Wang, J., Pan, Y., Shen, B. and Wu, C., 2019. Review of biochar for the management of contaminated soil: Preparation, application and prospect. *Science of the Total Environment*, *659*, pp.473-490.

Chapter 3: Physicochemical characterization of macadamia nutshells for fluoride and pathogen removal from groundwater

Abstract

Groundwater is regarded as one of the main sources of drinking water in most of the rural areas of South Africa. However, groundwater is contaminated by fluoride and pathogens which causes dental and skeletal fluorosis. Presence of pathogens in water leads to adverse health effects, such as gastrointestinal illness, reproductive problems, and neurological disorder. This chapter aims is to explore the physicochemical composition of macadamia nutshells (MNS) and its efficiency in fluoride and pathogen removal from groundwater. Physiochemical and mineralogical compositions of MNS were determined using X-ray fluorescence (XRF), Fourier Transform Infra-red (FTIR) spectroscopy, X-ray diffraction (XRD), scanning electron microscopy (SEM) and Brunauer Emmett Teller (BET) techniques. Batch experiments were used to evaluate the potential of MNS in fluoride removal. Anti-microbial activity of the MNS was investigated using Well disc diffusion assay method. A maximum fluoride sorption capacity of 1.26 mg/g was achieved at initial fluoride concentration of 5 mg/L using adsorbent dosage of 0.5 g/100 mL at pH 6 and shaking time of 120 min. The adsorption kinetics data for fluoride showed a better fit to pseudo second order model of reaction kinetics indicating the dominance of chemisorption mechanism for fluoride sorption. Adsorption isotherms data showed a better fit to Langmuir model suggesting that adsorption of fluoride occurred on a monolayer surface. Thermodynamic studies revealed negative ΔG^{O}, and positive ΔH^{O} and ΔS^{O} indicating that adsorption of fluoride ion by MNS is spontaneous, endothermic and fluoride ions were randomly distributed on the surface. The MNS was successfully regenerated and reused for up to 7 successive cycles using 0.01 M HCl as eluent. The MNS showed no effectiveness towards *Escherichia Coli, Staphylococcus Aureus* and *Klebsiella Pneumoniae*. It was concluded that the MNS has potential for use in fluoride removal and the authors suggested the surface modification to enhance its antimicrobial activity.

Keywords: Fluoride, Pathogens, Defluoridation, Macadamia nutshell powder, and Groundwater.

3.1 Introduction

Water scarcity is gradually becoming a potential threat to human health, food security and national ecosystems with more than 50% of the world projected to experience water shortage by 2025 (Hoekstra., 2014). This is mainly due to climate change and pollution from industries. For these reasons, majority of people in rural areas of Sub-Saharan Africa and other developing countries depend on groundwater as their source of drinking water and domestic usage (Gitari *et al*., 2015). Depending on the geographical location, groundwater often contains higher concentration of fluoride which is detrimental to human health (Ahmed, 2019; Ayinde *et al*., 2018; Odiyo and Makungo, 2012). Exposure to fluoride concentration greater than 1.5 mg/L causes dental fluorosis and skeletal fluorosis as the level and period of exposure increases (WHO, 2017).

In Africa, fluoride concentration above 1.5 mg/L has been reported in several countries including Algeria, Benin, Cameroon, Egypt, Ethiopia, Ghana, Ivory Coast, Kenya, Libya, Malawi, Nigeria, Rwanda, Sierra Leone, South Africa, Sudan, Tanzania, Togo, Tunisia, Uganda and Zimbabwe with an estimate of 80 million of people within the continent exhibiting varying degrees of fluorosis symptoms (Kimambo *et al*., 2019). In Limpopo Province of South Africa, a study conducted by Odiyo and Makungo (2012) in Siloam Village reported that 87% of household depend on groundwater and 85% of these household have family member with mottled teeth and about 50% of children between the age of 11 and 14 in Siloam primary school have mottled teeth. Other study conducted in South Africa by Ncube and Schutte (2005) reported 93.4% dental fluorosis mobidity Mogwase community in North West Province where groundwater is the main source of drinking water. Ncube and Schutte (2005) further recommend the development of economic effective and user-friendly technology for water defluoridation. Defluorination remain the solution in many countries to remove access fluoride from drinking water. Most innovative technique such as ion exchange, precipitation, adsorption, electrolysis and membrane filtration have been used for fluoride removal. Adsorption is very important and most used adsorbent to remove access fluoride from groundwater in many countries due to lower initial cost, flexibility and simplicity of design and easy to operation and maintenance.

Apart from fluoride, due to lack of proper sanitation measures groundwater is vulnerable to contamination by pathogens (Soupir *et al*., 2018; Ayinde *et al*., 2018). South Africa is experiencing high number of children at five suffering from diarrhoea, cholera and typical fever

has been reported in Mpumalanga, Limpopo and KwaZulu Natal provinces (Potgieter *et al.*, 2018). The presence of pathogens in water can lead to adverse health effects, including diarrhoea, cholera, gastrointestinal illness, reproductive problems, and neurological disorders (Newell *et al*., 2010). According to the World Health Organization reports, about 844 million people lack basic quality drinking-water service, with about 3.4 million people, mostly young children died annually from pathogen related diseases, mostly in the developing countries (WHO, 2017; Ayinde *et al*., 2018). The method used to disinfect pathogens from ground include chlorination of drinking water, boiling of water, ceramic filters and ultraviolet (UV) (Dhillon *et al*., 2015; Ayinde *et al*., 2018).

Most fluoride in groundwater is naturally due to weathering of rocks rich in fluoride, combustion of fossil fuels also account for high fluoride and phosphate containing fluoride fertiliser add up to high fluoride in groundwater (Mukherjee and Singh, 2018). Sources by which disease causing viruses enter groundwater are land disposal of sewage, overflow from septic systems, and livestock waste. Leachate from solid waste landfills also can contain viruses (Sargunar, 2020). Owing to the co-existence of fluoride and pathogen in groundwater there is need of to find multifunctional adsorbent that is capable of removing both fluoride and pathogen. Macadamia nut shells (MNS) are mainly consisting of cross-linked polymeric chains such as lignin, cellulose, and hemicellulose which usually account for exchange and complexion properties of this class of adsorbent of various pollutants in water (Saini *et al*., 2015). In addition, they are known to have high surface area, well-developed producible microporous structure which accounts for high adsorption capacity (Antal and Gronli, 2003; Marsharll, 2001). Pakade *et al.* (2017) reported their potential application of MNS towards the removal of hexavalent chromium from aqueous solution. Their results showed that MNS has higher sorption efficiency towards Cr (VI) and it was also demonstrated that the prepared materials can be recycled more than once with removal efficiencies greater than 80%. Therefore, this chapter aims at evaluating the effectiveness of MNS in fluoride and its potency towards pathogen removal from groundwater. The following specific objectives were set: i) to determine the physicochemical characteristics of MNS powder, ii) to evaluate the effect of contact time, dosage, pH, adsorbate concentration and co-existing ions in fluoride removal, iii) to model the adsorption data using adsorption kinetics and isotherm models, iv) to evaluate the reusability of MNS towards fluoride removal and lastly, v) to determine the anti-microbial potency of the MNS.

3.2 Methods and materials

3.2.1 Sample collection

Macadamia nutshells were collected from Levubu Royal Macadamia in Vhembe district Limpopo Province, South Africa. The analytical grade reagents used in this study includ sodium hydroxide (NaOH), hydrochloric acid (HCl), potassium chloride (KCl), sodium fluoride (NaF) and Total Ionic Strength Adjustment Buffer (TISAB III) were purchased from Rochelle Chemicals, South Africa. All chemicals were used without further purification.

3.2.2 Preparation and characterization of macadamia nutshell powder

Macadamia nut shells were washed to remove dust and soil with Milli-Q (18.2MΩ/cm) water and then air dried at room temperature overnight to dry off. Thereafter, the shells were milled to pass through <250 µm sieve and stored in a zip locked sample bag. The elemental composition of the macadamia nutshell powder was determined using Thermo Flash 2000 Series CHNS/O organic Elemental analyser and also by Bruker S1 Titan/Titan/Tracer S Handheld X-Ray Fluorescence. The functional groups were determined using Bruker Alpha Platinum-ATR Fourier transformation infrared spectroscopy (FTIR). The crystallinity was determined using D8 advanced X-ray diffract meter (XRD) (Bruker) with Cu-Kα Radiation as source. Surface morphology was determined using scanning electron microscope (SEM) (Leo1450 SEM, at kv, working distance 14 mm). Pore size distribution, pore volume and surface area were determined using Barrett Joyner Halenda (BJH) sorption model using a specific surface area analyser (Autosorb-IQ and quadrasorb SI, USA). The pHpzc was evaluated using solid addition method (Gitari et al., 2017).

3.2.3 Batch fluoride adsorption experiments

The effect of contact time, adsorbent dosage, pH and co-existing ions in fluoride removal were evaluated using batch adsorption experiments. To evaluate the effect of contact time, 100 mL of solution containing 5 mg/L of fluoride was prepared and pipetted into 250 mL plastic bottles. Thereafter, 0.5 g of MNS was added to make up 0.5 g/100 mL adsorbent dosage and mixtures were then agitated for 5, 10, 15, 20, 25, 30, 40, 50, 60, 90, 120, 180 and 240 min using reciprocating table shaker. After agitation, samples were filtered through 0.45 µm pore membrane and the residual fluoride concentration was determined using ion selective electrode attached to fluoride multi-meter and calibrated using four standards (0.1, 1, 10 and 100 mg/L) containing ratio TISAB III to solution of 1:10. The same ratio was maintained for sample analysis. The effect of pH on fluoride sorption by MNS was evaluated by varying the initial solution pH from 2 to 12 using 0.1 M NaOH and 0.1 M HCl to adjust. Adsorbent dosage of

0.5g/100 mL and initial concentration of 5 mg/L were used. Mixtures were agitated for 120 mins. The effect of adsorbent dosage was evaluated by varying the adsorbent dosage from 0.1 to 0.6 g/100 mL using initial concentration of 5 mg/L. Solution pH was adjusted to 6±0.5 and mixtures were agitated for 120 mins. The effect of initial fluoride concentration was evaluated by varying initial fluoride concentration from 5 to 30 mg/L at a temperature of 298, 308 and 318 K. Adsorbent dosage of 0.5 g/ 100 mL and initial pH of 6±0.5 were used. Mixtures were agitated for 120 mins. To evaluate the effect ions in fluoride removal was done using 5 mg/L of SO_4^{2-}, Cl^-, NO_3^-, CO_3^{2-}, Ca^{2+} and Mg^{2+} were prepared separately and mixed with 5 mg/L of fluoride solution. The adsorbent dosage of 0.5 g/100 mL and initial pH of 6±0.5 and mixtures were shaken for 120 mins. All experiments were conducted in triplicate for better accuracy and the average value were reported. The percentage of fluoride removal and the adsorption capacity of MNS were computed using equation (3.1) and (3.2) respectively.

$$\%\ Fluoride\ removal = \left(\frac{C_0 - C_e}{C_0}\right) \times 100 \qquad (3.1)$$

$$Q = \left(\frac{C_0 - C_e}{m}\right) \times V \qquad (3.2)$$

Where: C_o is the initial fluoride ion concentration (mg/L); C_e is the fluoride ion concentration at equilibrium (mg/L); V is the volume of the solution (L) and m mass of the adsorbent (g).

3.2.4 Regeneration and reuse of the adsorbent

The regeneration of the adsorbent was carried out as follows: 0.5 g of MNS loaded with fluoride desorbed through agitation with a solution of 100 mL containing 0.1 M KCl and 0.1 M HCl for 120 min reciprocating shaker. After agitation, mixtures were filtered through 0.45 µm pore membrane and the collected residues were washed using Milli-Q water to a neutral pH and then oven dried at 110 ^{O}C for 3 h. The regenerated adsorbent was then reused for defluoridation and the procedure was repeated for up to six (6) KCl and seven (7) HCl successive regeneration re-use cycle.

3.2.5 Anti-microbial studies

Anti-microbial activity of the MNS was investigated using Well disc diffusion assay method (Kirby-Bauer method) based on the observation minimal zone of inhibition. Measurements of diameter from exterior of absorbent to end point of the inhibition zone were done and subsequently the values were implemented on analysis of MNS adequacy on anti-bacterial activity. Briefly, a 100 mL Mueller-Hinton agar broth was prepared as follows; 2.1 g of Mueller-Hinton agar broth was dissolved in 100 mL of Milli-Q water. After the mixture is

dissolved completely, the mixture was autoclaved at 121 ^{O}C for 15 min. After autoclaving, ager was left to cool at room temperature. Three 15 mL tubes were labelled *E. coli*, *S. Aureus* and *K. Pneumoniae* and 5 mL broth was allocated to each tube, a 3-4 colonies were inoculated from each plate to the tube respectively the tubes were incubated at 37 ^{O}C for a period of 3 hours. Subsequently a swab was used to streak the culture onto fresh agar plate each respectively, and 100 µL of MNS solution was pipetted on the centre of the plate and kept at the 37 ^{o}C incubator for 48 hours period. Thereafter, the zone of inhibition was observed.

3.3 Results and discussion

3.3.1 Physiochemical characterization

3.3.1.1 Elemental composition

The elemental composition of Macadamia nutshell powder is presented in Table 3.1. The results showed that MNS is mainly composed of carbon (49.56%), oxygen (44.08%) and hydrogen (6.19%). A similar composition was reported for other lignocellulosic compounds such as walnut shells (Altun and Pehlivan 2012) and raw macadamia nutshell powder (Pakade *et al.*, 2017). The oxides of MgO, SiO_2, K_2O, CaO and Al_2O_3 were detected at trace levels.

Table 3.1: Chemical analysis of macadamia nutshell powder

Element / oxide	Composition (%)
C	49.56
O	44.08
H	6.20
MgO	0.97
SiO_2	0.44
K_2O	0.30
CaO	0.25
N	0.20
AI_2O_3	0.16
P_2O_2	0.01

3.3.1.2 Functional groups

The functional groups of MNS were determined using FTIR and the results are presented in Figure 3.1. The raw MNS spectra showed wide transmittance band at wavelength regions 3351 cm^{-1} which is attributed to stretching and vibration of hydroxyl (OH^-) groups associated with the hydrogen bond in absorbed moisture and cellulose structure (Zhao *et al.*, 2013). The band intensity at 2928 cm^{-1} is linked to aliphatic group (C-H). The band at 1738 cm^{-1} is linked to carboxylic group (C=O). The bands at 1454 cm^{-1} can be assigned to the stretching of C-C bond. The band at 1248 cm^{-1} indicating the C-OH together with the band of C-O at 1030 cm^{-1} linked to the vibration and stretching of the phenols, ketones, ethers and esters in the surface of the adsorbent. After defluoridation there was a decrease in peak intensity and shift in band to 3361, 1741, 1456, 1268 and 1091 cm^{-1}. Similar observations were reported in the literature where the changes in intensities and shifts of absorption bands at 1454 and 1244 cm^{-1} were attributed to oxidation of lignin when contacted by Cr (VI) ions (Yang *et al.*, 2021; Albadarin *et al.*, 2011). The difference before and after adsorption confirm the participation of functional groups in removal of fluoride.

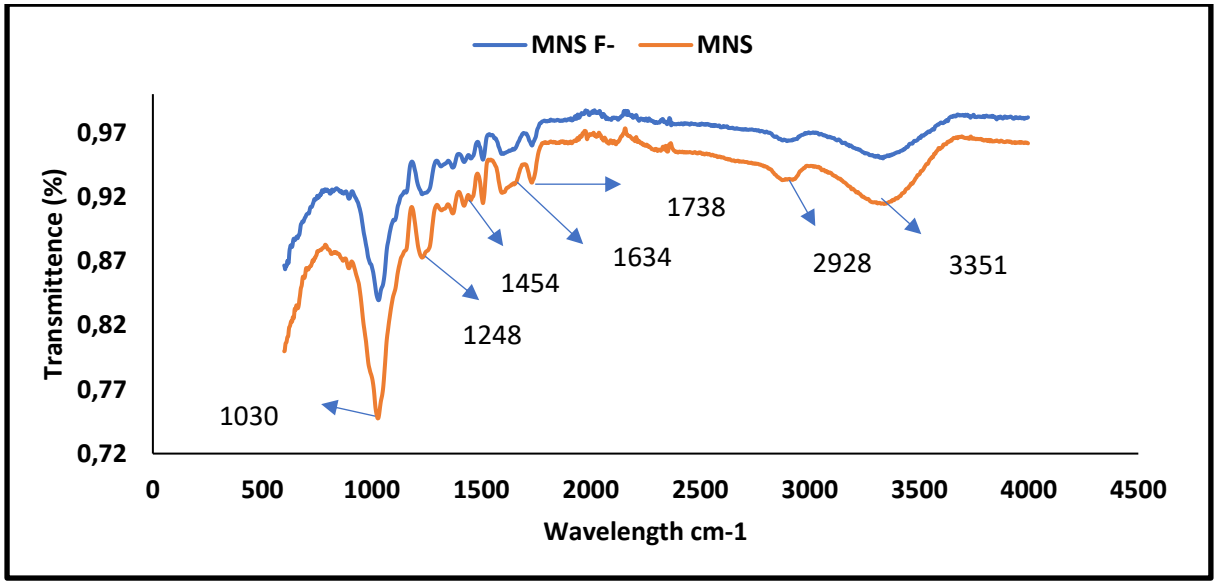

Figure 3.1: FTIR spectra of raw macadamia nutshell powder and the residual macadamia nutshell powder.

3.3.1.3 XRD studies

The x-ray diffraction spectra of MNS before and after fluoride removal is depicted in Figure 3.2. The spectra showed the major diffraction peak at 2θ degree = 17.31°, 22.17° and 34.35° which are native cellulose ($C_6H_{12}O_6$) peaks. The material shows the crystalline peak at 22.17° 2-degree theta and also it appears to be amorphous. The x-ray diffraction spectra after fluoride removal show similar peaks.

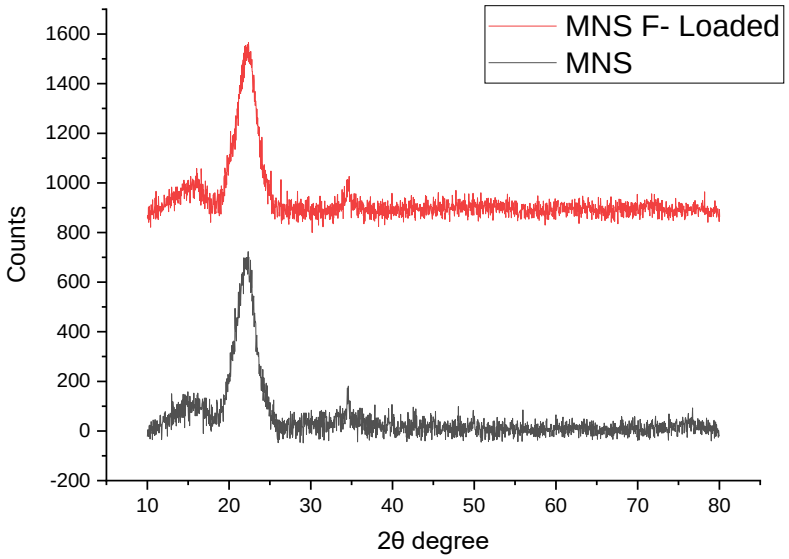

Figure 3.2: XRD spectra for raw macadamia nutshell power and macadamia nutshell powder residues.

3.3.1.4 Morphological analysis

The morphology MNS before and after fluoride removal is depicted in Figure 3.3a and b. The micrograph revealed that the MNS consisted of flaky fold-like structures with some crystals on top. The flaky like structures are linked to crystalline peak observed in XRD. After fluoride adsorption the surface appears to be much smooth than it was before fluoride removal. The change in structure after fluoride removal can be an indication that fluoride ion diffuses on the adsorbent when removing fluoride leading to deformation of the raw MNS structure.

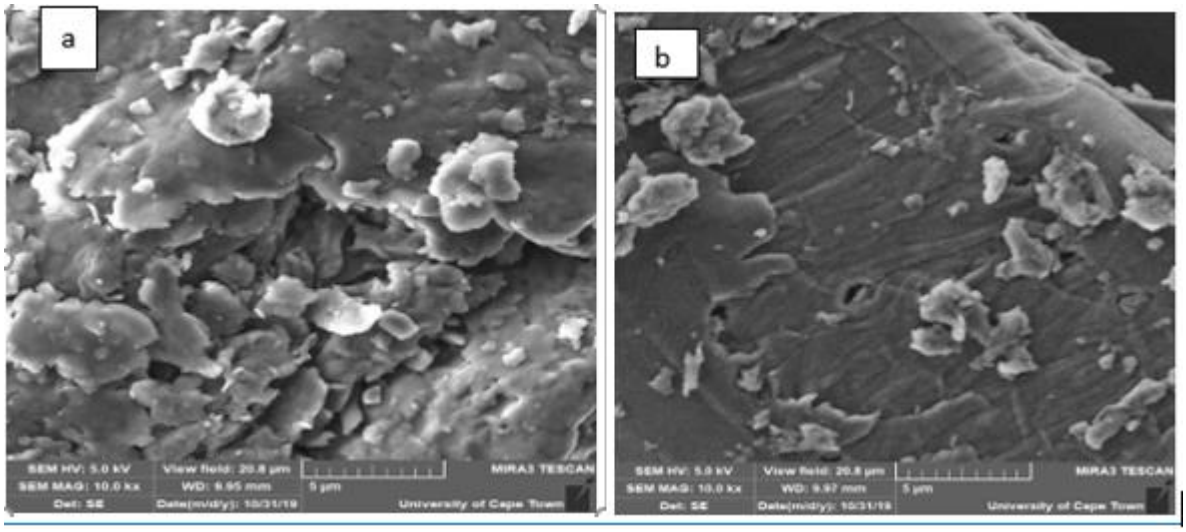

Figure 3.3: Micrographs of MNS before (a) and after (b) fluoride removal.

3.3.1.5 surface area, pore distribution and pore volume

Table 3.2 present the BET suface area, pore distribution and pore volume of MNS. The surface area of raw macadamia nutshell powder was 1.69 m^2/g. The avarage pore diameter of MNS was found to be 15.40 nm (Table 2). The pore distribution curve in Figure 3.4 shows that majority of the pores lies within 1.76 to 14.61 nm indicating that the pores of MNS ranges from microporous to mesoporous range. The fluoride ion diffuse in the surface of the adsorbent and when it diffuse, the floride ion was absorbed into the mesoporous adsorbent.

Table 3.2: surface area, and pore area and volume of the raw MNS

Surface area (m^2/g)	Pore diameter (nm)	Pore volume (cm^3/g)
1.69	15.4	0.01

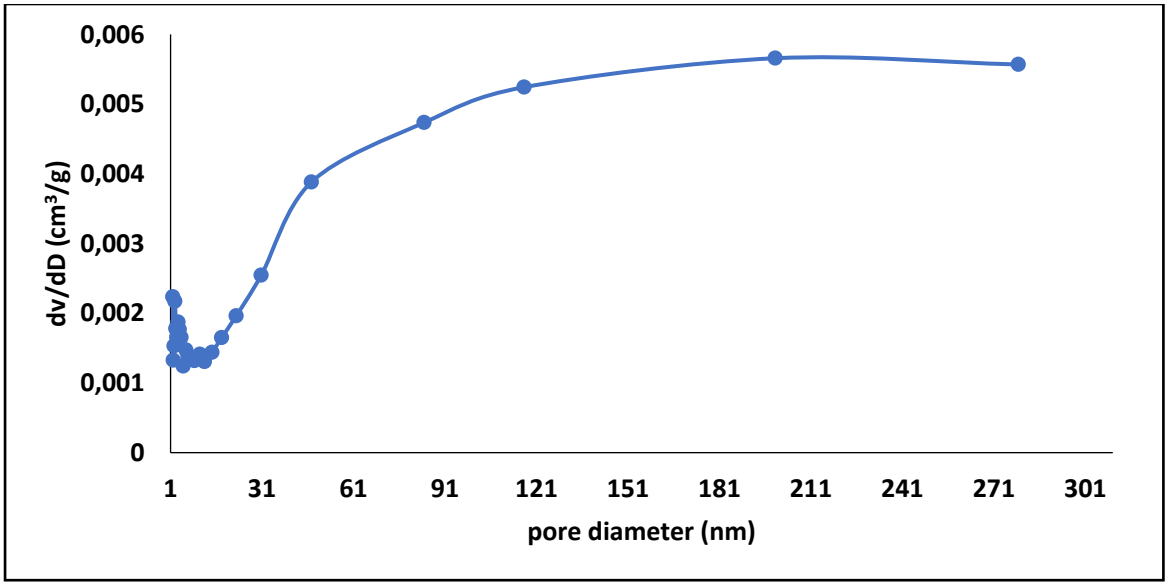

Figure 3.4: Pore distribution curve for MNS.

3.4 Batch adsorption experiment

3.4.1 The effect of contact time and adsorption kinetics

The effect of contact time on percentage F^- removal and adsorption kinetics is depicted in Figure 3.5. It is observed that the fluoride removal adsorption capacity increased gradually with increasing contact time. The increase in F^- adsorption capacity could be due to available active surface of the adsorbents for fluoride ions in the solution. The steep slope between 5 and 10 min could be ascribed to the fast movement of F^- from the bulk solution onto the adsorbent

while the plateau between 10 and 120 min could be an indication of diffusion of fluoride ions onto the mesopores of the adsorbent followed by adsorption within the pores as the time progresses to 180 min. Therefore 120 min was chosen to be the optimum contact time for subsequent experiments.

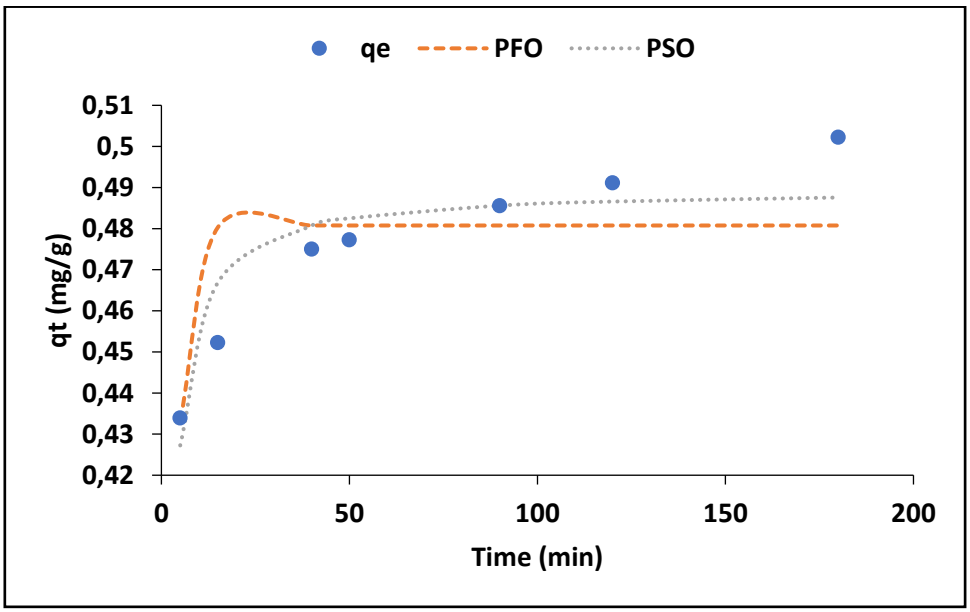

Figure 3.5: Adsorption capacity and adsorption kinetics for fluoride removal by raw macadamia nutshell powder (5 mg/L initial F^- concentration, pH 6, 0.5 g dosage, shaking speed 200 rpm).

The data obtained from the effect of contact time was fitted to pseudo-first order (PFO) and the pseudo-second order (PSO) non-linear reaction kinetics models as well as the intra-particle diffusion model in order to evaluate the mechanism and the rate limiting steps for fluoride adsorption by MNS. The pseudo-first order is used to describe physisorption of the material as well as solid-liquid adsorption system. It is given by the equation 3.3 as follows (Gupta and Bhattcharyya, 2011).

$$q_t = q_e(1 - e^{-k1t}) \qquad (3.3)$$

Pseudo second order on the other hand is given by equation 3.4 and it is used to describe chemisorption as well as cation exchange reactions (Simon *et al.*, 2016; Gupta and Bhattcharyya, 2011).

$$q_t = \frac{q_e^2 k_2 t}{1 + k_2 q_e t} \qquad (3.4)$$

Where q_t (mg/g) is adsorption capacity at a given time t, qe (mg/g) is the maximum sorption capacity at equilibrium and k_1 (min^{-1}) and k_2 (g/mg.min) are the pseudo first and second order rate constant, respectively. Figure 3.5 depicts the pseudo first and second order plots, respectively. The constant values of pseudo first and second order are presented in Table 3.3. From the results, the R^2 value of pseudo first order is 0.39 and for pseudo second order is 0.75 indicating that pseudo second order show the better fit meaning that fluoride removal happen via chemisorption. From the results (Table 3.3), the rate constant k_1 (pseudo first order) is 0.35 min^{-1} and k_2 (pseudo second order) is 1.26 min^{-1}, which suggest that chemisorption was much faster and dominant as compared to physisorption. The chi-square (X^2) determines the goodness of fit, that is the lower the value the better the fit. The pseudo second order shows chi-square of 0.000569 which indicate that pseudo second order show the better fit than pseudo first order.

Table 3.3: Calculated parameters for pseudo first order and pseudo second order reaction kinetics of raw MNS

		PFO			PSO		
K_1 (min^{-1})	Qe (mg/g)	R^2	X^2	K^2 (g/mg.min)	Qe (mg/g)	R^2	X^2
0.35	0.51	0.39	0.001412	1.26	0.53	0.75	0.000569

During adsorption, adsorbate molecules move from the bulk solution into the boundary layer and further diffuse onto the interior of the adsorbent (Ayinde *et al.*, 2018 and Mudzielwana *et al.*, 2017). To further confirm the particle diffusion and understanding the rate limiting steps, Weber–Morris intra-particle diffusion was applied (Weber and Morris, 1964). Weber-Morris model is depicted by equation 3.5.

$$q_t = k_i t^{0.5} + C_i \quad (3.5)$$

Where q_t is the amount adsorbed (mg g^{-1}) at a given time, t (min); K_i (mg $g^{-1}min^{-1}$) is the intra-particle diffusion rate constant and is determined from the slope of $t^{0.5}$ vs q_t and C_i is the constant obtained from the intercept and reflects the thickness of the boundary layer. The larger the intercept, the greater the boundary layer effect. The positive value of C_i indicates that intra-particle is the main mechanism for adsorption and external diffusion occurred to some degree. Figure 3.6 shows the intra-particle diffusion plot for fluoride adsorption by MNS. It is observed

that the plot did not pass through the origin instead the data yielded three clear phases. The first phase attributed to boundary layer adsorption occurred between 5 and 15 min. The second between 40 and 50 min is associated with the intra-particle diffusion which is followed by subsequent adsorption within the pores of adsorbent after 90 min agitation time (Bullen *et al*., 2021; Gupta and Bhattcharyya, 2011). During the boundary layer adsorption (phase 1) fluoride ions are attracted via electrostatic forces to the surface of the adsorbent which is followed by the diffusion into the mesoporous structures of the MNS (phase 2) where it starts interacting with the atoms within the pores resulting in chemisorption (phase 3). The rate of constant for phase 1, phase2, and phase 3 (K_1, K_2, and K_3) are shown in Table 3.4. It is observed that K_1 is higher than K_2 and K_3 indicating that boundary layer adsorption occurred much faster than the subsequent intra-particle diffusion and the adsorption at equilibrium.

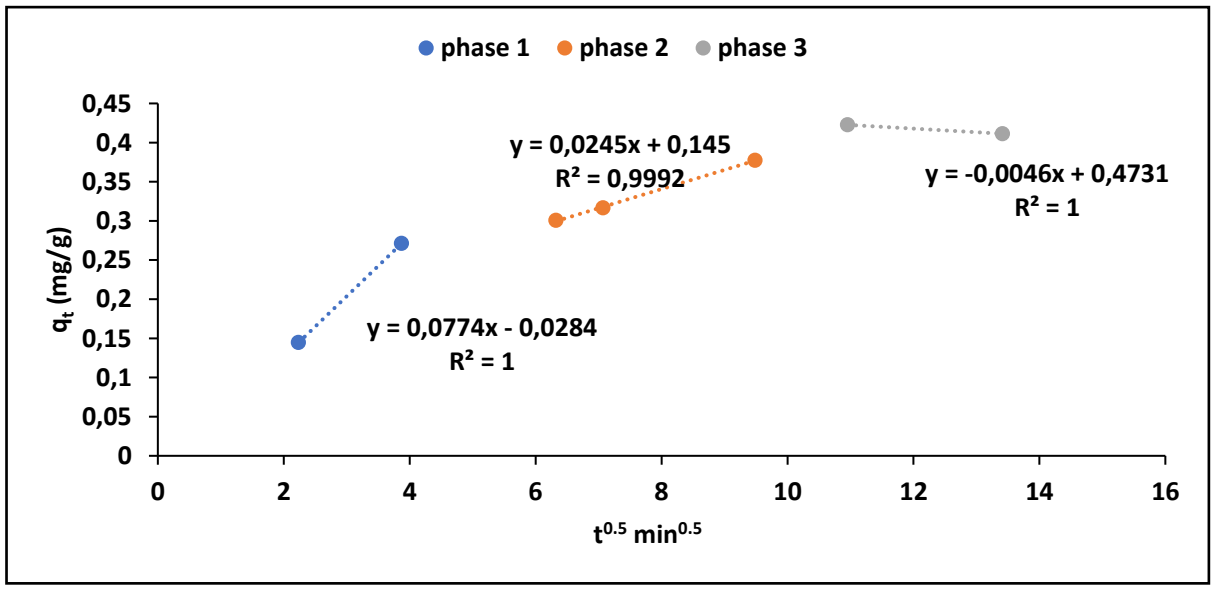

Figure 3.6: Intra-particle diffusion plot for fluoride adsorption onto MNS.

Table 3.4. Constant values of intra particle diffusion

Model		MNS
Intra particle diffusion	K_1 (mg/g min^{-1})	0.08
	K_2 (mg/g min^{-1})	0.02
	K_3 (mg/g min^{-1})	0.005
	R^2 (phase 1)	1
	R^2 (phase 2)	0.99
	R^2 (phase 3)	1

3.4.2 Effect of pH

Figure 3.7a show the effect of pH on the fluoride removal by MNS. The results showed that the sorption of fluoride by MNS is favoured at initial pH of 6 where maximum percent fluoride removal of 48% was achieved. The percentage fluoride removal decreased as the solution pH reduced to acidic range and also as it increased to alkaline range. The pH of the solution influences the adsorbent's surface charges and consequently affect the behaviour of fluoride adsorption. To establish the surface charges, the pH point of zero charge (pHpzc) of MNS was evaluated using the titration method figure 3.7b. It is observed that the pH of the material is at pH of 7.2±0.5. Indicating that at this pH the surface is neutrally charged while at pH below this level, the material is positively charged and at pH 7.2±0.5 the surface is negatively charged. Therefore, the decrease at acidic pH where H^+ ions dominate the surface could be attributed to the formation of weak HF acid in the solution leading to lower fluoride removal (Eq. 3.6). The fluoride adsorption at acidic level could be attributed to electrostatic attraction between the positively charged surface and negative fluoride ion (Eq. 3.7). At near neutral pH where optimum uptake occurred, fluoride adsorption could be due to ion exchange and as a result of weak van der Waal forces (Eq. 3.8). Conversely at alkaline pH where OH^- dominate the surface could be attributed the electrostatic repulsion between negatively charged surface and negative fluoride ion. However, fluoride could also be adsorbed as a results of ion exchange (Eq. 3.9 and 3.10).

$$H^+ + F^- \rightarrow HF \quad (3.6)$$

$$MOH + F^- + H_3O^+ \rightarrow MOH_2^+ - F^- + H_2O \quad (3.7)$$

$$MOH + F^- + H_3O^+ \rightarrow M^+ - F^- + 2H_2O \quad (3.8)$$

$$MOH + F^- \rightarrow MF + OH^- \quad (3.9)$$

$$M(OH)2^- + 2F^- \rightarrow MF^- + 2OH^- \quad (3.10)$$

Where M represent the elements in the adsorbent (MNS) surface.

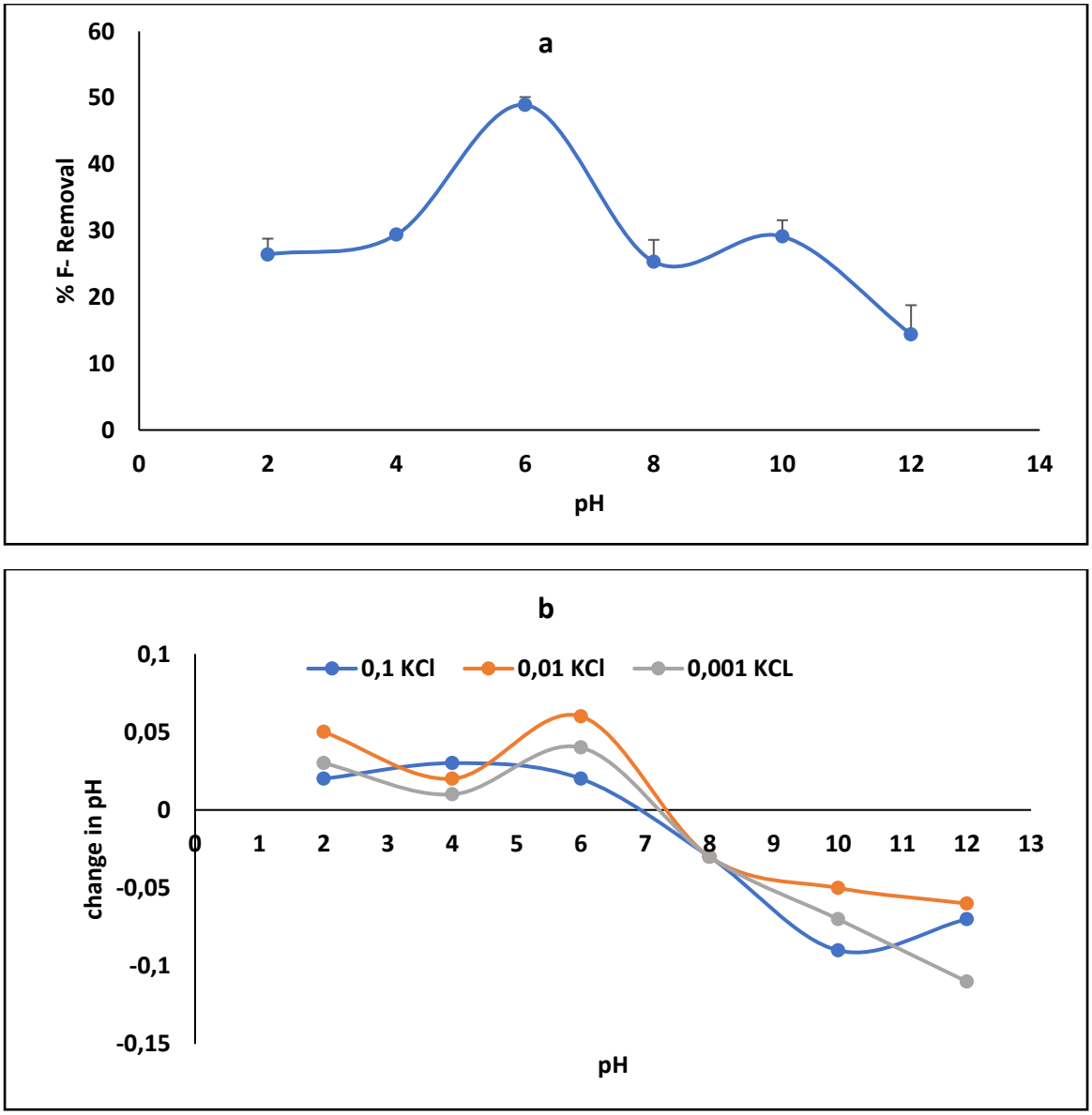

Figure 3.7: (a) Effect of pH on fluoride removal (5 mg/L initial F^- concentration, 0.5 g dosage, shaking speed 200 rpm) and b) point of zero charge (0.1, 0.01 and 0,001 M KCl, dosage of 0.5 g/100 mL shaking time of 120 min and shaking speed 200 rpm).

3.4.3 The effect of adsorbent dosage

Figure 3.8 depicts the effect of adsorbent dosage on fluoride removal. The percentage of fluoride removal increase as the adsorbent dosage increases from 0.1 g to 0.5 g/100 mL and slight change was observed as the dosage increases to 0.6 g/100 mL. Conversely, the adsorption capacity decreased with increasing adsorbent dosage. These trends could be attributed to increasing number of adsorption sites for limited fluoride ions as the adsorbent dosage increases. Adsorbent dosage of 0.5 g/100 mL was therefore selected as the optimum for subsequent experiments.

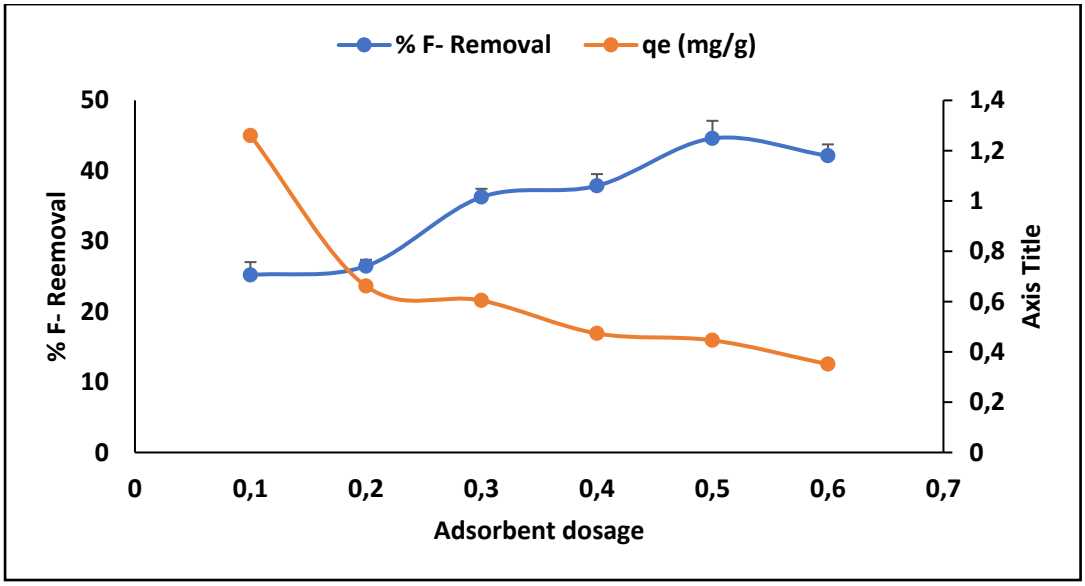

Figure 3.8: Variation $\%F^-$ removal and adsorption capacity by raw macadamia nutshell powder as a function of adsorbent dosage (contact time of 120 min, initial F^- concentration of 5 mg/L at 100 mL solution volume, pH 6 and shaking speed 200 rpm).

3.4.4 Effect of initial concentration and adsorption isotherms

Figure 3.9 shows the effect of initial concentration on the fluoride removal efficiency at different temperature. The initial concentration was varied from 5 to 30 mg/L and the experiment was repeated at a temperature of 298, 308 and 318 K. It was observed that fluoride adsorption capacities increase with increasing equilibrium concentration at 298 K. The adsorption capacity decreases with increasing initial concentration at temperature of 308 K and 318 K.

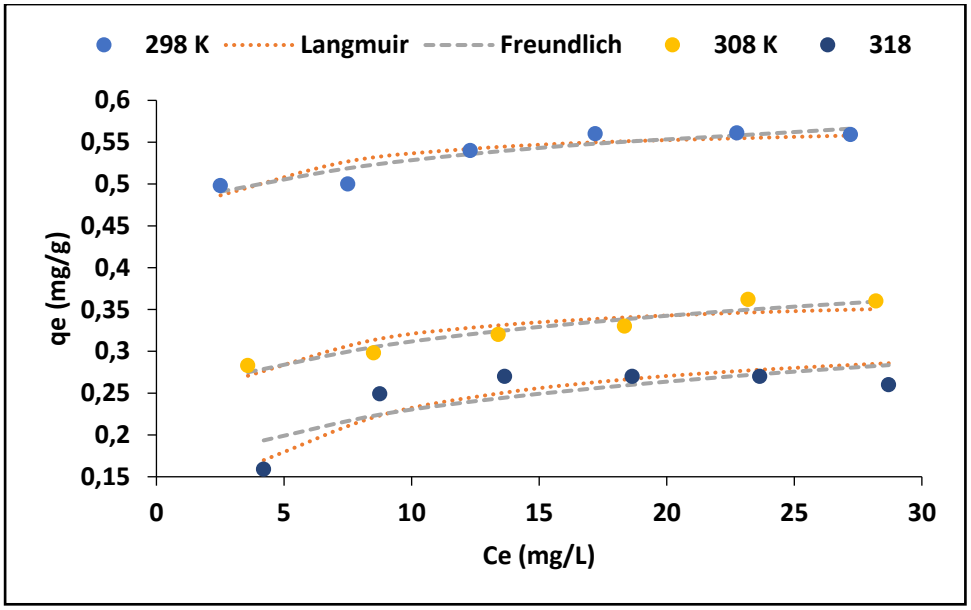

Figure 3.9: Variation of adsorption capacity and equilibrium fluoride concentration and nonlinear adsorption isotherm plots (contact time 120 min, dosage 0.5 g/ 100 mL F^- solution, pH 6 and shaking speed of 200 rpm).

Adsorption isotherm were employed to further explain the interaction between the fluoride ions and the MNS surface. The commonly used Langmuir and Freundlich adsorption non-linear isotherms were used. Langmuir isotherm model is based on the assumption that adsorption occurs on monolayer surface. Once fluoride ion is adsorbed on the surface of the adsorbent, no other ion is adsorbed on that adsorption site (Foo and Hammed, 2010). Langmuir isotherm model is represented by equation (3.11).

$$q_e = \frac{q_{max} K_L c_e}{1 + K_L c_e} \qquad (3.11)$$

where C_e is the equilibrium concentration (mg/L); q_e is the amount of fluoride ion adsorbed (mg/g); q_m is q_e for a complete monolayer (mg/g); K_L is adsorption equilibrium constant (L/mg).

The Freundlich adsorption isotherm model on the other hand assumes that adsorption occurs on a heterogeneous surface and consider multilayer adsorption (Foo and Hammed, 2010). Freundlich is represented by equation 3.12:

$$q_e = K_f c_e^{1/n} \qquad (3.12)$$

Where C_e is the equilibrium concentration (mg/L); q_e is the amount of ion adsorbed at equilibrium (mg/g); K_f is the Freundlich constant related to adsorption capacity and 1/n is the

adsorption intensity. When 0< 1/n<1, the adsorption is favourable; when 1/n =1, the adsorption is irreversible; and when 1/n > 1, the adsorption is unfavourable.

Figure 3.9 depicts the plot for Langmuir isotherm model and Freundlich isotherm model respectively while the model's constant values are presented in Table 5. The adsorption data at both temperatures yielded higher correlation co-efficient values when fitted to Langmuir model than Freundlich model. The better fit to Langmuir isotherm model suggests monolayer coverage. To further establish the favourability of the adsorption process, the equilibrium dimensionless parameter, R_L which is depicted by equation 3.12 was also calculated based on Langmuir isotherm adsorption constant and initial concentration.

$$R_L = \frac{1}{1+k_L C_i} \tag{3.12}$$

where K_L is the Langmuir isotherm constants and C_i is the initial concentration of fluoride (mg/L). R_L value indicates the sorption system to be favourable if $0 < R_L < 1$. The R_L value equal to 1 indicate linear adsorption and if value of R_L is equal to 0, the adsorption is irreversible. Calculated value of R_L for different initial concentration is presented in figure 3.10. All calculated value of R_L lies between 0 and 1 indicating that the adsorption of fluoride onto MNS at both initial concentrations was favourable. The chi-square (X^2) determines the goodness of fit, that is the lower the value the better the fit. Based on the chi-square value, the smallest values are observed in Langmuir isotherm, meaning that the fluoride adsorption for both temperatures better fit to Langmuir isotherm.

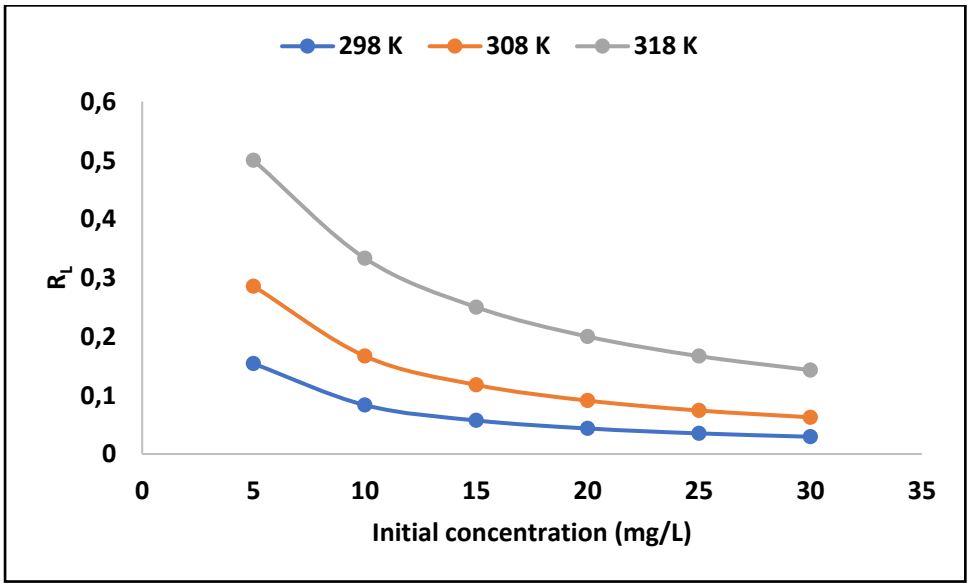

Figure 3.10: R_L values for the adsorption of fluoride onto MNS.

Table 3.5. Calculated Langmuir and Freundlich isotherm parameters

	Langmuir isotherm				Freundlich isotherm			
Temperature(K)	q_m(mg/g)	K_L (L/mg)	X^2	R^2	1/n	K_f	R^2	X^2
298	0.57	1.10	0.00188	0.99	0.08	0.43	0.86	0.01156
308	0.37	0.33	0.00294	0.99	0.15	0.22	0.99	0.00107
318	0.05	0.20	0.00269	0.98	0.21	0.14	0.96	0.01160

3.4.5 Adsorption thermodynamics

Adsorption thermodynamics is the calculation of phase equilibrium between a gaseous mixture and a solid adsorbent. To further establish the adsorption mechanism of fluoride adsorption unto MNS, thermodynamics parameters such as Gibbs energy change (ΔG°), the enthalpy change (ΔH°) and the entropy change (ΔS°) were computed using equation (3.13) and (3.14).

$$\Delta G^{\circ} = -RT \ln K_c \quad (3.13)$$

$$\ln K_c = -\frac{\Delta H^0}{RT} + \frac{\Delta S^0}{R} \quad (3.14)$$

Where ΔG° is the standard Gibbs free energy change calculated using equation (12) and R is the molar gas constant, 8.314 J mol^{-1} K^{-1} and T is absolute temperature in Kelvin. ΔH° is the standard enthalpy change while ΔS° is the entropy change and they are determined from slope and the intercept of $\ln K_c$ against 1/T. The equilibrium constant K_c is calculated from Langmuir's adsorption isotherm constant (L/mg) by multiplying it with 18.998×10^3 where 18.998 is the atomic mass of fluoride and it must be dimensionless therefore the equilibrium constant K_c equation (3.13) must be a parameter without unit (Tran *et al.*, 2016). The plot for lnKc is presented in Figure 3.11 while the constant parameters are presented in Table 3.6. The value ΔG° was found to be negative indicating that adsorption of fluoride by MNS occurred spontaneously. The value of ΔS° was found to be positive, which suggests fluoride ions were randomly distributed on the surface of the adsorbent. The enthalpy change (ΔH°) value was found to be positive indicating that adsorption of fluoride was endothermic and chemisorption process.

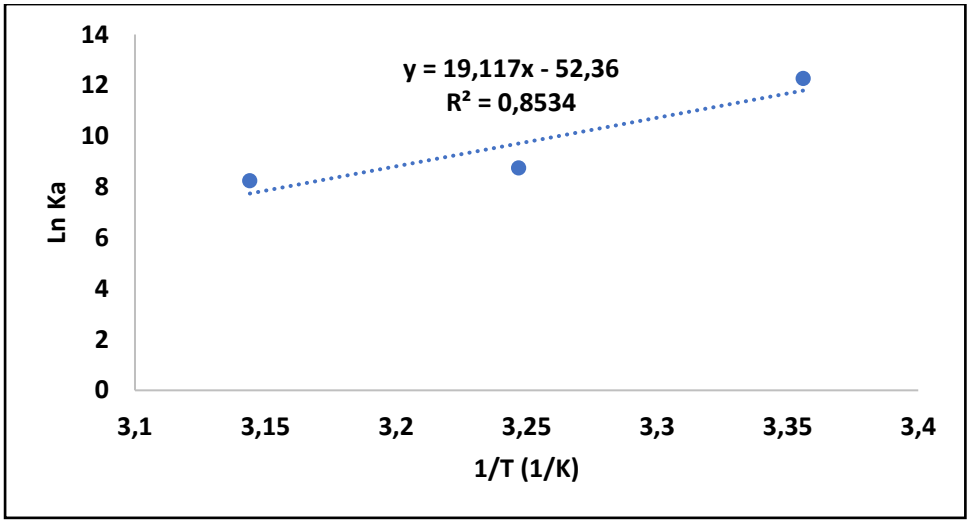

Figure 3.11: lnKc as a function of reciprocal of adsorption temperatures.

Table 3.6. Adsorption thermodynamic parameters

ΔG^o (kj / mol)	ΔH^o (kj/ mol)	ΔS^o (kj/mol)
298 K = -30393.6		
308 K = -22388	158.93	435.32
318 K = -21791		

3.4.6 The effect of co-existing ions

Figure 3.12 shows the effect of co-existing ion unto fluoride ion removal by MNS. The results show that the presence of magnesium (Mg^{2+}), calcium (Ca^{2+}), sulphate (SO_4^{2-}), nitrates (NO_3^-), chloride (Cl^-), and carbonate (CO_3^{2-}) enhances the percentage removal of fluoride uptake by MNS. This could be an indication that the co-existing ions are creating more surface charges of the adsorbent leading to high fluoride percentage removal. These results indicate that MNS has a better advantage for application in groundwater defluoridation since its performance is not affected by the presence of other co-existing ions.

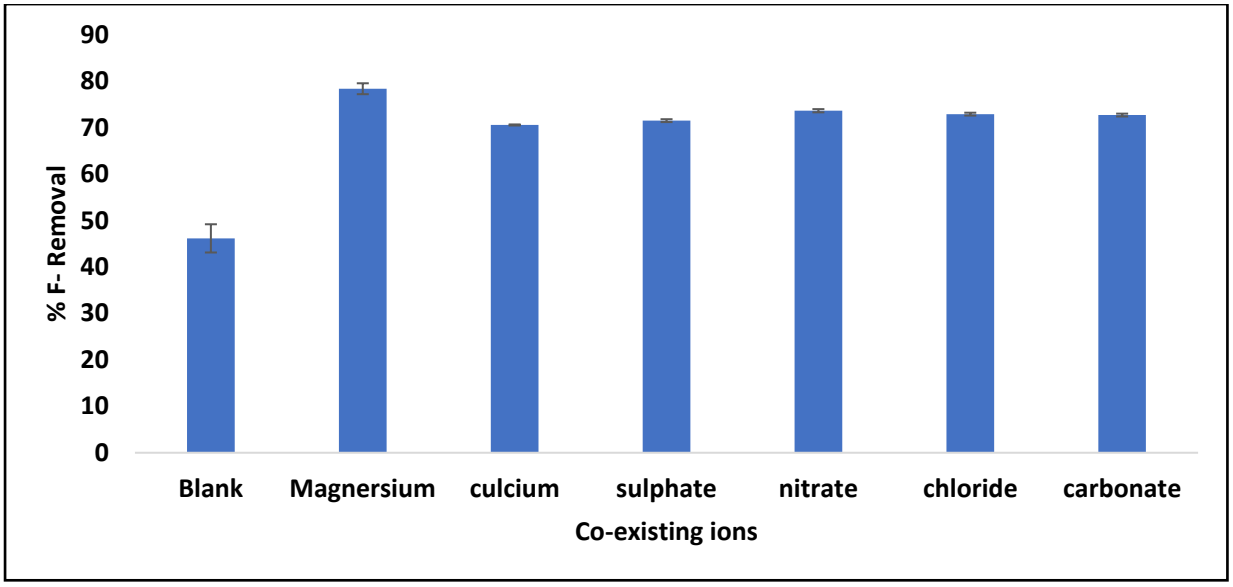

Figure 3.12: Effect of co-existing ions on fluoride removal by MNS (contact time 120 min, dosage 0.5 g/ 100 mL F^- solution, pH 6 and shaking speed of 200 rpm).

3.4.7 Regeneration and re-use of the adsorbent

The regeneration and reuse potential of the MNS was evaluated using 0.1 M KCl and 0.01 M HCl as the regenerant and the results are presented in Figure 3.13. The percentage of fluoride removal by MNS decrease from 42.4% to 15.2% when KCl was used. The decrease in fluoride adsorption when using KCl is probably due to the gradual dissolution of MNS at alkaline conditions from the surface of the adsorbent during the regeneration process. Conversely, when HCl was used the percentage fluoride removal increased from 46.4% to 62.2% after first cycle and thereafter decreased as the reuse-regeneration cycles increases. This indicates that HCl has the potential to activate the surface charges leading to increased fluoride removal. This was also observed by Pakade *et al*., (2017) for biosorption of hexavalent chromium from aqueous solution using MNS. Therefore, HCl was selected as the best regenerant.

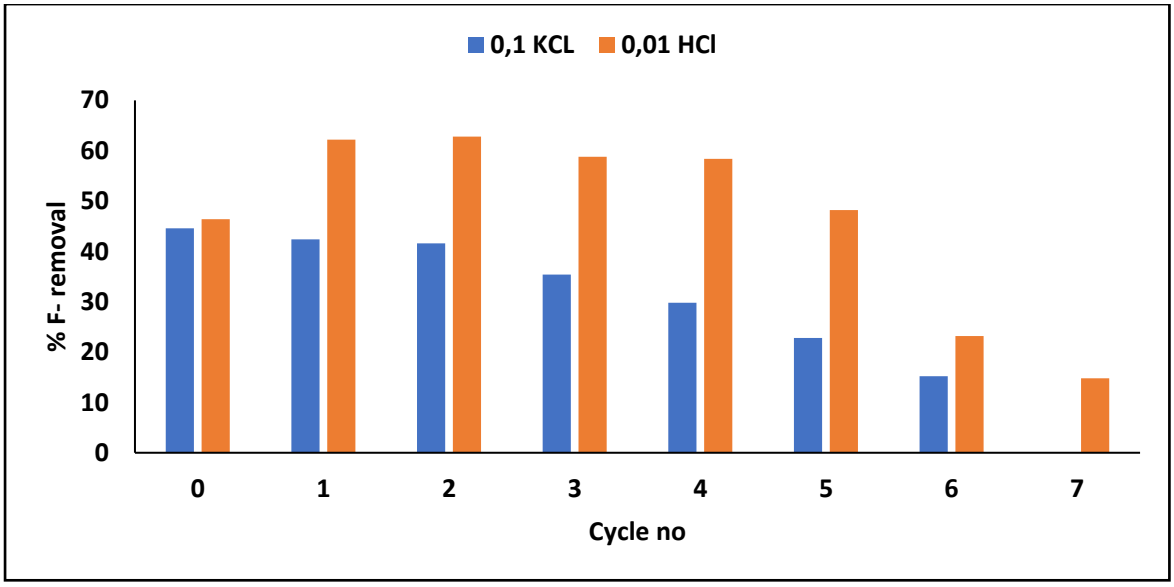

Figure 3.13: Effect of co-existing ions on fluoride removal by raw macadamia nutshell powder (5 mg/L initial F^- concentration, pH 6, 0.5 g dosage, shaking speed 200 rpm).

3.4.8 Comparison of MNS powder with other adsorbents

Comparison of defluoridation capacity between raw MNS powder and other reported adsorbents for removal of other toxic metals in water is presented in Table 3.7. The composition of an adsorbent at different conditions and other experimental conditions has an influence in adsorption capacity of the sorbents. The MNS powder have low adsorption capacity as compared to those given in Table 3.7. Adsorption capacity is a function of initial fluoride used and the adsorbent dosage used. Moreover, the percentage of fluoride removal was above 40%. The low adsorption capacity is because the material used in this study was raw as compared to other materials used in other studies because the materials were modified.

Table 3.7: Comparison of binding capacities

Adsorbent	Treatment	Adsorption capacity (mg/g)	Experimental conditions	reference
Macadamia nutshell (RMN)	Raw	45.23	pH 2, contact time 600 min, 100 mg/L Cr (VI) and 0.2 g	Pakade(a) *et al.*, 2017
Macadamia nutshell (ARMN)	HCl	44.83	pH 2, contact time 600 min, 100 mg/L Cr (VI) and 0.2 g	Pakade(b) *et al.*, 2017
Rice husk & corn cob activated carbon	HCl & NaOH	7.9	pH 4, contact time 4hrs, 2 g and 18 mg/L	Gebrewold *et al.*, 2018
Macadamia nutshell (BRMN)	NaOH	42.44	pH 2, contact time 600 min, 100 mg/L Cr (VI) and 0.2 g	Pakade(c) *et al.*, 2017
Sugarcane bagasse	Raw	1.79	pH 2, contact time 60 min, 10 g	Aloma *et al.*, 2014
Raw MNS powder	Raw	1.26	pH 6, contact time 120 min, shaking speed 200 rpm, 5 mg/L fluoride and 0.5 g	This study

3.4.9 Antibacterial activity of MNS

Antibacterial activity of the raw MNS was evaluated using the sensitivity method of Kirby-Bauer (Jorgensen and Turnidge, 2007) by observing the minimal zone of inhibition and is presented in Figure 3.14. Three bacterial strains *Escherichia Coli*; gram-negative, Figure 3.14 (a), *Staphylococcus Aureus;* gram-positive, Figure 3.14(b) and *Klebsiella Pneumoniae;* gram-positive, Figure 3.15 (c) were check using MNS adsorbent for antibacterial activity. The results indicated the extract had no antibacterial properties and produced a null result in the inhibition zone observed meaning that MNS has no antibacterial activity. This was also observed by Dang *et al*. (2019) and it was attributed to the variation of cell wall composition of the bacteria were MNS raw was used. However, this aspect of the research needs further research to establish

the exact mechanisms involved and to further modify the adsorbent with nanoparticles to enhance its effectiveness towards microbes.

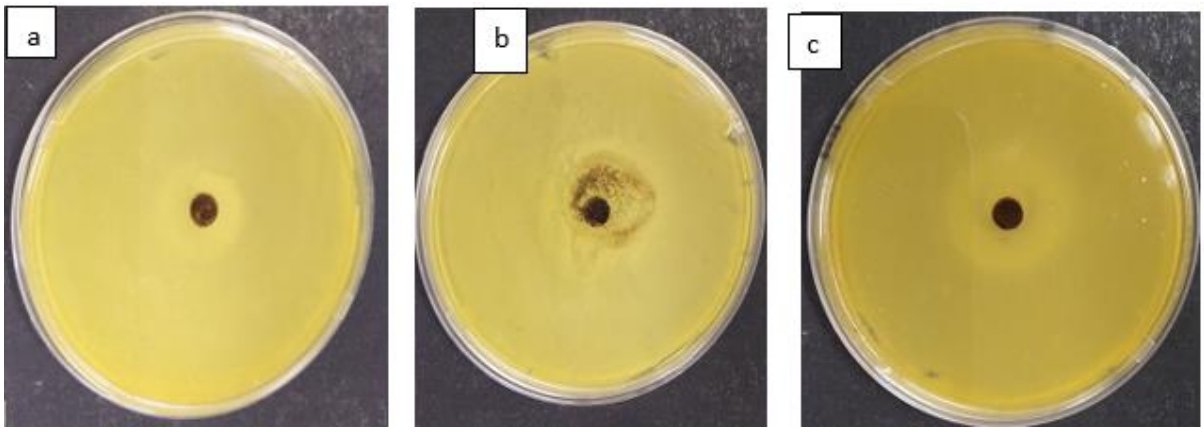

Figure 3.14: A representative petri dish of different bacteria (a) *Escherichia Coli*, (b) *Staphylococcus Aureus* and (c) *Klebsiella Pneumoniae.*

3.5 Conclusion

In this chapter, the physicochemical characteristics of MNS and its application towards fluoride and pathogen removal were studied. The results showed that the material consist of carbon 49.56% (C), hydrogen (H), nitrogen 0.20% (N) and oxygen 44.08% (O). Batch experiments showed the maximum fluoride removal of 42.27% from 5 mg/L initial fluoride concentration when 0.5 g/100 mL adsorbent dosage was used at pH 6 after 120 min contact time. The presence of co-existing ions enhanced the performance of fluoride removal. Moreover, regeneration studies demonstrated that the adsorbent can be regenerated for up to 7 cycles using 0.01 M HCl. The adsorption of fluoride onto MNS powder follow pseudo second order of reaction kinetics model indicating that fluoride ions removed through chemisorption. The adsorption data fitted better to Langmuir than Freundlich adsorption isotherm model which suggest monolayer coverage. The value ΔG^{o} was found to be negative indicating that adsorption of fluoride onto MNS was spontaneous and favourable. According to the findings MNS possesses no anti-microbial activity. Although the MNS showed potential towards F^{-} removal, this study further recommends the modification of MNS with nanoparticles and other metal oxides to enhance its efficiency towards fluoride removal as well as the potency towards anti-microbes.

3.6 References

Ahmed, M., 2019. Characterization of the Yousoufia Morocco mine fluoride contaminated water and their detrimental effects on human health. In *Fluoride Pollution-Facts and Fundamental Findings of Health and Environmental Remediation*, p3.

Albadarin, A.B., Ala'a, H., Al-Laqtah, N.A., Walker, G.M., Allen, S.J. and Ahmad, M.N., 2011. Biosorption of toxic chromium from aqueous phase by lignin: mechanism, effect of other metal ions and salts. *Chemical Engineering Journal*, *169*(1-3), pp.20-30.

Alomá, I.D.L.C., Rodriguez, I., Calero, M. and Blazquez, G., 2014. Biosorption of Cr6+ from aqueous solution by sugarcane bagasse. *Desalination and Water Treatment*, *52*(31-33), pp.5912-5922.

Altun T. and Pehlivan E., 2012 Removal of Cr (VI) from aqueous solutions by modified walnut shells. *Food Chemistry* 132, pp.693–700.

Antal, M.J. and Grønli, M., 2003. The art, science, and technology of charcoal production. *Industrial & Engineering Chemistry Research*, *42*(8), pp.1619-1640.

Ayinde, W.B., Gitari, W.M., Munkombwe, M. and Amidou, S., 2018. Green synthesis of Ag/MgO nanoparticle modified nanohydroxyapatite and its potential for defluoridation and pathogen removal in groundwater. *Physics and Chemistry of the Earth, Parts A/B/C*, 107, pp.25-37.

Bullen, J.C., Saleesongsom, S., Gallagher, K. and Weiss, D.J., 2021. A Revised Pseudo-Second-Order Kinetic Model for Adsorption, Sensitive to Changes in Adsorbate and Adsorbent Concentrations. *Langmuir*.

Dhillon, J., Liang, Y., Kamat, A.M., Siefker-Radtke, A., Dinney, C.P., Czerniak, B. and Guo, C.C., 2015. Urachal carcinoma: a pathologic and clinical study of 46 cases. *Human pathology*, *46*(12), pp.1808-1814.

Foo, K.Y. and Hameed, B.H., 2010. Insights into the modelling of adsorption isotherm systems. *Chemical engineering journal*, *156*(1), pp.2-10.

Gebrewold, B.D., Kijjanapanich, P., Rene, E.R., Lens, P.N. and Annachhatre, A.P., 2018. Fluoride removal from groundwater using chemically modified rice husk and corn cob activated carbon. *Environmental technology*.

Gitari, W.M., Izuagie, A.A. and Gumbo, J.R., (2017). Synthesis, characterization and batch assessment of groundwater fluoride removal capacity of trimetal Mg/Ce/Mn oxide-modified diatomaceous earth. http://dx.doi.org/10.1016/j.arabjc.2017.01.002

Gitari, W.M., Ngulube, T., Masindi, V. and Gumbo, J.R., 2015. "Defluoridation of groundwater using Fe^{3+} modified bentonite clay: optimization of adsorption conditions". *Desalination and Water Treatment*, 53(6), pp.1578-1590.

Gupta, S.S. and Bhattacharyya, K.G., 2011. Kinetics of adsorption of metal ions on inorganic materials: a review. *Advances in colloid and interface science*, *162*(1-2), pp.39-58.

Hoekstra, A.Y., 2014. Water scarcity challenges to business. *Nature climate change*, *4*(5), p.318.

Izuagie, A.A., Gitari, W.M. and Gumbo, J.R., 2016. Defluoridation of groundwater using diatomaceous earth: optimization of adsorption conditions, kinetics and leached metals risk assessment. *Desalination and Water Treatment*, 57(36), pp.16745-16757.

Kimambo, V., Bhattacharya, P., Mtalo, F., Mtamba, J. and Ahmad, A., 2019. Fluoride occurrence in groundwater systems at global scale and status of defluoridation state of the art. *Groundwater for Sustainable Development*, p.100223.

Marshall, J., Kushnir, Y., Battisti, D., Chang, P., Czaja, A., Dickson, R., Hurrell, J., McCARTNEY, M.I.C.H.A.E.L., Saravanan, R. and Visbeck, M., 2001. North Atlantic climate variability: phenomena, impacts and mechanisms. *International Journal of Climatology: A Journal of the Royal Meteorological Society*, *21*(15), pp.1863-1898.

Mudzielwana, R., Gitari, W.M. and Ndungu, P., 2018. Evaluation of the adsorptive properties of locally available alumino-silicate clay in As (III) and As (V) remediation from groundwater. *Physics and Chemistry of the Earth, Parts A/B/C*.

Mukherjee, I. and Singh, U.K., 2018. Groundwater fluoride contamination, probable release, and containment mechanisms: a review on Indian context. *Environmental geochemistry and health*, *40*(6), pp.2259-2301.

Ncube, E.J. and Schutte, C.F., 2005. "The occurrence of fluoride in South African groundwater: A water quality and health problem". *Water SA*, 31(1), pp.35-40.

Newell, D.G., Koopmans, M., Verhoef, L., Duizer, E., Aidara-Kane, A., Sprong, H., Opsteegh, M., Langelaar, M., Threfall, J., Scheutz, F. and van der Giessen, J., 2010. "Food-borne diseases—the challenges of 20 years ago still persist while new ones continue to emerge". *International journal of food microbiology*, 139, pp3-15.

Odiyo, J.O. and Makungo, R., 2012. Fluoride concentrations in groundwater and impact on human health in Siloam Village, Limpopo Province, South Africa. *Water SA*, *38*(5), pp.731-736.

Pakade, V.E., Ntuli, T.D. and Ofomaja, A.E., 2017. Biosorption of hexavalent chromium from aqueous solutions by Macadamia nutshell powder. *Applied Water Science*, *7*(6), pp.3015-3030.

Saini, S., Belgacem, M.N., Missoum, K. and Bras, J., 2015. Natural active molecule chemical grafting on the surface of microfibrillated cellulose for fabrication of contact active antimicrobial surfaces. *Industrial Crops and Products*, *78*, pp.82-90.

Sargunar, C.G., 2020. Occurrence of indicator bacteria and pathogens in the waters of the noyyal river near its source and downstream in Coimbatore district. *Kongunadu Research Journal*, *7*(2), pp.68-80.

Simonin, J.P., 2016. On the comparison of pseudo-first order and pseudo-second order rate laws in the modelling of adsorption kinetics. *Chemical Engineering Journal*, *300*, pp.254-263.

Soupir, M.L., Hoover, N.L., Moorman, T.B., Law, J.Y. and Bearson, B.L., 2018. Impact of temperature and hydraulic retention time on pathogen and nutrient removal in woodchip bioreactors. *Ecological Engineering*, *112*, pp.153-157.

Tran, H.N., You, S.J. and Chao, H.P., 2016. Thermodynamic parameters of cadmium adsorption onto orange peel calculated from various methods: a comparison study. *Journal of Environmental Chemical Engineering*, *4*(3), pp.2671-2682.

Weber Jr, W.J. and Morris, J.C., 1964. Equilibria and capacities for adsorption on carbon. *Journal of the Sanitary Engineering Division*, *90*(3), pp.79-108.

WHO/UNICEF Joint Water Supply, Sanitation Monitoring Programme, World Health Organization, WHO/UNICEF Joint Monitoring Programme for Water Supply, Sanitation and UNICEF., 2017. Water for life: Making it happen. World health organization.

World Health Organization and UNICEF, 2017. "Progress on drinking water, sanitation and hygiene: update and SDG baselines".

Yang, H., Dong, Z., Liu, B., Chen, Y., Gong, M., Li, S. and Chen, H., 2021. A new insight of lignin pyrolysis mechanism based on functional group evolutions of solid char. *Fuel*, *288*, p.119719.

Zhang, Y. and Huang, K., 2019. Grape pomace as a bio-sorbent for fluoride removal from groundwater. *RSC advances*, *9*(14), pp.7767-7776.

Zhao X., Chen J., Chen F., Wang X., Zu Q. and Ao Q., 2013. Surface characterization of corn stalk superfine power studied by FTIR and XRD. *Colloids Surf B Biointerface 104*, pp. 207-212.

CHAPTER 4: Fabrication of macadamia nutshell powder-Al/Fe metal oxide Modified diatomaceous earth composite beads for fluoride and pathogen removal.

Abstract

In the previous chapter, the efficiency of Macadamia nutshell (MNS) towards fluoride and pathogen removal from groundwater was evaluated. It was found that the optimum fluoride removal of 48% was achieved at initial pH of 6 using adsorbent dosage of 0.5 g. Furthermore, the material showed no antimicrobial activities. This chapter aims at improving the percentage fluoride removal of MNS by fabricating a composite bead from MNS and Al/Fe metal oxides Modified diatomaceous earth (DE) using sodium alginate as binder and further evaluate their efficiency towards fluoride and pathogen removal from drinking water. The physicochemical compositions of the material were characterized using SEM, FTIR, SEM EDX and XRF. The fluoride removal efficiency of the material was evaluated using batch and fixed bed column experiments while the anti-microbial potency was evaluated using the well assay diffusion methods. A maximum fluoride sorption capacity of 2.61 mg/g was achieved at initial fluoride concentration of 5 mg/L using adsorbent dosage of 0.9 g/100 mL at pH 4 and shaking time of 120 min. The presence of co-existing ions decreased the fluoride removal efficiency. The kinetics data for fluoride adsorption by MNS-Al/Fe metal oxides Modified DE composite beads followed pseudo-second order model of reaction kinetics implying that the dominant mechanism for fluoride removed is chemisorption. The isotherm data fitted better to Langmuir isotherm model as compared to Freundlich adsorption isotherm which suggest monolayer coverage. The thermodynamics parameters such as ΔG^{o} and ΔH^{o} revealed that adsorption of fluoride by the composite adsorbent is endothermic and spontaneous and ΔS^{o} indicated that fluoride ions where randomly distributed on the surface of the adsorbent. The column experiments showed that the bed height of 40 mm is the most effective towards fluoride removal showing the maximum adsorption capacity of 0.49 mg/g and treated 1.8 L at breakthrough point and 9.2 L at exhaustion point with adsorption capacity of 1.43 mg/g. The MNS-Al/Fe Modified DE composite beads were successfully regenerated and reused for up to 5 successive cycles using deionised water as regenerating eluent. The developed beads showed a minimal inhibition zone towards *Klebsiella Pneumoniae* and no inhibition towards *Escherichia Coli* and *Staphylococcus Aureus*. This chapter concluded that the beads have potential for use in defluoridation as well as in anti-microbial towards *Klebsiella Pneumoniae*.

Keywords: Fluoride, Pathogens, Defluoridation, anti-microbial activity, and groundwater.

4.1 Introduction

Groundwater contamination by fluoride and pathogen world-wide has become the great concern worldwide. High intake of water contaminated by fluoride and pathogens leads to dental and skeletal fluorosis, cholera, and diarrhoea (Ahmad *et al*., 2020 and Palansooriya *et al.*, 2020). Contamination of groundwater by fluoride occurs through natural and anthropogenic sources. The natural process includes weathering of fluoride-bearing minerals, volcanic eruptions, and the marine aerosols. The anthropogenic source includes the application of fertilizers in agricultural field, coal combustion and cement manufacturing are also contributing to the release of fluoride into the groundwater (Sahu, 2019; Malago *et al*., 2020). Groundwater contamination by pathogen occurs through run-off water from farms, sewage and hospital waste (Arun *et al.*, 2020).

Because of the health concerns caused by exposure to water contaminated by pathogens and fluoride, there is a need to develop a cheap and effective multi-functional adsorbent to use for fluoride and pathogen removal from groundwater. Obijole *et al*., 2021 use mechanochemically activated aluminosilicate clay for fluoride and pathogen removal from water and it showed optimum fluoride sorption capacity of 2.75 mg/g with about 52% fluoride removal. Moreover, when testing the adsorbent for microbial potency it showed promising antibacterial potency against the *E. coli.* Ayinde *et al*., 2018 use Ag/MgO nanoparticle modified nanohydroxyapatite for pathogen and fluoride removal and find that the optimum adsorption capacity of 2.146 mg/g at 298 K was achieved with more than 90% fluoride removal and also show strong antibacterial activity against *E. coli and K. pneumonia*.

Diatomaceous earth is commonly known for its application in water treatment. Izuagie *et al.* (2016) synthesized Al/Fe metal oxide modified diatomaceous earth for fluoride removal in groundwater. Their results showed optimum adsorption capacity was 7.633 mg/g for initial concentration 100 mg/L fluoride at 297 K. The same material was further tested by Nekhavhambe (2017) for its applicability at household fluoride removal using gravity flow column set up experiments. The results showed that Al/Fe metal oxide modified diatomaceous is limited by low flow rate. Flow rate significantly affects the performance of column in continuous mode study, and it is an important parameter for evaluating the efficiency of adsorbent in continuous treatment process (Afroze *et al*., 2016; Patel, 2019). The low flow rate is caused by the compaction of the material when packing the column (Patel, 2019). When the flow rate of influent is low, the influent has more time to contact with the adsorbent resulting in shallow adsorption as well as high percentage removal (Gong *et al*., 2015; Afroze *et al*.,

2016). At higher flow rate, the influent has no time to interact with the adsorbent there by leading to faster saturation point and also reduction in removal efficiency (Afroze *et al*., 2016).

In the bid to enhance the hydraulic properties of Al/Fe metal oxide modified diatomaceous earth and to enhance the effectiveness of macadamia nutshells, in this chapter, composite beads were prepared from MNS and Al/Fe metal oxides modified diatomaceous earth using sodium alginate as a binder. The material was thereafter tested for its efficiency towards fluoride and pathogen removal from groundwater. The following specific objectives were set for this chapter: i) to evaluate the optimum ratio for preparing MNS–Al/Fe metal oxides modified DE composite beads , ii) to determine the physicochemical characteristics of MNS-Al/Fe Modified DE alginate composite beads iii) to evaluate the effectiveness of the beads in fluoride removal using batch and column experiments, iv) to model the adsorption data using adsorption kinetics and isotherm models, v) to evaluate the reusability of MNS-Al/Fe Modified DE alginate composite beads towards in fluoride removal and lastly, vi) to determine the anti-microbial potency of the MNS-Al/Fe Modified DE alginate composite beads.

4.2 Methods and materials

4.2.1 Sample collection

Macadamia nutshells were collected from Levubu Royal Macadamia in Vhembe district Limpopo Province, South Africa. The diatomaceous earth (DE) was collected from Karandusi in Gilgil District, Nakuru, Kenya. Sodium hydroxide (NaOH), hydrochloric acid (HCl), potassium chloride (KCl) sodium fluoride (NaF), Total Ionic Strength Adjustment Buffer (TISAB III), calcium chloride ($CaCl_2$), Aluminium sulphate $Al_2(SO_4)_3.18H_2O$, Iron(lll) chloride hexahydrate ($FeCl_3.6H_2O$), sodium alginate and other chemical reagents used in this study were of analytical grade reagents and were purchased from Rochelle Chemicals, Johannesburg, South Africa. All chemicals were used without further purification.

4.2.2 Preparation Al/Fe metal oxide modified diatomaceous earth

The modification of DE by Al/Fe metal oxides was carried out following the procedure optimized by Izuagie *et al*. (2017). Briefly, the modification was carried out as follows: solutions of 0.25 M Al^{2+} and 0.25 M Fe^{3+} were prepared by dissolving 8.33 g of [$Al_2(SO_4)_3.18H_2O$ and 6.76 g of ($FeCl_3.6H_2O$)] in 100 mL volumetric flask, respectively. The two solutions were added in 1000 mL plastic bottle at a ratio of 1:1. Thereafter, 15 g of clean DE was dispersed in the solution and shaken using reciprocating shaker at 200 rpm for 20 min for proper soaking. Precipitation of the solution was affected by adjusting the pH to 8.2 using

NaOH. The mixture was agitated on a reciprocating shaker at 100 rpm for 50 min. The mixture was then centrifuged to remove excess NaOH while the solid was washed with Milli-Q water until it could turn phenolphthalein to red. After the equilibration the mixture was centrifuged to recover the solid by discarding the supernatant. The washed solid was dried in the EcoTherm oven model no.920, Labotec at 110 °C for 8 h, cooled in the desiccator and then stored in corked plastic bottles for subsequent use.

4.2.3 Macadamia nutshell powder-Al/Fe metal oxides modified DE composite beads

The MNS-Al/Fe metal oxides modified DE composite beads (MNS-Al/Fe metal oxides DE beads) were prepared as follows; a mass of 3 g sodium alginate was weighed and dissolved in 100 mL of Milli-Q water until homogeneous was obtained. MNS and Al/Fe oxides modified DE were then added onto the prepared sodium alginate solution at mass ratios of 1:1, 1:2, 2:1, 3:1 and 3:1 and the suspensions were stirred at 350 rpm for 6 hours at room temperature. Thereafter, homogenised mixtures were slowly dropped using a funnel into 800 mL beaker containing 0.1 M of $CaCl_2$ to form beads of roughly uniform size. Therefore, the beads were kept in $CaCl_2$ solution over night to allow the beads harden. Thereafter, the beads were then separated from $CaCl_2$ and washed using deionized water and dried in an EcoTherm oven at temperature of 80 °C for overnight. Figure 4.1 depicts the schematic diagram for beads formation process. Batch defluoridation were carried out to determine the optimum mass ratio for preparing the composite beads as follows: 3 g of DE and 1 g of MNS were weighed and added into the 250 mL plastic bottles each containing 100 mL of 5 mg/L of fluoride solution. Mixtures were shaken using table shakers at 250 rpm for 60 min and the final concentration of fluoride was measured using ion selective electrode attached to fluoride multi-meter and calibrated using four standards (0.1, 1.0, 10 and 100 mg/L) containing ratio TISAB III to solution of 1:10. The mass ratio with the highest fluoride removal was then used in further experiments.

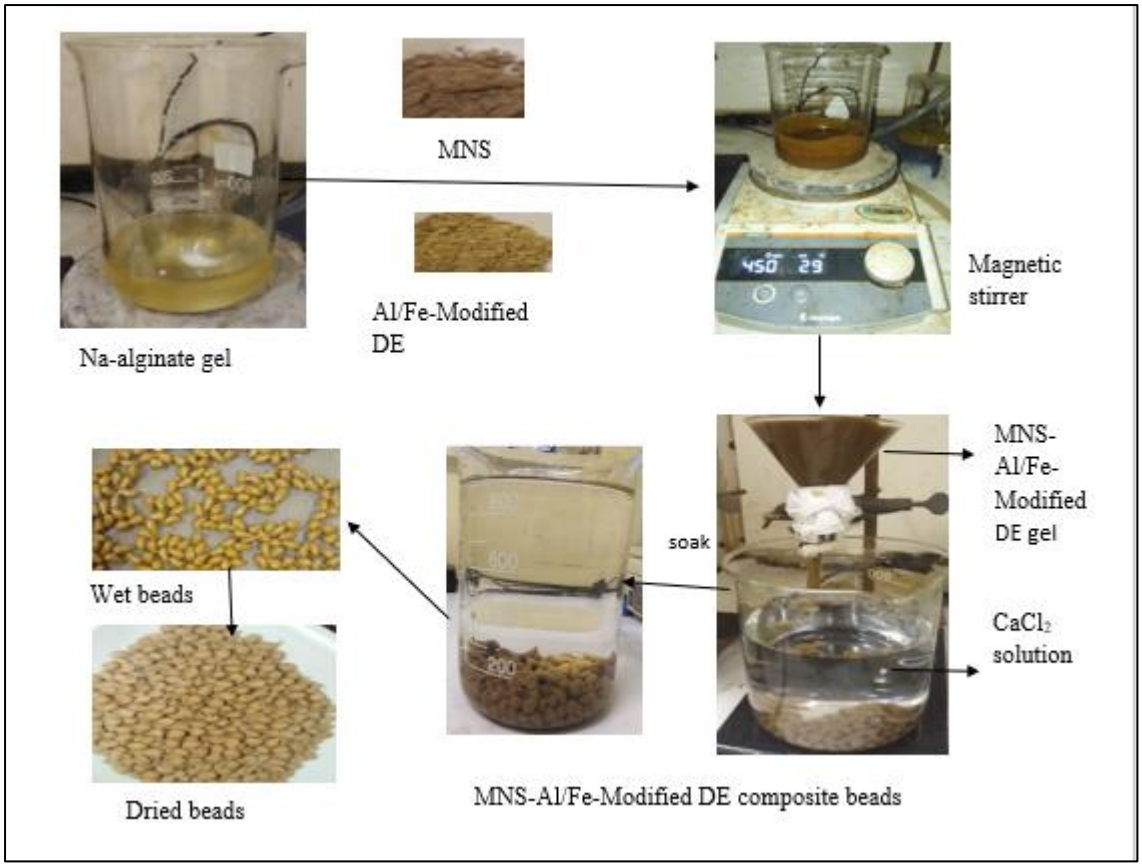

Figure 4.1: Schematic diagram for preparation of MNS-Al/Fe metal oxides DE beads.

4.2.4 Characterisation of the adsorbent

The elemental compositions of MNS-Al/Fe metal oxides DE beads were determined using Thermo Flash 2000 Series CHNS/O organic Elemental analyser and also by Bruker Titan S1 Handheld X-Ray Fluorescence. The functional groups of the materials were determined using Bruker Alpha Platinum-ATR Fourier transformation infrared spectroscopy (FTIR). The crystallinity was determined using D8 advanced X-ray diffract meter (XRD) (Bruker) with Cu-Kα Radiation as source. Surface morphology was determined using scanning electron microscope (SEM) (Leo1450 SEM, at kv, working distance 14 mm). Pore size distribution, pore volume and surface area were determined using Barrett Joyner Halenda (BJH) sorption model using a specific surface area analyser (Autosorb-IQ and quadrasorb SI, USA). The pHpzc was evaluated using solid addition method (Gitari et al., 2017). Physical parameters such as size was measured using a ruler in mm. the volume of the beads was measured using volume displacement method using equation (4.1). Further, moisture level of the beads was analysed by calculating the percentage difference between the wet weight and the dry weight and the bulk density for the dried beads was calculated based on mass (g) and volume obtained.

$$m\% = \frac{initial\ weight - final\ weight}{initial\ weight} \quad (4.1)$$

4.2.5 Batch fluoride adsorption experiment

Batch experiments were used to determine the optimum conditions (such as contact time, adsorbent dosage, adsorbate concentration and pH) for fluoride removal. To evaluate the contact time, 100 mL of solution containing 5 mg/L of fluoride was prepared and pipetted into 250 mL plastic bottles. Thereafter, 0.9 g of MNS-Al/Fe metal oxides DE beads was added to make up 0.9 g/100 mL adsorbent dosage and mixtures were then agitated for 5, 10, 15, 20, 25, 30, 40, 50, 60, 90, 120, and 150 min using reciprocating table shaker. After agitation, samples were filtered through 0.45 µm pore membrane and the residual fluoride concentration determined using ion selective electrode attached to fluoride multi-meter and calibrated using four standards (0.1, 1.0, 10 and 100 mg/L) containing ratio TISAB III to solution of 1:10. The same ratio was maintained for sample analysis. The effect of pH on fluoride sorption by MNS-Al/Fe metal oxides DE beads was evaluated by varying the initial solution pH from 2 to 12 using 0.1 M NaOH and 0.1 M HCl to adjust the solution pH. Adsorbent dosage of 0.9 g/100 mL and initial concentration of 5 mg/L were used. Mixtures were agitated for 120 mins. The effect of adsorbent dosage was evaluated by varying the adsorbent dosage from 0.1 to 1 g/100 mL using initial concentration of 5 mg/L. Solution pH was adjusted to 4±0.9 and mixtures were agitated for 120 min. The effect of initial fluoride concentration was evaluated by varying initial fluoride concentration from 5 to 30 mg/L. The experiment was conducted at temperature of 298, 308 and 318 K. Adsorbent dosage of 0.9 g/ 100 mL and initial pH of 4±0.9 were used. Mixtures were agitated for 120 mins. To evaluate the effect ions in fluoride removal was done using 5 mg/L of SO_4^{2-}, Cl^-, NO_3^-, CO_3^{2-}, Ca^{2+} and Mg^{2+} were prepared separately and mixed with 5 mg/L of fluoride solution. The adsorbent dosage of 0.9 g/100 mL and initial pH of 4±0.9 and mixtures were shaken for 120 mins. All experiments were conducted in duplicate for better accuracy and the average value were reported. The percentage of fluoride removal and the adsorption capacity of MNS were computed using equation 4.2 and 4.3 respectively.

$$\%\ Fluoride\ removal = \left(\frac{C_0 - C_e}{C_0}\right) \times 100 \quad (4.2)$$

$$Q = \left(\frac{C_0 - C_e}{m}\right) \times v \quad (4.3)$$

Where: Co is the initial fluoride ion concentration (mg/L); Ce is the fluoride ion concentration at equilibrium (mg/L); v is the volume of the solution (L) and m mass of the adsorbent (g).

4.2.6 Column Experiments

For column experiments, two syringes of about 135 mm height with a diameter of 26 mm were used. Beads weighing 14 and 18 g were added into the column to make up the bed height of 30 and 40 mm, respectively. The beads were fused in between the glass wool, the glass wool was used to support the column and to avoid the breaking of column. Figure 4.2 depicts the column setup. A feed water containing initial F^- concentration of 5 mg/L was poured continuously to pass through the bed on a gravity flow mode. Effluents were collected at intervals of 1 hour throughout the experiment. The final fluoride concentration, EC, TDS and pH of the effluent collected were measured immediately after collection. Equation 4.4 and 4.5 were used to calculate the adsorption capacity at breakthrough point and at exhaustion point, respectively.

$$q_b = \int_0^{V_b} \left(\frac{C_o - C_e}{m}\right) v \quad \text{..... (4.4)}$$

$$q_e = \int_0^{V_e} \left(\frac{C_o - C_e}{m}\right) v \text{..... (4.5)}$$

Where: V_b and V_e is volume at breakthrough point and exhaustion point, respectively (L), C_e is concentration at breakthrough, m is the mass of adsorbent in g, while V is the volume of fluoride solution in L.

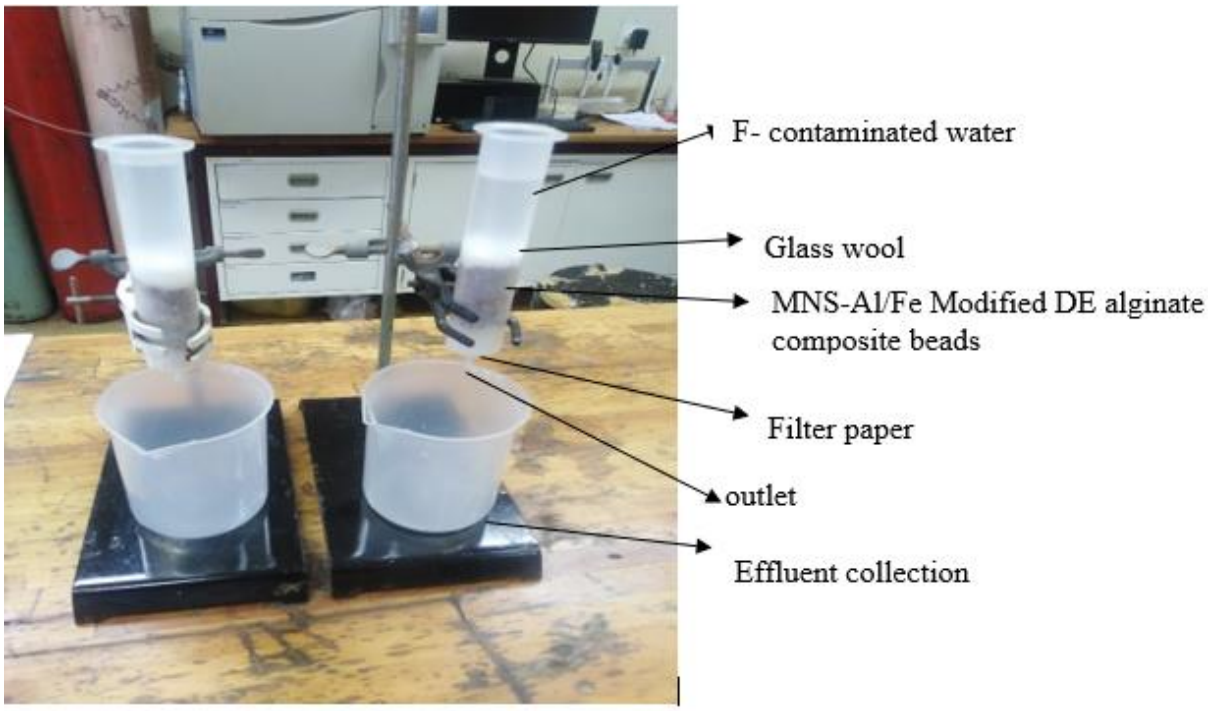

Figure 4.2: Fixed-bed column experimental set up.

The column performance was assessed by calculating the bed volume (BV) as well as the adsorbent exhaustion rate (AER) using equation 4.6 and 4.7, respectively.

$$BV = \frac{volume\ of water\ treated\ at\ breakthrough\ point\ (L)}{volume\ of\ adsorbent\ bed\ (L)} \quad (4.6)$$

$$\text{AER} = \frac{mass\ of\ adsorbent}{volume\ of\ water\ treated} \quad (4.7)$$

4.2.7 Regeneration and re-use of the adsorbent

The regeneration of the adsorbent was carried out as follows: 0.9 g of MNS-Al/Fe metal oxides modified DE beads loaded with fluoride desorbed through agitation with 100 mL of deionised water for 120 min reciprocating shaker. After agitation, beads were recovered by filtering the mixtures through 0.45 µm pore membrane and then kept in an oven dried at 110 ^{O}C for 3 h. The regeneration was evaluated through batch shaking experiment.

4.2.8 Anti-microbial studies

Anti-microbial activity of the MNS-Al/Fe metal oxides modified DE beads was investigated using well disc diffusion assay method (Kirby-Bauer method). A solution of 100 mL of Mueller-Hinton agar broth was prepared by dissolving 2.1 g in milli-Q water. The solution was autoclaved for 15 min at 121 ^{O}C for sterilisation. After autoclaving the solution was left to cool

at room temperature. Thereafter, 5 mL of the broth was pipetted into 15 mL different tubes and about 3-4 colonies of *E. coli, S. Aureus* and *K. Pneumoniae* bacterial strains were inoculated in each of the tube containing broth. Bacterial strains were grown at 37 ^{o}C in an incubator for a period of 3 hours. Thereafter, about 20 mL of agar was dispersed in the plates and bacterial strains were spread on the surface of the agar plate using a swab. Therefore, 0.1 g of the adsorbent was weighed and was dissolved in 1 mL of milli-Q water and left for overnight to completely dissolve. The well was dug in the agar in order to put the adsorbent in it. The adsorbent was introduced onto the well in the agar plate and stored in an incubator at 37 ^{o}C for 48 hrs. Thereafter, measurements of diameter from exterior of absorbent to end point of the inhibition zone were done and subsequently the values were implemented on analysis of MNS-Modified DE composite beads adequacy on anti-bacterial activity.

4.3. Results and discussion

4.3.1 Effect of MNS-Al/Fe metal oxide beads ration on fluoride removal

The results of the batch experiments conducted with the beads prepared at varying mass ratio are prepared in Table 4.1. Results showed that the beads prepared at the ratio of 1:3 yielded higher percentage fluoride removal (55.26%) as compared to the other materials prepared at other ratios. Therefore, ratio of 1:3 was adopted as the optimum ratio for preparing the composite beads and was therefore characterized and further used on subsequent fluoride removal experiments.

Table 4.1. Percent fluoride removal by Raw MNS and Al/Fe oxide-modified DE, Na-alginate composite beads containing different ratios (5 mg/L F^-, 60 min, 250 rpm and pH 6.25)

MNS: Modified DE	Final pH	F^- (mg/L)	% Fluoride removal
1:1	6.38	3.61	40.03
1:2	6.15	3.62	40.00
2:1	6.53	3.57	40.64
3:1	6.29	3.26	45.79
1:3	6.23	2.69	55.26

4.3.2 Physical characteristics and the surface area, pore distribution and pore volume

The size (diameter) of the beads was ranging between 2 to 3 mm. The volume displacement method revealed that the beads have a volume of 0.8 mL and the density of 1.13 g/mL. The surface area, pore volume and pore size are depicted in Table 4.2. The surface area of MNS and the Al/Fe metal oxide modified DE were found to be 1.69 and 27.60 m^2/g, respectively. The MNS-Al/Fe metal oxide DE beads had lower surface area as compared to the parent materials with the surface area of 6.72 m^2/g. This could be attributed to the fact the that the introduction of low surface area MNS affects the surface area of the resulting composite and also binder dilute the surface area of the composite. The beads were also found to be having lower pore volume and pore diameter as compared to MNS and the Al/Fe metal oxide modified DE (Table 4.2). The surface area, pore volume and pore diameter further decreased after fluoride removal to 4.35 m^2/g, 0.006 cm^3/g and 5.246 nm, respectively. This could be attributed to the fact that fluoride ions covered up the surface space of adsorbent surface. The decrease in pore volume is because of the introduction of binder which cover up the surface pore limiting the flow rate in column experiment. In comparison with Al/Fe modified DE the flow rate was low.

Table 4.2. The surface area, pore volume and pore size MNS-Al/Fe oxide modified DE beads

	Surface area (m^2/g)	Pore volume (cm^3/g)	Pore diameter (nm)
Al/Fe metal oxide DE	27.60	0.041	6.021
MNS	1.69	15.4	0.01
MNS-Al/Fe metal oxide DE beads	6.27	0.00082	5.504
F^- loaded MNS-Al/Fe metal oxide DE beads	4.35	0.006	5.246

4.3.3 Elemental composition

The elemental composition of raw MNS, raw DE, Al/Fe metal oxide modified DE, MNS-Al/Fe metal oxides modified DE beads (composite beads), and composite beads F^- loaded is presented in Table 4.3. The results showed that MNS is mainly composed of carbon (49.56%), oxygen (44.08%) and hydrogen (6.19%). The raw DE show that is mainly compose of SiO_2 and CaO

as the main oxides averaging 83.92 and 7.5%, respectively. After modification of raw DE by Al and Fe oxides, the percentage composition of Al_2O_3 and Fe_2O_3 increased to 5.18 and 9.69% respectively and this confirm that raw DE was successfully coated with Al and Fe oxides. The beads were mainly consisting of SiO_2 (63.23%), CaO (12.73), Al_2O_3 (3.98%) and Fe_2O_3 (5.40%) as the major oxides in the adsorbent. The increase in CaO could be attributed the use of $CaCl_2$ as crosslinking agent. After F^- removal there was a decrease in SiO_2 (56.51%), CaO (11.63%), Al_2O_3 (1.81%) and Fe_2O_3 (3.29%). This could be due to dilution of F ions as a results of surface complexation.

Table 4.3: Chemical analysis of MNS-Al/Fe metal oxide modified DE beads

Element/ oxide	MNS (%)	Raw DE (%)	AL/Fe Modified DE (%)	Composite beads (%)	Composite beads F-loaded (%)
MgO	0.97	0.56	0.54	0.90	0.614
SiO_2	0.44	83.92	72.37	63.23	56.51
CaO	0.25	7.50	3.45	12.73	11.63
Al_2O_3	0.16	0.69	5.18	3.98	1.81
P_2O_5	0.01	0.19	0.04	0.06	0.07
FeO3	-	0.69	9.69	5.40	3.29
C	49.56		-	-	-
O	44.08		-	-	-
H	6.20		-	-	-

4.3.4 Functional groups

Figure 4.3 show the spectra of MNS, Al/Fe metal oxide DE, sodium alginate, MNS- Al/Fe metal oxide DE beads (composite beads) and F^- loaded MNS- Al/Fe metal oxide DE. The raw MNS spectra showed wide transmittance band at wavelength region of 3351 cm^{-1} which is attributed to stretching and vibration of hydroxyl (OH^-) groups associated with the hydrogen bond in absorbed moisture and cellulose structure (Zhao *et al.*, 2013). The band at 1738 cm^{-1} is linked to carboxylic group (C=O). The bands at 1454 cm^{-1} can be assigned to the stretching of C-C bond. The band at 1248 cm^{-1} indicating the C-OH together with the band of C-O at 1030 cm^{-1} linked to the vibration and stretching of the phenols, ketones, ethers and esters in the surface of the adsorbent. The transmittance bands of Al/Fe metal oxides modified DE (Fig

4.3b) were observed at wavelength range of 918 cm^{-1} and 797 cm^{-1}, 1069 cm^{-1} and 3360 cm^{-1}. The band at 3360 cm^{-1} is attributed to stretching and vibration of hydroxyl (OH^-) groups. The band at lower frequencies, a band between 1000 cm^{-1} and 1100 cm^{-1} was observed which may be due by stretching and vibration of Si-O groups in the DE. The smaller band at 918 cm^{-1} and 797 cm^{-1} show the stretching vibration of Si-O-Si, Fe-O-Al, Al-O-Si, and Si-O-Fe bands respectively. The spectra of sodium alginate (figure 4.3c) and the strong band and wide band appeared around 3357 cm^{-1} which can be attributed to -OH stretching vibration. The two-small band at 1601 and 1417 cm^{-1} corresponds to C=O of amide group and C–O stretching vibration bands in carboxyl groups, this band was also observed by Zhang *et al.*, (2020) and Qiusheng *et al*., (2015) for the pure sodium alginate and the band at 1032 cm^{-1} is due to the stretching of alcohols, ether, esters and carboxylic acids. The FTIR spectra of the composite beads (Figure 4.3d) showed a broad stretching of -OH band at 3343 cm^{-1} and band at 1599 and 1419 cm^{-1} is ascribed to carboxyl functional group. The band at 819, 915 and 1038 cm-1 are ascribed to Si-O-Si, Fe-O-Al, Al-O-Si, and Si-O-Fe bands, respectively. The similarities on bonds between the parent materials, sodium alginate and the composite beads is that they all have carboxyl functional group. After fluoride removal by MNS-Modified DE alginate composite beads, the band show similar peaks to the ones of composite beads with the decrease intensity. The decrease in intensity could be that the functional groups play a role in fluoride removal.

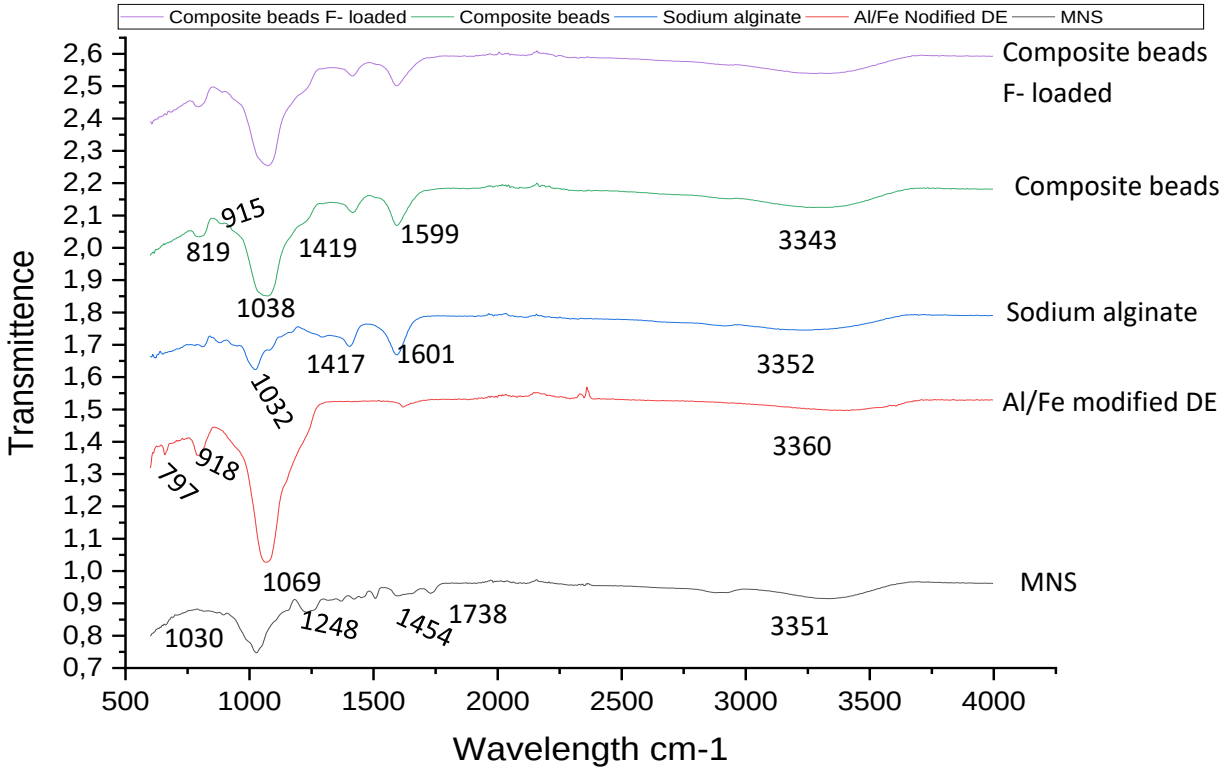

Figure 4.3: FTIR spectra of sodium alginate, MNS-Modified DE Na alginate composite beads and MNS-Modified DE Na alginate composite beads F^- loaded.

4.3.5 Scanning electron spectra analysis

Figure 4.4a-d present the surface micrograph of the raw MNS, MNS-Al/Fe metal oxide DE beads and F^- loaded MNS-Al/Fe metal oxide DE beads. The micrograph of MNS revealed some flaky fold-like structures morphology with some crystals on top (Fig. 4.4a). The micrograph of Al/Fe metal oxide modified DE on the other hand shows porous irregular shape features with some crystalline structures (Fig. 4.4b). After combining the two material and convert them into beads, the morphology appears to have irregular shaped granule with some pore visible (figure 4.4c). After fluoride removal, the surface appears to have broken down into with some cracks. This could be attributed to expansion of the material during fluoride ion adsorption (Fig. 4.4d).

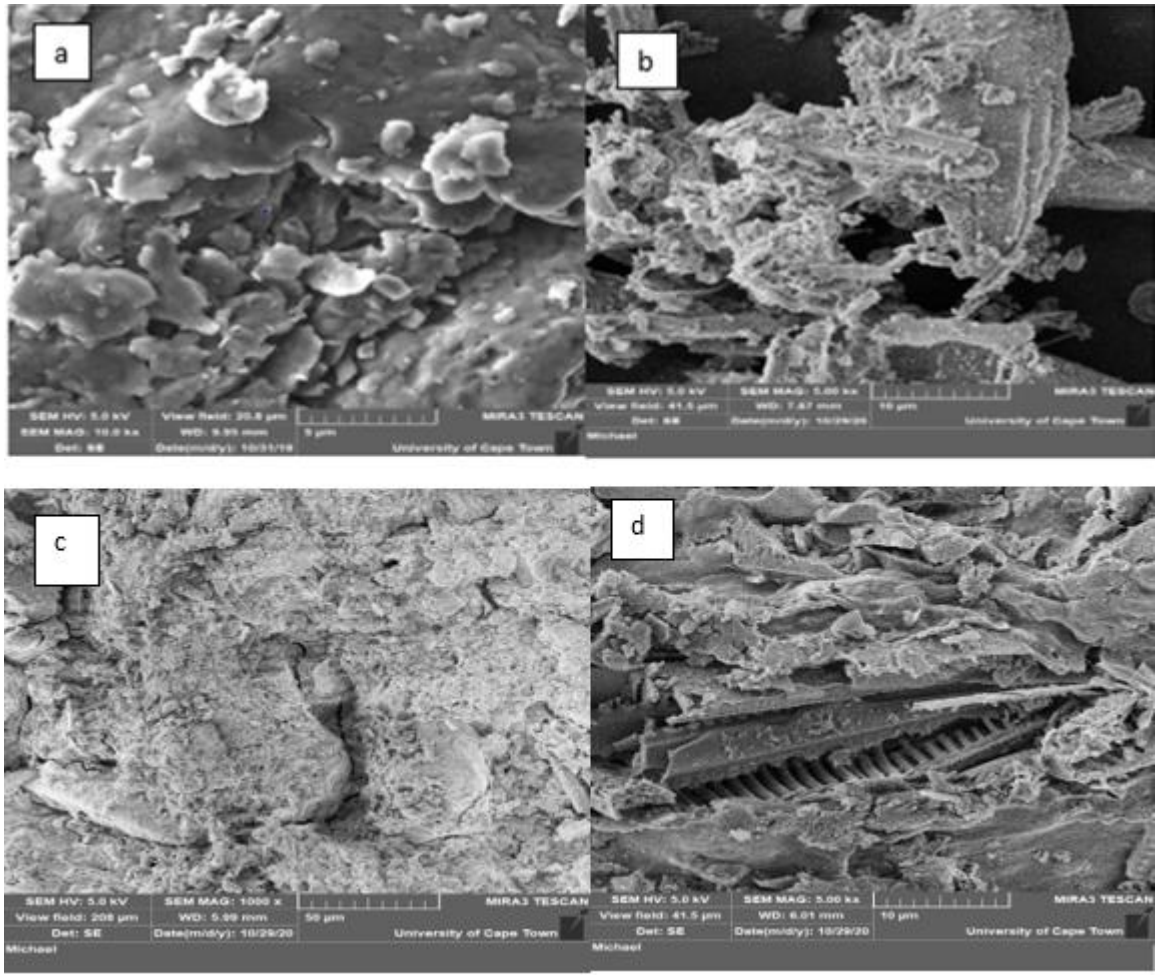

Figure 4.4: Scanning Electron Microscopy a) MNS, b) Al/F metal oxide DE, c) MNS-Al/Fe metal oxide DE beads and d) F^- loaded MNS-Al/Fe metal oxide DE beads.

4.3.6 XRD analysis

The X-ray diffraction patterns of MNS, Al/Fe metal oxide modified DE and MNS- Al/Fe metal oxide modified DE composite beads are depicted in Figure 4.5. The spectra of MNS showed the major diffraction peak at 2θ degree of 17.31^{O}, 22.17^{O} and 34.35^{O} which are related to crystalline native cellulose ($C_6H_{12}O_6$). The spectra of Al/Fe metal oxide modified DE showed major diffraction peaks at 2θ degree angles of 9.84^{O}, 14.71^{O}, 20.89^{O}, 25.63^{O}, 26.63^{O}, 29.72^{O}, 31.92^{O}, 42.25^{O}, 49.26^{O}, 54.08^{O}, and 59.87^{O}. The major mineral phases of Al/Fe metal oxide modified DE spectra are observed at these diffraction angles includes muscovite, calcium sulphate hydrate and quarts, respectively. The spectra of the MNS-Al/Fe metal oxide modified DE composite beads showed major diffraction peaks at 2 theta degrees angels of 24.56^{O} and 27.23^{O} which shows the presence of mainly quarts and a smaller broader bump which is albite intermediate at 34.42^{O}.

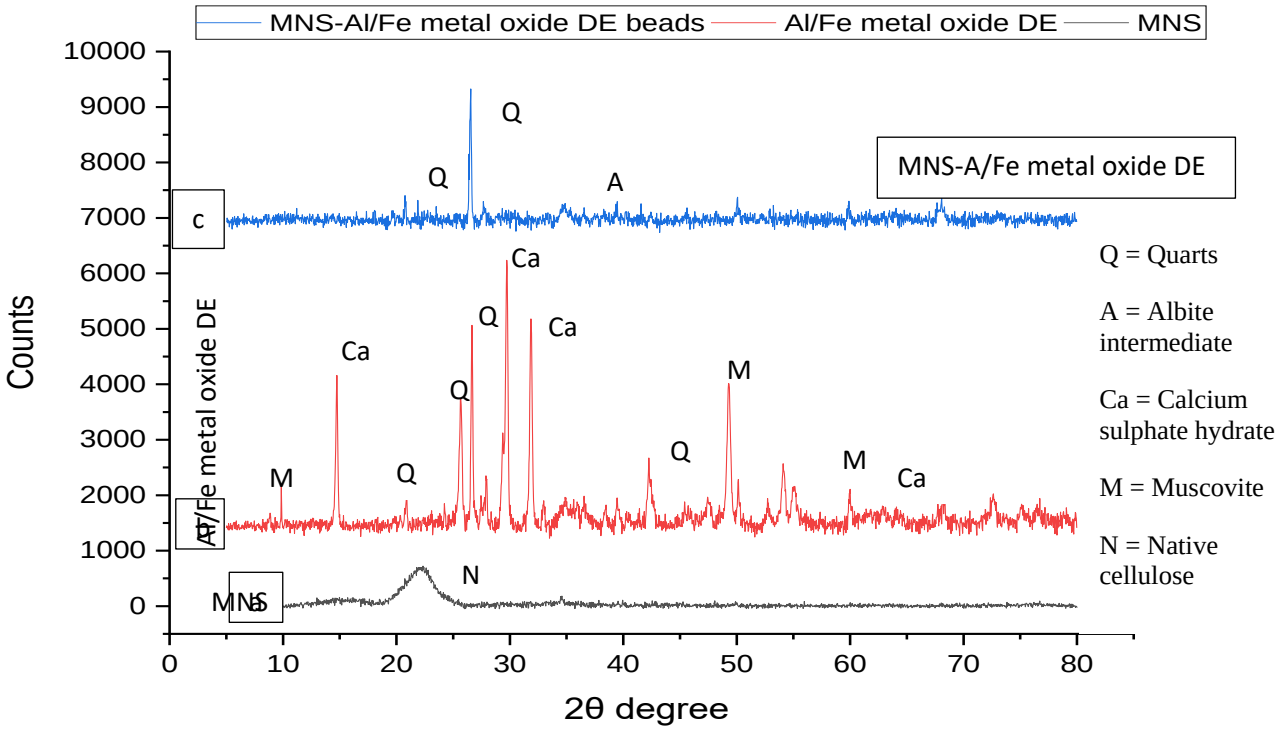

Figure 4.5: XRD patterns of MNS, Al/Fe metal oxide modified DE and MNS- Al/Fe metal oxide modified DE composite beads.

4.4 Batch adsorption experiment

4.4.1 The effect of contact time and adsorption kinetics

Figure 4.6 depicts the variation of adsorption capacity of prepared composite beads against contact time as well as the nonlinear plots for adsorption kinetics models. The fluoride adsorption capacity increase with the increasing contact time from 5 to 120 min where it reached plateau indicating that the system is has reached equilibrium. The rapid fluoride uptake at contact time below 120 min could be attributed to large number of active sites available for fluoride adsorption. Therefore, 120 min was therefore selected as the optimum contact time for used in subsequent experiments.

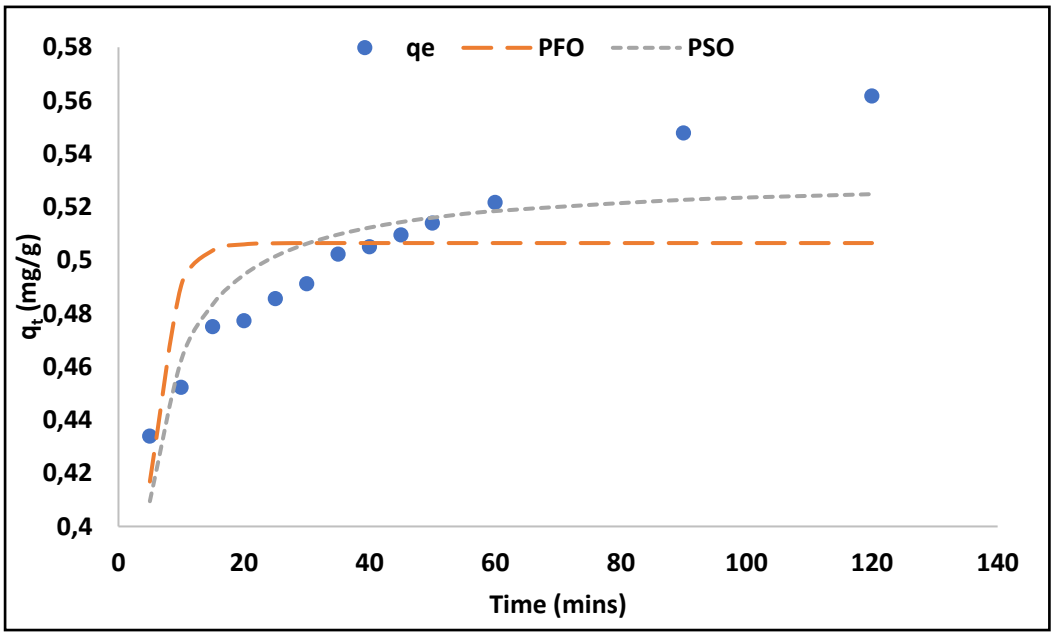

Figure 4.6: Variation of fluoride adsorption capacity as a function of contact time and adsorption kinetics (5 mg/L initial F^- concentration, pH 4, 0.9 g dosage, shaking speed 250 rpm).

In order to elucidate the adsorption mechanism for fluoride sorption by MNS-Al/Fe metal oxides modified DE beads as well as the fluoride adsorption rate limiting step, the adsorption data fitted onto nonlinear equation of pseudo first order and pseudo second order kinetics models as well as the intra-particle diffusion model of Weber and Morris (Gupta and Bhattcharyya, 2011). Pseudo-first order (PFO) is used to describe physisorption process as well as solid-liquid adsorption system. It is given by the equation 4.8 as follows (Gupta and Bhattcharyya, 2011).

$$q_t = q_e(1 - e^{-k1t}) \qquad (4.8)$$

Pseudo second order (PSO) on the other hand is given by equation 4.9 and it is used to describe chemisorption as well as cation exchange reactions (Simonin *et al*., 2016; Gupta and Bhattcharyya, 2011).

$$q_t = \frac{q_e^2 k_2 t}{1 + k_2 q_e t} \qquad (4.9)$$

Where q_t (mg/g) is adsorption capacity at a given time t, q_e (mg/g) is the maximum sorption capacity at equilibrium and k_1 (min^{-1}) and k_2 (min^{-1}) are the pseudo first and second order rate constant, respectively. The value of k_2 is determined by the slope and intercepts of t/q_t vs t

(min). Figure 4.6 depicts the pseudo first and second order plots, respectively while the constant values of pseudo first and second order are presented in Table 4.4. It is evident from the correlation coefficient that the data fitted better to pseudo second order (R^2 = 0.83) rather than pseudo first order (R^2 = 0.57). The better fitting to pseudo second order suggests that the fluoride adsorption by composite beads occurred via chemisorption. From the results (Table 4.4), the rate constant k_1 (pseudo first order) is 0.46 min^{-1} and k_2 (pseudo second order) is 2.80 min^{-1}, which suggest that chemisorption was much faster and dominant as compared to physisorption. The chi-square (X^2) determines the goodness of fit, that is the lower the value the better the fit. According to chi-square value, pseudo second order show the better fit than pseudo first order with X^2 of 0.000043.

Table 4.4. Calculated parameters for pseudo first order and pseudo second order reaction kinetics of raw MNS-Al/Fe metal oxides DE beads

PFO				PSO			
K_1 (min^{-1})	Qe (mg/g)	R^2	X^2	K^2 (g/mg.min)	Qe (mg/g)	R^2	X^2
0.46	0.48	0.57	0.000167	2.80	0.49	0.83	0.000043

The Weber and Morries (1963) intra-particle diffusion, represented by equation 4.10, was employed to explain the movement of fluoride ion from the bulk solution into the surface of the adsorbent (Tran *et al.*, 2016). During adsorption, adsorbate molecules move from the bulk solution into the boundary layer and further diffuse onto the interior of the adsorbent (Ayinde *et al*., 2018).

$$q_t = k_i t^{0.5} \quad (4.10)$$

Where q_t is the amount adsorbed (mg g^{-1}) at a given time, t (min); K_i (mg $g^{-1}min^{-1}$) is the intra-particle diffusion rate constant and is determined from the slope of $t^{0.5}$ vs qt. The intra-particle plot obtained from the adsorption data did not yield straight line indicating that intra-particle diffusion is not the only rate limiting step (Figure 4.7). The data exhibited two clearly defined phases indicating that there are two main adsorption steps are taking place. Phase I could be attributed to surface adsorption which completed within the first 90 min. Phase II at 240 min and beyond could be attributed to intra-particle diffusion adsorption at equilibrium. The rate of constant for phase 1 and phase 2 (K_1 and K_2,) are shown in Table 4.5. It is observed that K_1 is

higher than K_2, these indicates that boundary layer adsorption occurred much faster than the subsequent intra-particle diffusion and the adsorption at equilibrium. The pore diffusion in phase I and phase II is positive, meaning that the boundary layer and intra-particle diffusion are the main mechanism for adsorption.

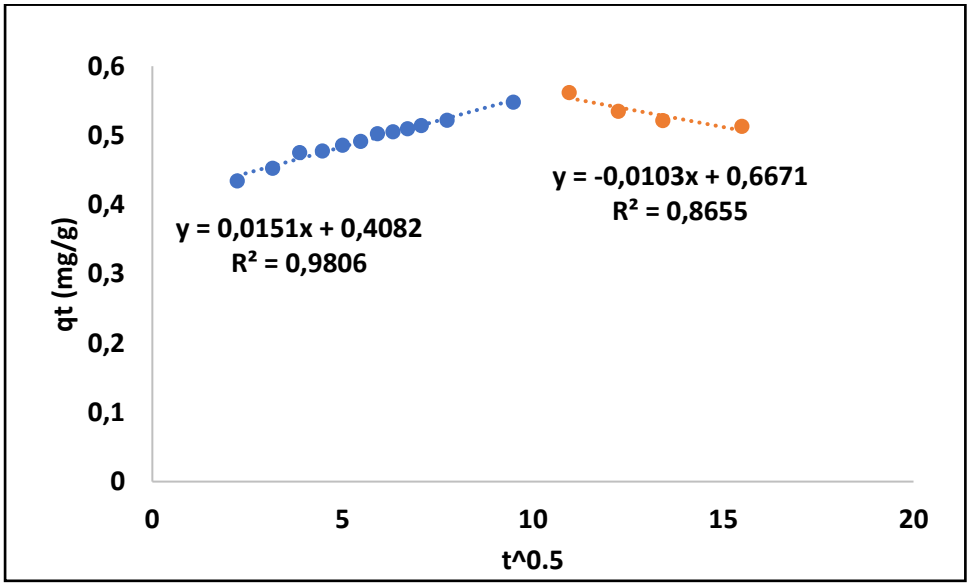

Figure 4.7: Intra-particle diffusion plot for fluoride adsorption onto MNS-Al/Fe metal oxides DE beads.

Table 4.5. Constant values of intra particle diffusion

Model		MNS-Al/Fe Modified DE alginate composite beads.
Intra particle diffusion	K_1 (mg/g min^{-1})	0.02
	K_2 (mg/g min^{-1})	0.01
	R^2 (phase 1)	0.98
	R^2 (phase 2)	0.87

4.4.2 The effect of adsorbent dosage

Figure 4.8 depicts the variation of percentage fluoride removal and adsorption capacity against adsorbent dosage. The percentage of fluoride removal increase as the adsorbent dosage increases from 0.1 g to 0.9 g/100 mL. The increase in adsorption with increase in MNS-Al/Fe Modified DE composite beads dosage could be due to increasing active binding sites as the

adsorption dosage increases. Conversely, the adsorption capacity decreased with increasing adsorbent dosage form 2.61 mg/g to 0.47 mg/g. Adsorbent dosage of 0.9 g/100 mL was therefore selected as the optimum for subsequent experiments.

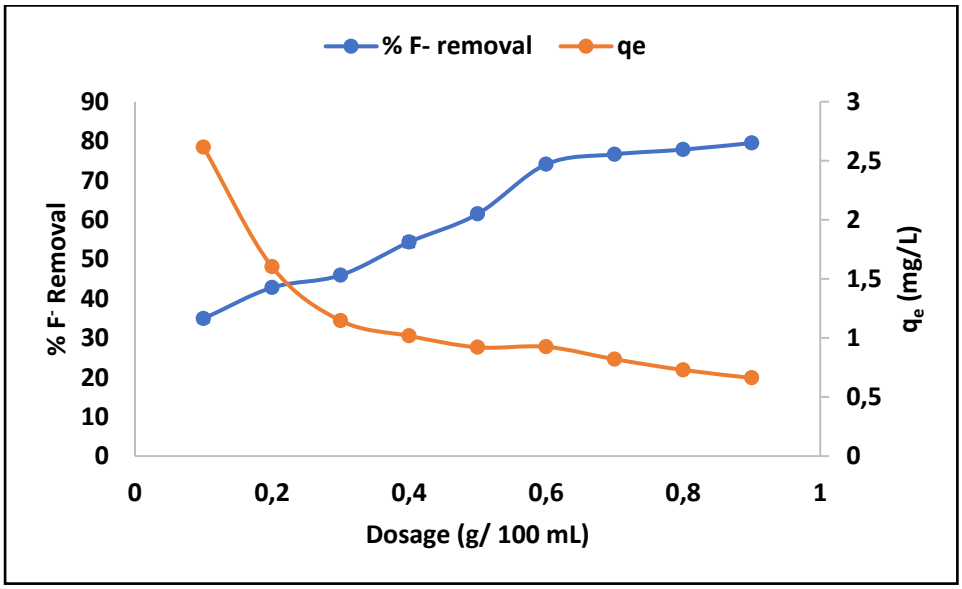

Figure 4.8: Variation % F^- removal and adsorption capacity by MNS-Al/Fe modified DE composite beads as a function of adsorbent dosage (contact time of 120 min, initial F^- concentration of 5 mg/L at 100 mL solution volume, pH 6 and shaking speed 250 rpm).

4.4.3 Effect of pH

The pH solution has an influence on the adsorbent's surface charges which in turn affect the behaviour of fluoride adsorption. The effect of pH on the adsorption of fluoride by the composite beads was evaluated by varying initial solution pH from 2 to 12 and the results are presented in Figure 4.9 a). It is observed that fluoride removal is optimum at a pH of 2 to 6 with the percentage removal of 89.16% to 84.81%. As the pH increases from 6 to 8, a sharp decrease in fluoride percentage removal to 65.11% was observed. Thereafter, a slight increase in fluoride percentage removal at pH 10 and 12. To further understand the behaviour of fluoride ion at various pH levels and to establish the surface charges, the pH point of zero charge (pH_{pzc}) of MNS-Al/Fe metal oxide modified DE beads was evaluated using the titration method and the results are presented in Figure 4.9 b). It is observed that the pH of the material is at pH of 5±0.9 indicating that at this pH the surface is neutraly charged while at pH below this level the material is positively charged and at pH above this level 5±0.9 the surface is negatively charged. Therefore, at pH below the 5±0.9 where H^+ dominate, adsorption may be attributed to possible electrostatic attraction between the negatively charge fluoride ion and the positively charged surface area of the adsorbent (equation 4.11). The fluoride adsorption above the pHpzc

where the surface of the adsorbent is negatively charged and where OH^- dominates, the decrease in fluoride removal could be attributed to competition between F^- and OH^- for adsorption site (equation 4.12). However, at neutral pH fluoride could also be adsorbed as a result of ion exchange and is presented by equation 4.13 and 4.14 respectively. Where M represent adsorbent's surface.

$$MOH + F^- + H_3O^+ \rightarrow MOH_2^+ - F^- + H_2O \quad (4.11)$$

$$MOH + F^- + H_3O^+ \rightarrow M^+ - F^- + 2H_2O \quad (4.12)$$

$$MOH + F^- \rightarrow MF + OH^- \quad (4.13)$$

$$M(OH)2^- + 2F^- \rightarrow MF^- + 2OH^- \quad (4.14)$$

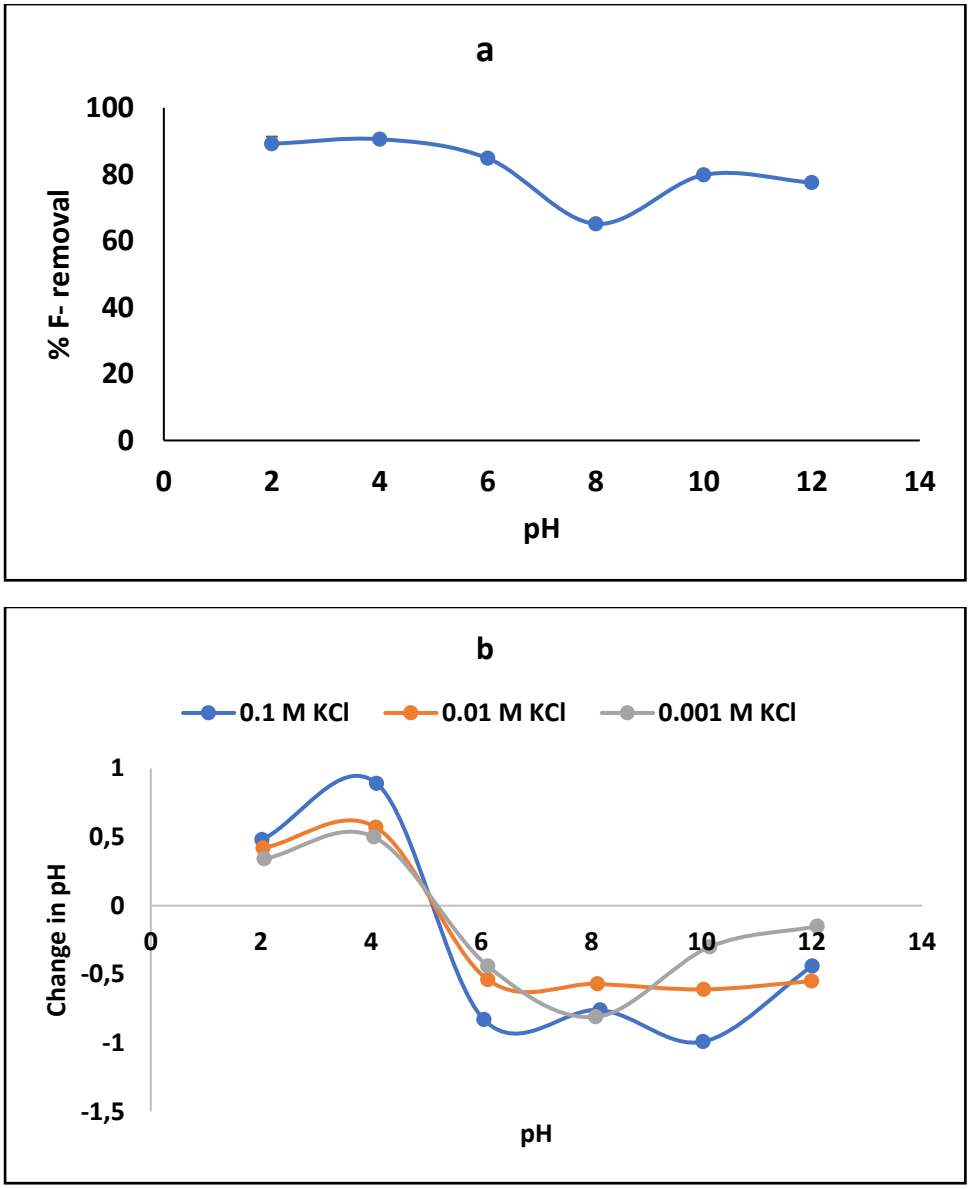

Figure 4.9: (a) Effect of pH and (b) point of zero charge on fluoride removal (5 mg/L initial F^- concentration, 0.9 g dosage, shaking speed 250 rpm) and b) point of zero charge.

4.4.4 Effect of initial concentration

The effect of initial concentration on the fluoride removal onto MNS-Al/Fe metal oxides DE beads as well as the adsorption isotherm were studied by varying the initial concentration from 5 to 30 mg/L. The experiment was repeated at different temperatures (298, 308 and 318 K) in order to study the thermodynamics. Figure 4.10 depicts the variation of adsorption capacity of fluoride concentration. Based on the findings, the adsorption capacity increases gradually with increasing initial concentration increase. The increase in adsorption capacity is due to the ratio of adsorbent mass to available fluoride ions in the solution. Increasing temperature from 298 to 308 K increases the adsorption capacity of fluoride removal while further increase to 318 K decreases the adsorption capacity.

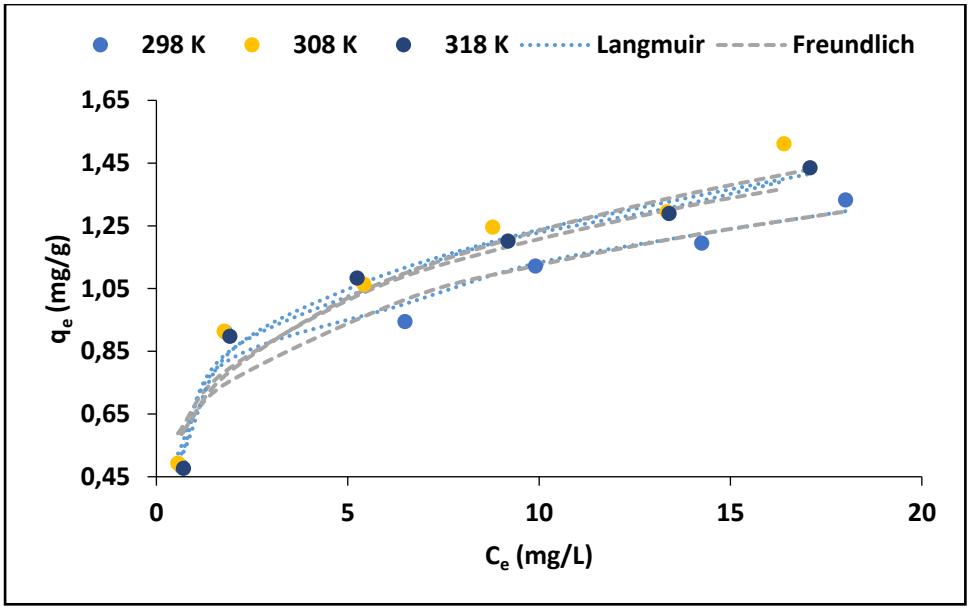

Figure 4.10: Variation of adsorption capacity with varying equilibrium concentration and adsorption isotherms for fluoride adsorption by composite beads (5 mg/L initial F^- concentration, pH 6, 0.9 g dosage, shaking speed 250 rpm).

Nonlinear equations of Langmuir and Freundlich adsorption isotherm were employed to further explain the interaction between the fluoride ions and the adsorbent's surface. Langmuir isotherm model is based on the assumption that adsorption occurs on monolayer surface. Once fluoride ion adsorbed on the surface of the adsorbent, no other ion is adsorbed on that adsorption site (Foo and Hammed, 2010). Langmuir isotherm model is represented by the following nonlinear equation 4.15.

$$q_e = \frac{q_m K_L c_e}{1+K_L c_e} \quad (4.15)$$

Where C_e is the equilibrium concentration (mg/L); q_e is the amount of ion adsorbed (mg/g); q_m is q_e for a complete monolayer (mg/g); K_L is adsorption equilibrium constant (L/mg). The Freundlich adsorption isotherm model on the other hand assumes that adsorption occurs on a heterogeneous surface and consider multilayer adsorption (Foo and Hammed, 2010). Freundlich is represented by equation 4.16.

$$q_e = K_f c_e^{1/n} \quad (4.16)$$

Where Ce is the equilibrium concentration (mg/L); q_e is the amount of ion adsorbed at equilibrium (mg/g); K_f is the Freundlich constant related to adsorption capacity and 1/n is the adsorption intensity. When 0< 1/n<1, the adsorption is favourable; when 1/n =1, the adsorption is irreversible; and when 1/n > 1, the adsorption is unfavourable. Nonlinear plots for Langmuir and Freundlich isotherm models are included in Figure 4.10 while the model's constant values

are depicted in Table 4.6. Based on the correlation coefficient (R^2) for initial concentration at different temperature, Langmuir adsorption data fitted better than Freundlich adsorption isotherm model. The better fit of the Langmuir isotherm suggests monolayer coverage. To further establish the favourability of the adsorption process, the equilibrium dimensionless parameter. Therefore, a dimensionless parameter, R_L, equation 4.17 was also calculated from the Langmuir isotherm adsorption process.

$$R_L = \frac{1}{1+K_L C_i} \qquad (4.17)$$

Where K_L is the Langmuir isotherm constants and C_i is the initial concentration of fluoride (mg/L). R_L value indicates the sorption system to be favourable if $0 < R_L < 1$. The R_L value equal to 1 indicate linear adsorption and if value of R_L is equal to 0, the adsorption is irreversible. Calculated value of R_L for different initial concentration is presented in figure 4.11. The calculated value of R_L lies between 0 and 1 indicating that the adsorption of fluoride onto MNS-Al/Fe metal oxides DE beads was favourable. The chi-square (X^2) determines the goodness of fit, that is the lower the value the better the fit. The chi-square values of Langmuir isotherm show small values for both temperatures as shown in Table 4.6 indicating better fit to Langmuir than Freundlich isotherms.

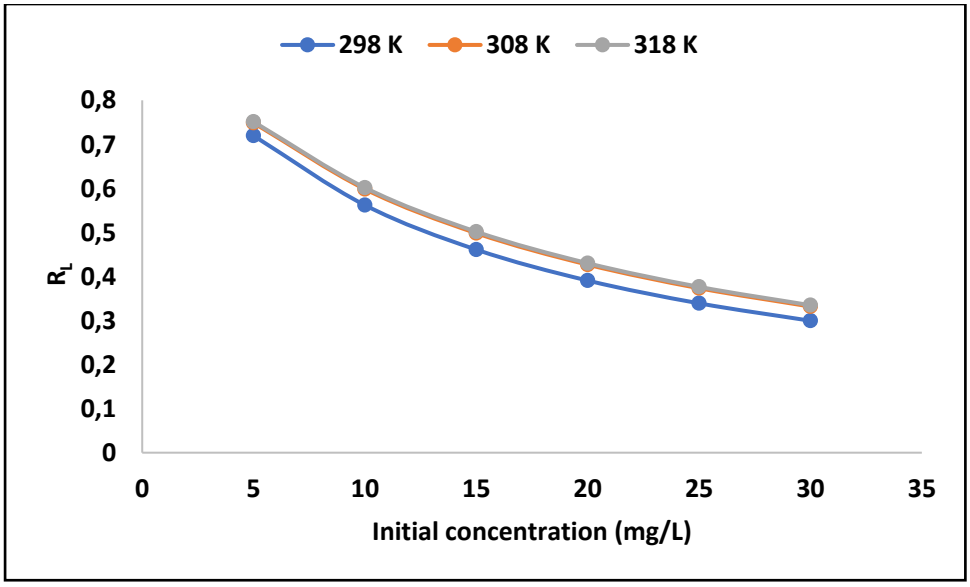

Figure 4.11: R_L values for the adsorption of fluoride onto MNS-Al/Fe metal oxides DE beads.

Table 4.6. Calculated Langmuir and Freundlich isotherm parameters.

		Langmuir isotherm			Freundlich isotherm			
Temperature(K)	q_m(mg/g)	R^2	K_L (L/mg)	X^2	1/n	K_f (mg/g)	R^2	X^2
298	1.84	0.96	0.08	0.017	0.24	0.65	0.98	0.044
308	2.08	0.96	0.07	0.022	0.25	0.68	0.90	0.048
318	2.12	0.99	0.07	0.007	0.28	0.66	0.94	0.030

4.4.5 Adsorption thermodynamics

To further elucidate adsorption mechanisms for fluoride onto MNS-Al/Fe metal oxide modified DE, the Gibbs energy change (ΔG^o), the enthalpy change (ΔH^o) and the entropy change (ΔS^o) were determined using the equation (4.18) and (4.19).

$$\Delta G^{\circ} = -RT \ln K_c \quad (4.18)$$

$$\ln K_c = -\frac{\Delta H^0}{RT} + \frac{\Delta S^0}{R} \quad (4.19)$$

Where ΔG^o is the standard Gibbs free energy change calculated using equation 4.18 and R is the molar gas constant, 8.314 J mol^{-1} K^{-1} and T is absolute temperature in Kelvin. ΔH^o is the standard enthalpy change while ΔS^o is the entropy change and they are determined from slope and the intercept of $\ln K_c$ against 1/T. The equilibrium constant, K_c is a dimensionless parameter derived from Langmuir's adsorption isotherm constant (L/mg) by multiplying it with 18.998×10^3 where 18.998 is the atomic mass of fluoride (Tran *et al*., 2016). The plot for $\ln K_c$ is presented in Figure 4.12 while the constant parameters are presented in Table 4.7. The results show the negative value of ΔG^o at all temperature, an indication that the fluoride adsorption on MNS-Al/Fe metal oxide modified DE composite beads surface is spontaneous. The enthalpy change (ΔH^o) value was found to be positive indicating that adsorption of fluoride by prepared composite beads was endothermic nature which absorb the heat from its surrounding and is unequivocally attributable to chemisorption. The value of ΔS^o was also found to be positive, suggesting that fluoride ions were randomly distributed on the surface of the adsorbent.

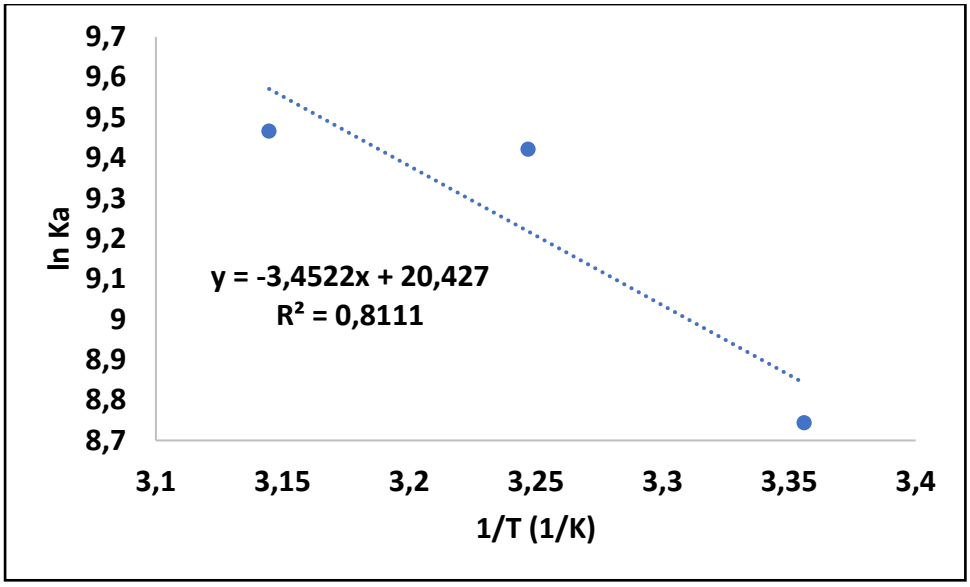

Figure 4.12: lnK_c as a function of reciprocal of adsorption temperatures.

Table 4.7. Adsorption thermodynamic parameters

ΔG^o (kj /mol)	ΔH^o (kj/mol)	ΔS^o (kj/mol)
298 K = -21662.5	28.70	170.20
308 K = -24125.3		
318 K = -25027.8		

4.4.6 The effect of co-existing ions

Figure 4.13 depict the effect of co-existing ions in fluoride adsorption by the prepared beads. Co-existing ions considered were magnesium (Mg^{2+}), calcium (Ca^{2+}), sulphate (SO_4^{2-}), nitrates (NO_3^-), chloride (Cl^-), and carbonate (CO_3^{2-}). From the results, the presence of co-existing decreases the fluoride uptake active sites. The same trend was observed during fluoride adsorption by zirconium-Na-attapulgite and Porous zirconium alginate beads (Zhang *et al.*, 2020; Qiusheng *et al*., 2015). This was attributed to the lower affinity of zirconium alginate for fluoride and a competition between the fluoride ions and the co-existing ions and may be since these ions compete with fluoride ions for the surface functional groups on bead surface and thereby decreasing the fluoride removal. Fluoride removal with the present on co-existing ions increased in the order of Ca^{2+}> CO_3^{2-}> SO_4^{2-}> Mg^{2+}> NO_3^-> Cl^-.

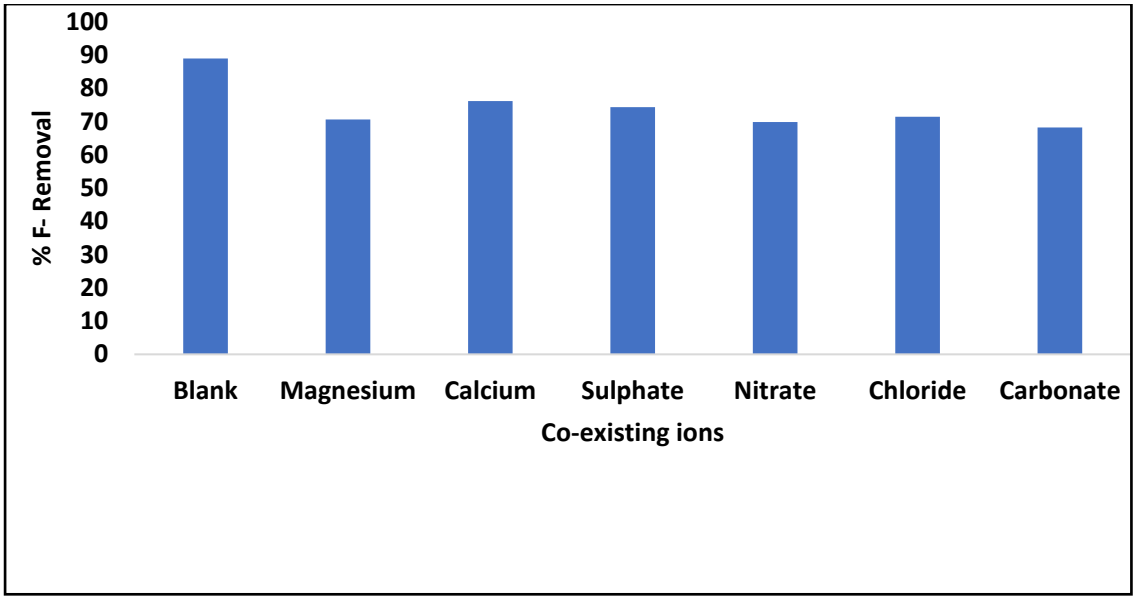

Figure 4.13: Effect of co-existing ions on fluoride removal by MNS-Al/Fe metal oxides DE beads (contact time 120 min, dosage 0.9 g/ 100 mL F^- solution, pH 4 and shaking speed of 250 rpm).

4.4.7 Regeneration and re-use of the adsorbent

The regeneration and reuse potential of the MNS-Al/Fe Modified DE alginate composite beads were evaluated using deionised water as the regenerant and the results are presented in Figure 4.14. The fluoride removal decreases with the increase in number of regeneration cycle from 86.5% to 61.6%. The decrease in fluoride removal could be attributed to diminishing adsorbent's active sites with continuous reuse. Deionized water was used as regenerant to avoid deformation of beads as it was observed by Zhang *et al.*, 2012 and Qiusheng *et al.*, 2015 when using HCl and NaOH as regenerant.

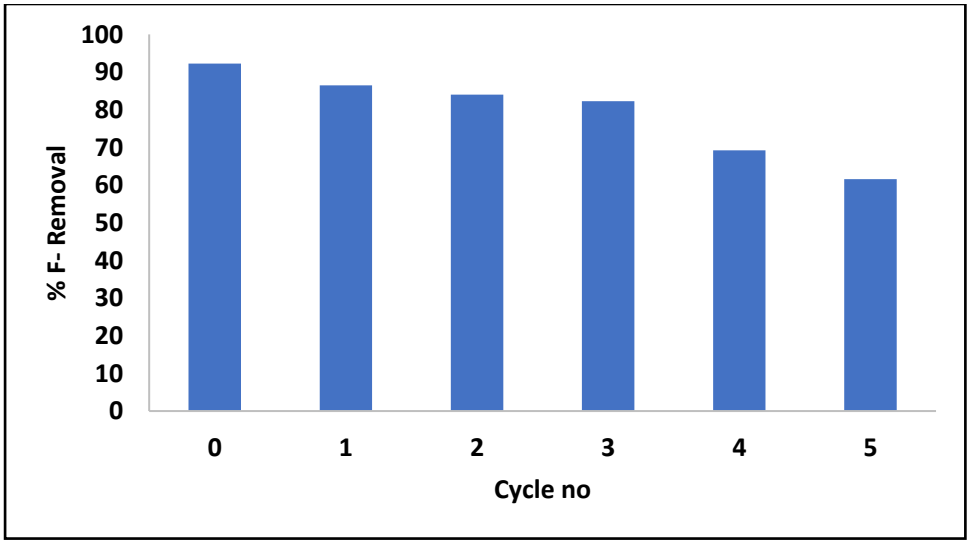

Figure 4.14: The regeneration and reuse of MNS-Al/Fe Modified DE alginate composite beads (5 mg/L initial F^- concentration, pH 4, 0.9 g dosage, shaking speed 250 rpm).

4.4.8 Defluoridation of field water

The efficiency of MNS-Al/Fe Modified DE alginate composite beads on fluoride removal was tested by using field groundwater collected from Siloam borehole at the established optimum conditions of pH, contact time, and adsorbent dosage. The experiment was conducted at optimized pH (pH 4). Table 4.8 shows physicochemical parameters of the field water before and after treatment. Percentage Fluoride removal of 79.79 % from field water was achieved at optimized conditions. Although the material is effective for fluoride removal at acidic pH, it is not applicable for household use. Moreover, the final pH is 6.22 which is suitable for human consumption. The treatment with acidic pH was because the optimum pH for fluoride that was effective was found to be at pH 4.

Table 4.8: Physicochemical parameters of field water before and after treatment (contact time 120 min, dosage 0.9 g/ 100 mL F^- solution, 5 mg/L F^-, pH 4 and shaking speed of 250 rpm)

Parameters	Before fluoride treatment	After fluoride treatment
pH	4.03	6.22
Total dissolved solids (mg/L)	750	385
Conductivity (µs/cm)	1050	543
F- (mg/L)	4.86	0.982

4.4.9 Column experiment

The column experiment was conducted using a bed height of 30 and 40 mm using the initial fluoride concentrations of 5 mg/L and the results are presented in Figure 4.15. It was observed that the breakthrough point, and the exhaustion point increases with an increase in bed height. This could be attributed to the fact that an increase in the bed height provides more adsorption sites and increases the resident time for the solution within the column resulting in efficient fluoride removal. The breakthrough adsorption capacities for 30 mm and 40 mm bed height were found to be 0.42 and 0.49 mg/g, respectively. The volume of water treated at each breakthrough point for bed height of 30 and 40 mm were found to be 1.3 and 1.8 L respectively. The breakthrough point was reached after 15 hours for bed height of 40 mm and 6 hours for bed height of 30 mm. The adsorption capacity at exhaustion points for 30 mm and 40 mm bed height were found to be 1.63 and 1.48 mg/g. The volume collected at exhaustion point for 30

mm and 40 mm bed height was found to be 9.6 and 9.2 L. The exhaustion point was reached after 28 hours for bed height of 40 mm and 33 hours for bed height of 30 mm. The flow rate was estimated to be 2.80 mL/min for 20 mm bed height and 0.32 mL/ min. In comparison with work done by Nekhavhambe, 2017 using Al/Fe metal oxide modified DE with the mass of 20 g, the breakthrough point was reached after 62 hours and the breakthrough point of 18 g of MNS-Al/Fe metal oxide modified DE beads was reach after 15 hours. In summary the one with 20 g (Al/Fe metal oxide modified DE) adsorbent show better fluoride removal than the adsorbent of 18 g (MNS-Al/Fe metal oxide modified DE beads). This could be because the MNS-Al/Fe metal oxide modified DE beads has low surface area than Al/Fe metal oxide modified DE. The flow rate in the present study when using 18 g of adsorbent did not increase.

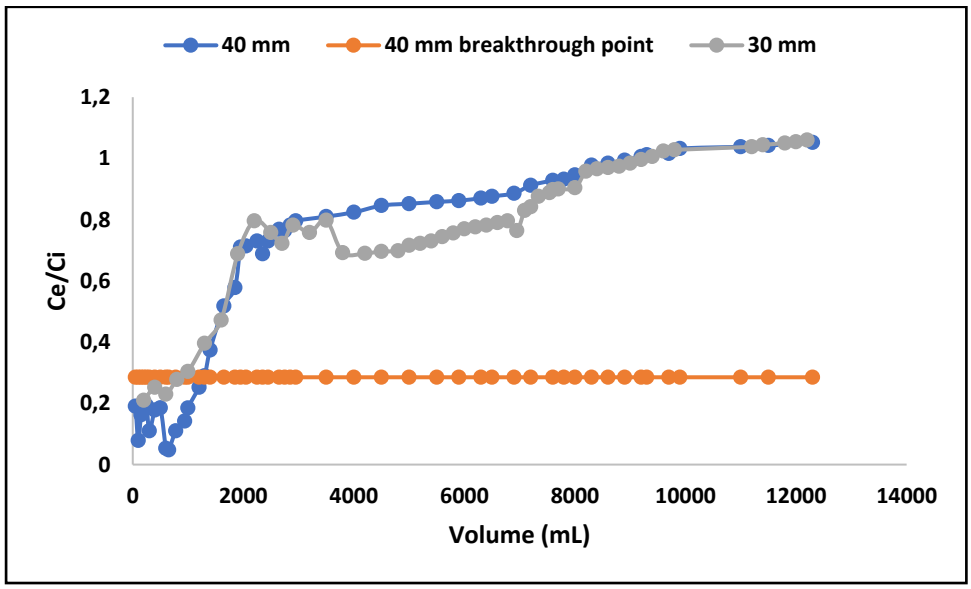

Figure 4.15: The breakthrough curve with bed height of 30 and 40 mm.

4.4.10 Column Performance indicator

The number of bed volume (BV) is essential for indicating the performance of fixed bed column. For a given bed mass, the adsorption is directly related to the number of volumes that have been processed before the breakthrough point (Setshedi *et al*., 2014). The calculated BV values are shown on Table 4.9. The BV value of 30 mm bed height was found to be 92.85 and the BV for the bed height of 40 mm was found to be 161 respectively. The bed height of 40 mm showed the high BV meaning that column with bed height of 40 mm perform better than the column with bed height of 30 mm. During operation, the adsorbent is deactivated. The rate of the deactivated will determined the frequency by which the adsorbent is replaced. The rate of deactivation is expressed as adsorbent exhaustion rate (AER), which is defined as the mass

of adsorbent deactivated per volume of water treated at breakthrough point (Setshedi *et al*., 2014). The calculated AER values are shown on Table 4.9 below. The AER value of column with bed height of 30 mm was found to be 1.45 g/L and the AER for column with bed height of 40 mm was found to be 0.92 g/L. The column with bed height of 40 mm has lower AER value meaning that it performs better. In summary, when the BV is high, and the AER is lower it indicate that fluoride removal was effective.

Table 4.9 Performance parameters of the adsorbent

	Bed height (mm)	
	30	40
Bed volume	92.85	161
Adsorption exhausting rate (g/L)	1.45	0.91

4.5 Comparison with other adsorbents

The comparison of defluoridation adsorption capacity between Al/Fe Modified DE and other reported adsorbents for defluoridation is shown in Table 4.10. The results showed that the adsorption capacity prepared composite bead is 2.61 mg/g. This was found to be lower compared to the other used adsorbent. Despite lower sorption capacity compared to other materials the material was able to bring the fluoride concentration to with the acceptable levels and when treating field water, the percentage fluoride removal was found to be 79.79 % and the final pH of 6.22 which shows that the material has the potential for use in real life application.

Table 4.10 Comparison between MNS-Al/Fe metal oxide modified DE beads and other adsorbent

Adsorbent	Adsorption capacity (mg/g)	Experimental conditions	Temperature (^{o}c)	Reference
Porous zirconium alginate beads	32.79	pH 2, contact time 20 hrs	40	Qiusheng *et al.*, 2015
Hydrous ferric oxide doped alginate beads	8.9	pH 7, contact time 24 hrs	29	Sujana *et al.*, 2013
Protonated chitosan beads	7.22	pH 7, contact time 0.5 hrs	30	Viswanathan *et al.*, 2009
Raw MNS powder	1.26	pH 6, contact time 120 min, shaking speed 200 rpm, 5 mg/L fluoride and 0.5 g	25	This study
MNS-Al/Fe metal oxide modified DE beads	2.61	pH 4, contact time 120 min, 5 mg/L and 0,9 g	25	This study

4.6 Anti-microbial activity results

Antibacterial activity of the raw MNS-Al/Fe metal oxides DE beads was evaluated with the reference to the well assay diffusion method by Kirby-Bauer. This was achieved by observing the minimal zone of inhibition and the results are presented in Figure 4.16 a) *Klebsiella Pneumoniae;* gram-positive b) *Staphylococcus Aureus;* gram-positive, and c) *Escherichia Coli*; gram-negative. MNS-Al/Fe Modified DE composite beads show antimicrobial potency studies towards *Klebsiella Pneumoniae*, with 10 mm diameter inhibition zone. This implies that MNS-Al/Fe Modified DE composite beads can destroy the cell wall of *Klebsiella Pneumoniae*. The prepared composite beads showed no antimicrobial activity for *Staphylococcus Aureus* which is gram positive and *Escherichia Coli* which is gram negative.

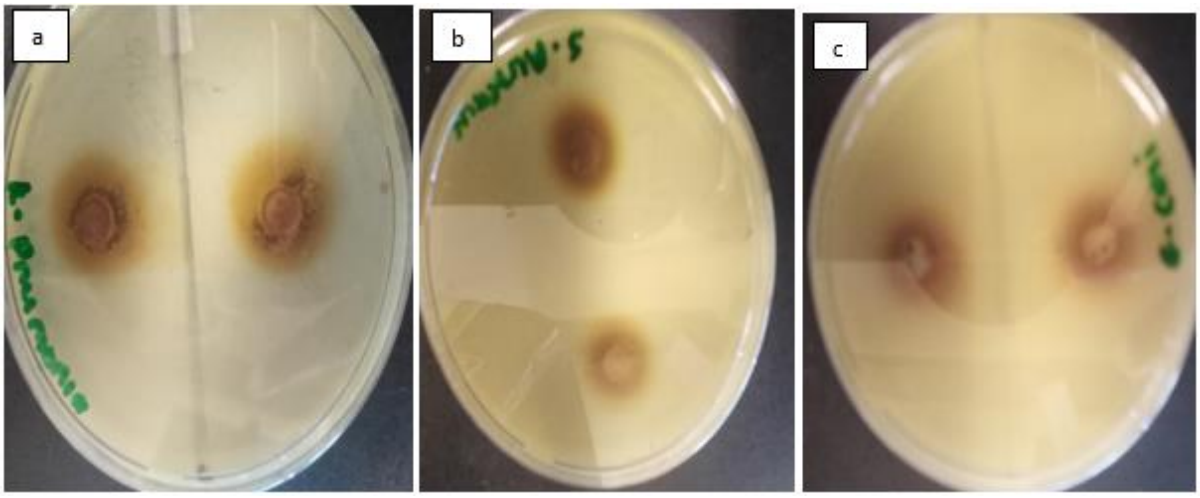

Figure 4.16: Representative petri dish of different bacteria (a) *Staphylococcus Aureus*, (b) *Klebsiella Pneumoniae* and (c) *Escherichia Coli.*

4.7 Summary

In this chapter, composite beads adsorbent was successfully prepared by blending MNS powder and Al/Fe metal oxides modified DE further applied towards fluoride and pathogen removal from water. The maximum adsorption capacity was found to be 2.61 mg/g and was achieved at pH 4.0 adsorbent dose 0.9 g and contact time 120 min and initial fluoride concentration of 5 mg/L. The adsorption of fluoride by the prepared composite beads followed pseudo second order of reaction kinetics model indicating that fluoride ions removed through chemisorption. The adsorption isotherms data better fit to Langmuir isotherm than Freundlich isotherm for both temperatures which suggest monolayer coverage. The thermodynamics parameters such as ΔG^{o} and ΔH^{o} revealed that adsorption of fluoride by the composite adsorbent is spontaneous and endothermic while ΔS^{o} indicated that fluoride ions where randomly distributed on the surface of the adsorbent. The presence of Mg^{2+}, Ca^{2+}, SO_4^{2-}, NO_3^{-}, Cl^{-}, and CO_3^{2-} reduced the percentage fluoride uptake by the prepared beads. The column with bed height of 40 mm was the most effective towards fluoride removal with the adsorption capacity of 0.49 mg/g at breakthrough point and treated 1.8 L and then treated 9.2 L at exhaustion point with adsorption capacity of 1.43 mg/g. MNS-Al/Fe metal oxides DE beads show antimicrobial potency studies towards *Klebsiella Pneumoniae*. Based on the finding the prepared beads has potential for use in fluoride and pathogenic removal from groundwater.

4.8 References

Afroze, S., Sen, T.K. and Ang, H.M., 2016. Adsorption performance of continuous fixed bed column for the removal of methylene blue (MB) dye using *Eucalyptus sheathiana* bark biomass. *Research on Chemical Intermediates*, *42*(3), pp.2343-2364.

Ahmad, M., Jamal, A., Tang, X.W., Al-Sughaiyer, M.A., Al-Ahmadi, H.M. and Ahmad, F., 2020. Assessing potable water quality and identifying areas of waterborne diarrheal and fluorosis health risks using spatial interpolation in Peshawar, Pakistan. *Water*, *12*(8), p.2163.

Arun, S., Kumar, R.M., Ruppa, J., Mukhopadhyay, M., Ilango, K. and Chakraborty, P., 2020. Occurrence, sources and risk assessment of fluoroquinolones in dumpsite soil and sewage sludge from Chennai, India. *Environmental Toxicology and Pharmacology*, *79*, p.103410.

Ayinde, W.B., Gitari, W.M., Munkombwe, M. and Amidou, S., 2018. Green synthesis of Ag/MgO nanoparticle modified nanohydroxyapatite and its potential for defluoridation and pathogen removal in groundwater. *Physics and Chemistry of the Earth, Parts A/B/C*, 107, pp. 25-37.

Foo, K.Y. and Hameed, B.H., 2010. Insights into the modelling of adsorption isotherm systems. *Chemical engineering journal*, *156*(1), pp.2-10.

Gitari, W.M., Izuagie, A.A. and Gumbo, J.R., 2017. Synthesis, characterization and batch assessment of groundwater fluoride removal capacity of trimetal Mg/Ce/Mn oxide-modified diatomaceous earth. *Arabian Journal of Chemistry*, *13*(1), pp.1-16.

Gong, J.L., Zhang, Y.L., Jiang, Y., Zeng, G.M., Cui, Z.H., Liu, K., Deng, C.H., Niu, Q.Y., Deng, J.H. and Huan, S.Y., 2015. Continuous adsorption of Pb (II) and methylene blue by engineered graphite oxide coated sand in fixed-bed column. *Applied Surface Science*, *330*, pp.148-157.

Gupta, S.S. and Bhattacharyya, K.G., 2011. Kinetics of adsorption of metal ions on inorganic materials: a review. *Advances in colloid and interface science*, *162*(1-2), pp.39-58.

Izuagie, A.A., Gitari, W.M. and Gumbo, J.R., 2016. Defluoridation of groundwater using diatomaceous earth: optimization of adsorption conditions, kinetics and leached metals risk assessment. *Desalination and Water Treatment*, 57(36), pp.16745-16757.

Malago, J., Makoba, E. and Muzuka, A.N., 2020. Spatial distribution of arsenic, boron, fluoride, and lead in surface and groundwater in arumeru district, northern Tanzania. *Fluoride*, *53*.

Obijole, O.A., Gitari, M.W., Mudzielwana, R., Ndungu, P.G., Samie, A. and Babatunde, A.W., 2021. Hydrothermally treated aluminosilicate clay (HTAC) for remediation of fluoride and pathogens from water: adsorbent characterization and adsorption modelling. *Water Resources and Industry*, p.100144.

Pakade, V.E., Ntuli, T.D. and Ofomaja, A.E., 2017. Biosorption of hexavalent chromium from aqueous solutions by Macadamia nutshell powder. *Applied Water Science*, *7*(6), pp.3015-3030.

Palansooriya, K.N., Yang, Y., Tsang, Y.F., Sarkar, B., Hou, D., Cao, X., Meers, E., Rinklebe, J., Kim, K.H. and Ok, Y.S., 2020. Occurrence of contaminants in drinking water sources and the potential of biochar for water quality improvement: A review. *Critical Reviews in Environmental Science and Technology*, *50*(6), pp.549-611.

Patel, H., 2019. Fixed-bed column adsorption study: a comprehensive review. *Applied Water Science*, *9*(3), pp.1-17.

Qiusheng, Z., Xiaoyan, L., Jin, Q., Jing, W. and Xuegang, L., 2015. Porous zirconium alginate beads adsorbent for fluoride adsorption from aqueous solutions. *RSC advances*, *5*(3), pp.2100-2112.

Sahu, P., 2019. Fluoride pollution in groundwater. In *Groundwater Development and Management*, pp. 329-350.

Setshedi, K.Z., Bhaumik, M., Onyango, M.S. and Maity, A., 2014. Breakthrough studies for Cr (VI) sorption from aqueous solution using exfoliated polypyrrole-organically modified montmorillonite clay nanocomposite. *Journal of Industrial and Engineering Chemistry*, *20*(4), pp.2208-2216.

Simonin, J.P., 2016. On the comparison of pseudo-first order and pseudo-second order rate laws in the modelling of adsorption kinetics. *Chemical Engineering Journal*, *300*, pp.254-263.

Sujana, M.G., Mishra, A. and Acharya, B.C., 2013. Hydrous ferric oxide doped alginate beads for fluoride removal: Adsorption kinetics and equilibrium studies. *Applied Surface Science*, *270*, pp.767-776.

Tran, H.N., You, S.J. and Chao, H.P., 2016. Thermodynamic parameters of cadmium adsorption onto orange peel calculated from various methods: a comparison study. *Journal of Environmental Chemical Engineering*, *4*(3), pp.2671-2682.

Viswanathan, N., Sundaram, C.S. and Meenakshi, S., 2009. Removal of fluoride from aqueous solution using protonated chitosan beads. *Journal of Hazardous Materials*, *161*(1), pp.423-430.

Weber Jr, W.J. and Morris, J.C., 1964. Equilibria and capacities for adsorption on carbon. *Journal of the Sanitary Engineering Division*, *90*(3), pp.79-108.

Zhang, B., Wang, Z., Shi, J. and Dong, H., 2020. Sulfur-based mixotrophic bio-reduction for efficient removal of chromium (VI) in groundwater. *Geochimica et Cosmochimica Acta*, *268*, pp.296-309.

Chapter 5: Conclusion and Recommendations

5.1 Conclusion

The study was designed with the main aim of fabricating macadamia nutshell powder-Al/Fe modified DE composite beads for removal of fluoride, pathogen from groundwater. In order to achieve this main objective, the following specific objectives were set:

Specific objectives

- To determine the physicochemical composition of macadamia nutshell powder.
- To evaluate the effectiveness of macadamia nutshell powder in fluoride and pathogens removal from groundwater.
- To evaluate the optimum conditions for fabricating macadamia nutshell powder-Al/Fe oxides coated DE sodium alginate beads for fluoride and pathogen removal from groundwater.
- To evaluate the fluoride and pathogens removal efficiency of macadamia nutshell powder Al/Fe oxides coated DE sodium alginate beads composite.
- To determine the regeneration and reusability potential of the synthesized adsorbents using various chemical solution.

The above specific objectives were further subdivided into two main chapters of results and the following conclusions/ findings were made drawn from each chapter.

5.2 Physicochemical characterization of macadamia nutshells and its application in fluoride and pathogen removal

The MNS results showed that the material consists of carbon 49.56% (C), hydrogen (H), nitrogen 0.20% (N) and oxygen 44.08% (O). The raw MNS spectra showed the main functional group of OH, C-H, C=O, C-C, C-OH together with the band of C-O. The micrograph revealed that the MNS consisted of flaky fold-like structures with some crystals on top. MNS shows the crystalline peak at 2-degree theta and also it appears to be amorphous.

Batch experiments of MNS showed the maximum fluoride removal percentage of 42.27% from 5 mg/L initial fluoride concentration when 0.5 g/100 mL adsorbent dosage was used at pH 6 after 120 min contact time. The presence of co-existing ions enhanced the performance of fluoride removal. The adsorption of fluoride onto MNS powder follow pseudo second order of reaction kinetics model indicating that fluoride ions removed through chemisorption. The adsorption data fitted better to Langmuir than Freundlich adsorption isotherm model which

suggest monolayer coverage. The value ΔG^0 was found to be negative indicating that adsorption of fluoride onto MNS was spontaneous and favourable. According to the findings MNS elucidate that it possesses no anti-microbial activity furthermore, MNS has capabilities to extract fluoride from ground water. The regeneration studies of MNS demonstrated that the adsorbent can be regenerated for up to 7 cycles using 0.01 M HCl and this clearly indicates the reuse potential of the adsorbent.

5.3 Fabrication of macadamia nutshell powder-Al/Fe metal oxide Modified diatomaceous earth composite beads for fluoride and pathogen

The optimum fluoride ratio of 1:3 yielded the high percentage removal and was adapted for further experiments. MNS-Al/Fe Modified DE composite beads show that the adsorbent composes of SiO_2 (63.23%), CaO (12.73), Al_2O_3 (3.98%) and Fe_2O_3 (5.40%) as the major oxides in the adsorbent. The FTIR spectra MNS-Modified DE alginate composite beads show that the main functional group of -OH and carboxyl functional group. The SEM spectra analysis revealed that the surface of the of MNS-Modified DE composite beads some irregular shaped granule and have rough surface area with some pore visible. The XRD spectra shows that the MNS-Modified DE composite beads consist mainly quarts and a smaller broader bump which is albite intermediate.

Their application towards fluoride and pathogen removal were studied. The fluoride adsorption from aqueous solutions by MNS-Al/Fe Modified DE composite beads depended on solution pH, adsorbent dosage, initial fluoride concentration, and contact time. The maximum adsorption capacity was found to be 2.61 mg/g and was achieved at pH 4.0 adsorbent dose 0.9 g and contact time 120 min and initial fluoride concentration of 5 mg/L. The adsorption of fluoride onto MNS-Al/Fe Modified DE composite beads powder follow pseudo second order of reaction kinetics model indicating that fluoride ions removed through chemisorption. The thermodynamics parameters such as ΔG^o and ΔH^o revealed that adsorption of fluoride by the composite adsorbent is endothermic and spontaneous and ΔS^o indicated that fluoride ions where randomly distributed on the surface of the adsorbent. The value ΔG^0 was found to be negative indicating that adsorption of fluoride onto MNS-Al/Fe Modified DE composite beads was spontaneous and favourable. The presence of Mg^{2+}, Ca^{2+}, SO_4^{2-}, NO_3^-, Cl^-, and CO_3^{2-} reduced the percentage fluoride uptake by the prepared beads. Experimental data were well fitted to the Langmuir isotherm model and the pseudo-second order kinetic model. The material showed better performance compared to other reported in the literature. The column with bed

height of 40 mm was the most effective towards fluoride removal with the adsorption capacity of 0.49 mg/g at breakthrough point and treated 1.8 L and then treated 9.2 L at exhaustion point with adsorption capacity of 1.43 mg/g. MNS-Al/Fe Modified DE composite beads show antimicrobial potency studies towards *Klebsiella Pneumoniae*. MNS-Al/Fe Modified DE composite beads were regenerated up to 5 cycle. This clearly indicates the reuse potential of the adsorbent.

5.4 Recommendations

Based on the findings the materials are suitable for application in fluoride removal and pathogen removal. Moreover, the following recommendations were made for future studies:

- The fluoride percentage removal when using MNS was found to be lower compared to other materials and it is recommended future studies should look into modification of MNS using inorganic and organic chemical species in order to enhance its performance towards fluoride and pathogen removal.
- Antibacterial testing revealed the Macadamia nutshell extract had no effect on the bacterial strains and it is recommended to use Nanoparticles to enhance its effectiveness to bacteria.
- MNS-Al/Fe metal oxide DE beads show microbial potency towards *Klebsiella Pneumoniae* However, further research is needed to establish the exact mechanisms involved and to further modify the adsorbent to improve the effectiveness towards microbes.
- The flow rate was found to be slow therefore it is recommended that, there is need to use peristaltic pump to enhance the flow rate.